



NISTIR 5246

Performance of 1/3-Scale Model Precast Concrete
Beam-Column Connections Subjected to
Cyclic Inelastic Loads - Report No. 3

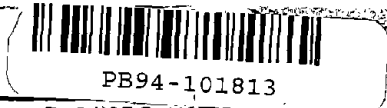
Geraldine S. Cheok
William C. Stone

August 1993
Building and Fire Research Laboratory
National Institute of Standards and Technology
Gaithersburg, MD 20899



U.S. Department of Commerce
Ronald H. Brown, *Secretary*
Technology Administration
Mary L. Good, *Under Secretary for Technology*
National Institute of Standards and Technology
Arati Prabhakar, *Director*

PROTECTED UNDER INTERNATIONAL COPYRIGHT
ALL RIGHTS RESERVED.
NATIONAL TECHNICAL INFORMATION SERVICE
U.S. DEPARTMENT OF COMMERCE



PB94-101813

T-114
EV. 9-92)
MAN 4.09

U.S. DEPARTMENT OF COMMERCE
NATIONAL INSTITUTE OF STANDARDS AND TECHNOLOGY

(ERB USE ONLY)

ERB CONTROL NUMBER <i>W93-1596</i>	DIVISION <i>861</i>
PUBLICATION REPORT NUMBER	CATEGORY CODE <i>140</i>
PUBLICATION DATE	NUMBER PRINTED PAGES

MANUSCRIPT REVIEW AND APPROVAL

INSTRUCTIONS: ATTACH ORIGINAL OF THIS FORM TO ONE (1) COPY OF MANUSCRIPT AND SEND TO:
SECRETARY, APPROPRIATE EDITORIAL REVIEW BOARD.

TITLE AND SUBTITLE (CITE IN FULL)
Performance of 1/3-Scale Model Precast Concrete Beam-Column Connections Subjected to Cyclic Inelastic Loads - Report No. 3

TRACT OR GRANT NUMBER <i>92-0A-055</i>	TYPE OF REPORT AND/OR PERIOD COVERED <i>NISTIR</i>
---	---

THOR(S) (LAST NAME, FIRST INITIAL, SECOND INITIAL) <i>Cheek, G. S. Stone, W. C.</i>	PERFORMING ORGANIZATION (CHECK (X) ONE BOX) <input checked="" type="checkbox"/> NIST/GAITHERSBURG <input type="checkbox"/> NIST/BOULDER <input type="checkbox"/> JILA/BOULDER
--	--

LABORATORY AND DIVISION NAMES (FIRST NIST AUTHOR ONLY)
Building and Fire Research Lab, Structures Division

SPONSORING ORGANIZATION NAME AND COMPLETE ADDRESS (STREET, CITY, STATE, ZIP)
*Concrete Research Council
P.O. Box 19150
22400 West Seven Mile Road
Detroit, MI 48219-0150*

*NIST Category No.
NIST-140*

RECOMMENDED FOR NIST PUBLICATION

<input type="checkbox"/> JOURNAL OF RESEARCH (NIST JRES)	<input type="checkbox"/> MONOGRAPH (NIST MN)	<input type="checkbox"/> LETTER CIRCULAR
<input type="checkbox"/> J. PHYS. & CHEM. REF. DATA (JPCRD)	<input type="checkbox"/> NATL. STD. REF. DATA SERIES (NIST NSRDS)	<input type="checkbox"/> BUILDING SCIENCE SERIES
<input type="checkbox"/> HANDBOOK (NIST HB)	<input type="checkbox"/> FEDERAL INF. PROCESS. STDS. (NIST FIPS)	<input type="checkbox"/> PRODUCT STANDARDS
<input type="checkbox"/> SPECIAL PUBLICATION (NIST SP)	<input type="checkbox"/> LIST OF PUBLICATIONS (NIST LP)	<input type="checkbox"/> OTHER _____
<input type="checkbox"/> TECHNICAL NOTE (NIST TN)	<input checked="" type="checkbox"/> NIST INTERAGENCY/INTERNAL REPORT (NISTIR)	

RECOMMENDED FOR NON-NIST PUBLICATION (CITE FULLY) U.S. FOREIGN

NISTIR 5246

PUBLISHING MEDIUM
 PAPER CD-ROM
 DISKETTE (SPECIFY) _____
 OTHER (SPECIFY) _____

SUPPLEMENTARY NOTES
In Comp 8-19-93

ABSTRACT (A 1500-CHARACTER OR LESS FACTUAL SUMMARY OF MOST SIGNIFICANT INFORMATION. IF DOCUMENT INCLUDES A SIGNIFICANT BIBLIOGRAPHY OR LITERATURE SURVEY, CITE IT HERE. SPELL OUT ACRONYMS ON FIRST REFERENCE.) (CONTINUE ON SEPARATE PAGE, IF NECESSARY.)

The tests results of hybrid post-tensioned precast concrete beam-to-column connections (Phase IV A) are presented. These tests are part of an experimental program on 1/3-scale model precast concrete moment resisting connections being conducted at the National Institute of Standards and Technology. Previous test results are summarized. The objective of the test program is to develop guidelines for an economical precast beam-to-column connection for regions of high seismicity. The basic concept of the study is to use of post-tensioning to connect the members and to eliminate the use of column corbels. Monolithic control specimens were designed to model interior moment resisting connections designed in accordance with the Uniform Building Code [ICBO, 1985 and 1988] criteria for seismic Zones 2 and 4. The precast specimens were designed to achieve moment and geometry compatibility with the monolithic design. To date, twenty specimens have been tested. Variables in the study include location of the post-tensioning steel, the use of post-tensioning bars versus strands, the use of fully and partially bonded and unbonded strands, and the combination of low strength steel and post-tensioning. Specimens were subjected to reversed cyclic loading according to a prescribed displacement history. Comparisons were made between the behavior of the precast specimens and monolithic specimens. The comparisons were based on connection strength, drift capacity of the connection, and energy dissipation characteristics.

KEY WORDS (MAXIMUM 9 KEY WORDS; 28 CHARACTERS AND SPACES EACH; ALPHABETICAL ORDER; CAPITALIZE ONLY PROPER NAMES)

Building technology; beam-column; concrete; connections; cyclic loading; joint; precast; post-tensioning; story drift.

AVAILABILITY

<input type="checkbox"/> UNLIMITED	<input type="checkbox"/> FOR OFFICIAL DISTRIBUTION. DO NOT RELEASE TO NTIS.
<input type="checkbox"/> ORDER FROM SUPERINTENDENT OF DOCUMENTS, U.S. GPO, WASHINGTON, D.C. 20402	
<input type="checkbox"/> ORDER FROM NTIS, SPRINGFIELD, VA 22161	

NOTE TO AUTHOR(S) IF YOU DO NOT WISH THIS MANUSCRIPT ANNOUNCED BEFORE PUBLICATION, PLEASE CHECK HERE.

11-11-11

ABSTRACT

Test results of hybrid post-tensioned precast concrete beam-to-column connections are presented. These tests represent Phase IV A of an experimental program on 1/3-scale model precast concrete moment resisting connections being conducted at the National Institute of Standards and Technology. Previous test results in Phases I through III are summarized. The objective of the test program is to develop guidelines for an economical precast beam-to-column connection for regions of high seismicity. The basic concept of the study is to use post-tensioning to connect the members and to eliminate the use of column corbels. Monolithic control specimens tested in Phase I were designed to model interior moment resisting connections designed in accordance with the Uniform Building Code [ICBO, 1985 and 1988] criteria for seismic Zones 2 and 4. The precast specimens were designed to achieve moment and geometric compatibility with the monolithic design. To date, twenty specimens have been tested. Variables in the study include the location of the post-tensioning steel (Phase I), the use of post-tensioning bars versus strands (Phase II), the use of fully and partially bonded and unbonded strands (Phase III), and the combination of low strength steel and post-tensioning (Phase IV, described in this report). Specimens were subjected to reversed cyclic loading according to a prescribed displacement history. Comparisons are made between the behavior of the precast specimens and monolithic specimens. The comparisons are based on connection strength, drift capacity of the connection, and energy dissipation characteristics.

KEYWORDS: Building Technology, beam-column, concrete, connections, cyclic loading, joint, precast, post-tensioning, story drift.



CONTENTS

	Page
ABSTRACT	iii
CONTENTS	v
LIST OF TABLES	vii
LIST OF FIGURES	ix
1.0 INTRODUCTION	1
2.0 SPECIMEN DESCRIPTION, DETAILS, AND TEST PROCEDURE	3
2.1 Summary of Previous NIST Tests	3
2.1.1 Prototype Structure	3
2.1.2 Phase I Tests	4
2.1.3 Phase II Tests	5
2.1.4 Phase III Tests	6
2.2 Phase IV A Tests	8
2.2.1 Introduction	8
2.2.2 Prototype Structure	9
2.2.3 I-P-Z4 and K-P-Z4 Specimen Details	10
2.2.5 J-P-Z4 Specimen Details	12
2.2.6 L-P-Z4 Specimen Details	14
2.3 Grouting Process of Phase IV A Specimens	18
2.4 Discussion of Specimen Design	18
2.5 Test Procedure	19
3.0 DISCUSSION OF TEST RESULTS	22
3.1 Failure Mode	22
3.1.1 Phase I-III Specimens	22
3.1.2 Phase IV A: Fully Bonded Mild and PT Steels [I-P-Z4 & K-P-Z4] ..	22
3.1.3 Phase IV A: Bonded Mild Steel and Unbonded PT Steel [J-P-Z4] ..	25
3.1.4 Phase IV A: Unbonded Mild and PT Steels (Replaceable System) [L-P-Z4, A, B, & C]	27
3.2 Story Drift	30
3.3 Connection Strength	35
3.4 Energy Dissipation	36
3.5 General Discussion	38
4.0 CONCLUSIONS AND FUTURE RESEARCH	41
4.1 Conclusions	41
4.2 Future Research at NIST	41

ACKNOWLEDGEMENTS	45
REFERENCES	47
APPENDIX A: DEVELOPMENT OF CODE CRITERIA	49
APPENDIX B: SPECIMEN DRAWINGS	57
APPENDIX C: MATERIAL PROPERTIES	77
APPENDIX D: ORGANIZATIONAL CHART	83
APPENDIX E: DOCUMENTATION FOR PROGRAM B6.FOR	85

LIST OF TABLES

	Page
Table 1. NIST Specimens	7
Table 2. Connection Strengths and Story Drifts	32
Table C1. Concrete and Grout Strengths	77

LIST OF FIGURES

	Page
Figure 1. Prototype Structure and Test Subassembly	3
Figure 2. Model Beam Cross Sections for Monolithic Zones 2 and 4	4
Figure 3. Model Beam Cross Sections for Precast Specimens - Phases I - III	5
Figure 4. Predicted Bilinear Elastic Behavior for Phase III Specimens [Priestley and Tao 1993].	6
Figure 5. Model Beam Cross Sections for Phase IV A Specimens I-P-Z4 & K-P-Z4	11
Figure 6. Steel cage for specimen I-P-Z4	12
Figure 7. Model Beam Cross Sections for Phase IV A Specimen J-P-Z4	13
Figure 8. Steel Cage for Specimen J-P-Z4	14
Figure 9. Model Beam Cross Sections for Phase IV A Specimens L-P-Z4 A-C	16
Figure 10. Details of the Block-out in Specimens L-P-Z4 C	17
Figure 11. Steel Cage for Specimen L-P-Z4	17
Figure 12. Boundary Conditions and Loading History	20
Figure 14. Specimen I-P-Z4 at Failure - 2.7% Story Drift	23
Figure 15. Mild Steel Bars Sliding Out of Duct at 4.6% Drift - I-P-Z4	24
Figure 16. Specimen K-P-Z4 at failure - story drift = 3.1%	25
Figure 17. Specimen J-P-Z4 at failure - story drift = 3.6%	26
Figure 18. Specimen L-P-Z4 C at story drift of 2%	29
Figure 19. Specimen L-P-Z4 C at story drift of 2%	30
Figure 20. Hysteresis curves for A-M-Z4	32
Figure 21. Hysteresis curves for A-P-Z4	32
Figure 22. Hysteresis curves for C-P-Z4	33
Figure 23. Hysteresis curves for E-P-Z4	33
Figure 24. Hysteresis curves for G-P-Z4	33
Figure 25. Hysteresis curves for I-P-Z4	33
Figure 26. Hysteresis curves for J-P-Z4	34
Figure 27. Hysteresis curves for K-P-Z4	34
Figure 28. Hysteresis curves for L-P-Z4 A	34
Figure 29. Hysteresis curves for L-P-Z4 B	34
Figure 30. Hysteresis curves for L-P-Z4 C	35
Figure 31. Comparison of the Normalized Cyclic Energy and Story Drift	37
Figure 32. Normalized Cumulative Energy Dissipated.	38
Figure 33. Generic Beam Details for Phase IV, B Production Specimens	43
Figure 34. Elevation View of Phase IV, B Production Specimens	44
Figure A1. Experimental Hysteresis Curves for NIST Specimen A-P-Z4	53
Figure A2. Predicted Hysteresis Curves Produced Using NIDENT 5.0 System Identification and IDARC 3.3 Inelastic Solution	53
Figure B1. Elevation View of Beams - I and K P-Z4	58

Figure B2.	Beam Cross Sections - I and K P-Z4	59
Figure B3.	Beam Ties - I and K P-Z4	60
Figure B4.	Column Cross Section - I and K P-Z4	61
Figure B5.	Top and Elevation Views of Column - I and K P-Z4	62
Figure B6.	Elevation View of Beams - J-P-Z4	63
Figure B7.	Beam Cross Sections - J-P-Z4	64
Figure B8.	Beam Top View and Longitudinal Reinforcement - J-P-Z4	65
Figure B9.	Column Cross Section - J-P-Z4	66
Figure B10.	Top and Elevation Views of Column - J-P-Z4	67
Figure B11.	Elevation View of Beams - L-P-Z4	68
Figure B12.	Beam Cross Section and Ties - L-P-Z4	69
Figure B13.	Beam Top View and Longitudinal Steel - L-P-Z4	70
Figure B14.	T-Section for L-P-Z4	71
Figure B15.	Column Cross Section - L-P-Z4	72
Figure B16.	Top and Elevation Views of Column - L-P-Z4	73
Figure B17.	Mild Steel Tube for Specimen L-P-Z4 C	74
Figure B18.	Modified Dywidag Bar	75
Figure C1.	Stress-Strain Curve for #3, Grade 40 Reinforcing Bar	78
Figure C2.	Stress-Strain Curve for #3, Grade 60 Reinforcing Bar	78
Figure C3.	Stress-Strain Curve for #4, Grade 60 Reinforcing Bar.	79
Figure C4.	Stress-Strain Curve for Smooth Wire Used for Ties	79
Figure C5.	Stress-Strain Curve for Dywidag Bar - J-P-Z4	80
Figure C6.	Stress-Strain Curve for Dywidag Bar - L-P-Z4 B	80
Figure C7.	Stress-Strain Curve for 9 mm, Grade 270 Strand - L-P-Z4 C	81
Figure C8.	Stress-Strain Curve for 11 mm, Grade 270 Strand - L-P-Z4 A	81
Figure C9.	Stress-Strain Curve for 13 mm, Grade 270 Strand - I and K P-Z4	82
Figure C10.	Stress-Strain Curve for 1026 Steel Tube - L-P-Z4 C	82
Figure E1.	Determination of Length Change in Steel Layer	86
Figure E2.	Flowchart for program B6.FOR	88
Figure E3.	Flowchart for Subroutine Calc_mom	89
Figure E4.	Flowchart for Subroutine Calc_mom (cont.)	90
Figure E5.	Flowchart for Subroutine Mom_check	91

1.0 INTRODUCTION

A study of the behavior of 1/3-scale model precast concrete interior beam-column connections subject to cyclic inelastic loading was initiated at the National Institute of Standards and Technology (NIST) in 1987. The objective of the ongoing experimental program is to develop guidelines for the design of an economical precast concrete beam-column connection for regions of high seismicity. The use of fully and partially bonded and unbonded post-tensioning in the connections is the major focus.

The test program consists of four phases. Phase I was an exploratory phase in which four monolithic specimens and two precast, post-tensioned concrete specimens were tested. Test results of the monolithic specimens served as references for the precast concrete tests. The results from the precast tests were used to determine the viability of the connection details. Phase II of the program involved testing six precast specimens. In an effort to improve the energy dissipation characteristics, the post-tensioning (PT) steel was moved closer to the beam center and the use of prestressing strands was compared with the use of post-tensioning bars. Because of stiffness degradation observed in the earlier precast specimens in the later stages of the tests, the use of partially bonded tendons was studied in Phase III. Two specimens were tested in this phase.

Phase IV, currently underway, examines the use of non-prestressed low strength steel used in conjunction with PT steel as a means of improving the energy dissipation characteristics of the precast specimens. The premise for this concept is that the mild steel will be used as an energy dissipator while the friction force developed between the beam and column by the post-tensioning force will be used to provide the necessary shear resistance. Initially, concerns were raised that the friction force would be insufficient to resist the applied shear loads in addition to gravity loads. To address this concern, simulated gravity loads were applied to the beams for the Phase IV tests. This had not been done in the earlier tests.

Phase IV is divided into two phases, A and B. Phase IV A involved three archetype designs and six tests. The test results from these specimens will be used to determine the specimen details in the next phase of testing, Phase IV B. One of the specimens in Phase IV A, which incorporated the concept of replaceable mild and PT steels, was tested three times. In Phase IV B, four "production" type tests are to be conducted. The term production is used as the precast beams and columns are to be fabricated by a precaster. The connections are then to be assembled and tested at NIST. The primary variable in this phase is the amount and type of mild and high strength steel.

A steering committee was formed to provide technical guidance for Phases I-III. The members of this committee include Mr. Dan Jenny (PCI), Dr. Robert Englekirk (Englekirk and Sabol, Inc.), Dr. S. K. Ghosh (PCA), Mr. Paul Johal(PCI), and Dr. Nigel Priestley (UC at San Diego). Partial funding was made available from ConREF (Concrete Research and Education Foundation) of the American Concrete Institute for the Phase IV tests and an

oversight committee was formed. Members of the oversight committee are listed in the organizational chart on page 83.

This report describes the Phase IV A specimens and summarizes the findings from Phases I - IV A. It is the third report in the series describing NIST work on precast moment resisting frames. Detailed results from Phases I, II and III may be found in NIST reports Cheok and Lew [1990, 1991], and in papers by Cheok, Stone, and Lew [1992], and Cheok and Lew [1993].

2.0 SPECIMEN DESCRIPTION, DETAILS, AND TEST PROCEDURE

2.1 Summary of Previous NIST Tests

2.1.1 Prototype Structure

The subassembly selected for testing is shown in Fig. 1. The test specimens were 1/3-scale models of an interior connection. The scale factor of 1/3 was the largest that could be accommodated in the test facility at NIST. The prototype monolithic interior connection is typical for a 15-story moment resisting frame office building, 4 x 8 bays in each direction, designed using UBC [ICBO, 1985] seismic Zones 2 and 4 criteria. The center-to-center spacing of the columns was 7.28 m and the story height was 3.96 m.

For the prototype structure, the total design base shear was 8518 kN. The required beam moment capacity at the 3rd floor was 2293 kN-m per beam at the column face. Based on this, the prototype beam dimensions were 762 mm x 1372 mm and 610 mm x 1219 mm. The prototype beam flexural steel consisted of 9 - #9 (29 mm, top) and 7 - #10 (32 mm, bottom) which resulted in an ultimate beam moment capacity of 2304 kN-m. The prototype column was 762 mm x 1372 mm with 24 - #10. The dimensions and steel areas for the models were obtained by scaling the prototype dimensions and areas by the appropriate scale factor.

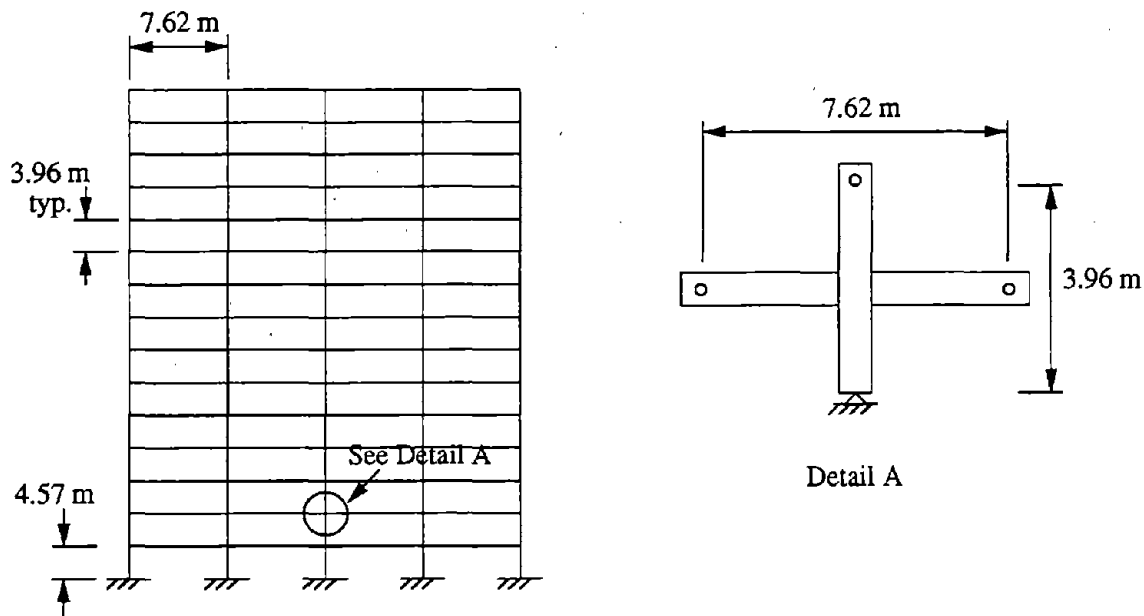


Figure 1. Prototype Structure and Test Subassembly.

2.1.2 Phase I Tests

Phase I was the exploratory phase of the test program. The objectives of the Phase I tests were to define benchmark behavior of a traditional monolithic connection, and to determine if the concept of using post-tensioning alone to connect the precast elements was viable. This concept of using PT alone was selected initially because it was simple to construct and if proven to be viable, would be economical as well since it would eliminate the use of shear keys and corbels.

In this phase, four monolithic specimens were tested. Two identical specimens, A-M-Z2 and B-M-Z2, were designed in accordance to the UBC seismic Zone 2 criteria [ICBO, 1985], and two other identical specimens, A-M-Z4 and B-M-Z4, were designed to UBC seismic Zone 4 criteria [ICBO, 1985]. The precast connection was designed to match the moment capacity of the monolithic Zone 4 specimens. The two identical precast specimens, A-P-Z4 and B-P-Z4, had the same dimensions as the monolithic Zone 4 specimens. A total of 6 specimens was tested in this phase. Dywidag¹ bars were selected to post-tension the precast specimens. This was so that load losses, which are a concern if short lengths of strands were used, would be minimized. Details of the Phase I beams are given in Figs. 2 - 3.

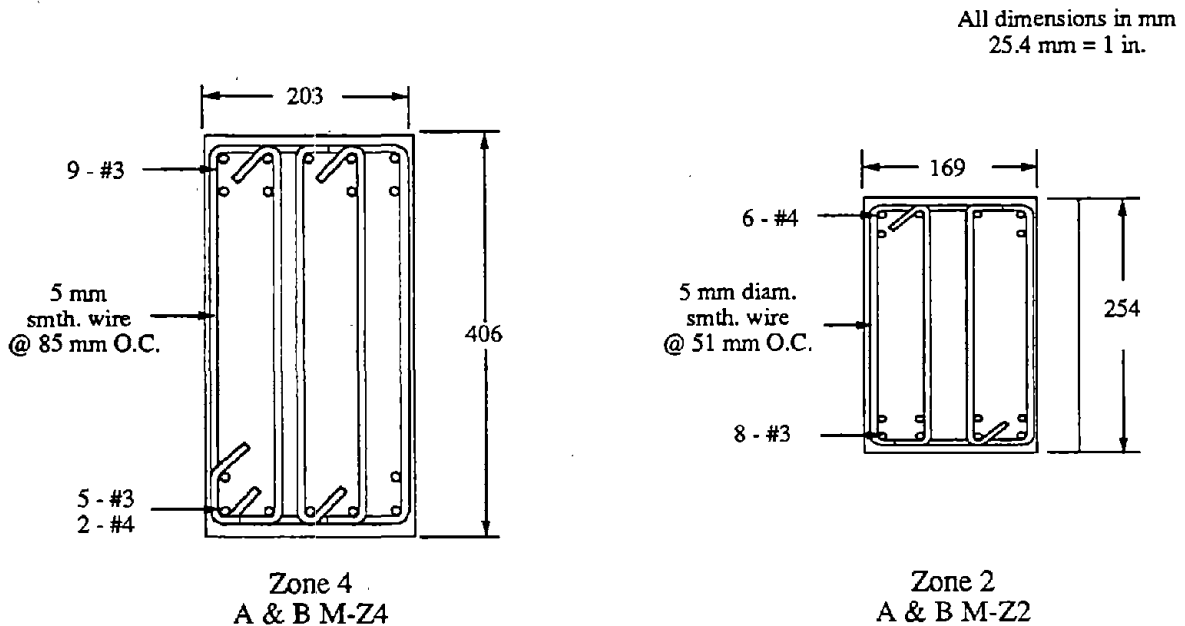


Figure 2. Model Beam Cross Sections for Monolithic Zones 2 and 4.

¹Certain trade names and company products are mentioned in the text or identified in an illustration in order to adequately specify the experimental procedure and equipment used. In no case does such an identification imply recommendation or endorsement by the National Institute of Standards and Technology, nor does it imply that the products are necessarily the best available for the purpose.

All dimensions in mm
25.4 mm = 1 in.

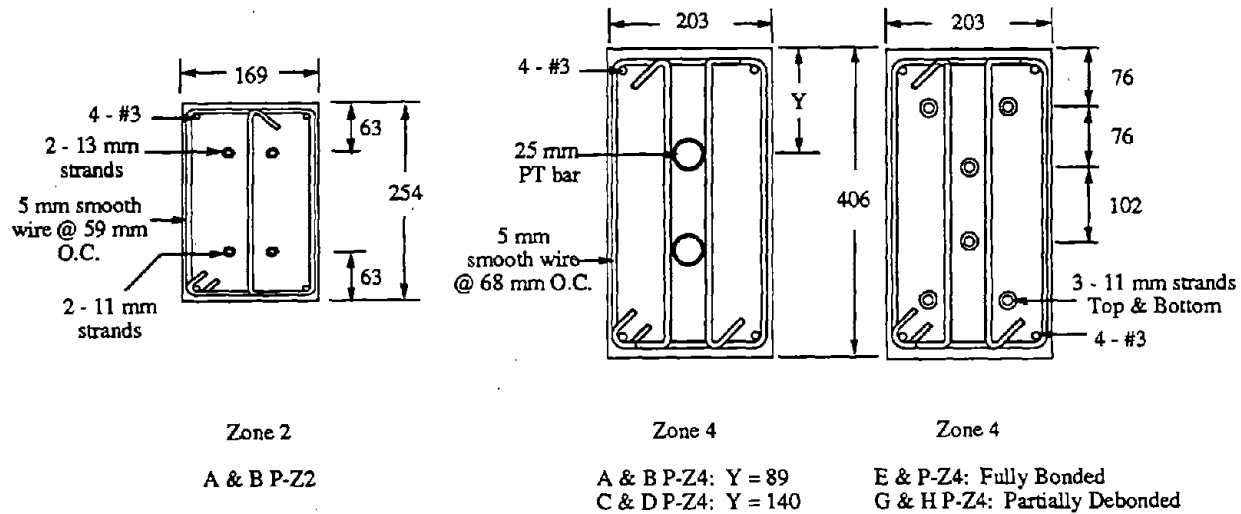


Figure 3. Model Beam Cross Sections for Precast Specimens - Phases I - III.

2.1.3 Phase II Tests

Results of the Phase I tests showed that a post-tensioned precast beam-to-column connection was a viable concept. However, the energy dissipation characteristics of the precast connections, as compared with the monolithic specimens, were poor. The objective of the Phase II tests was to improve the energy dissipation characteristics of the precast connections. One suggested method was to locate the post-tensioning bars closer to the beam center to delay the onset of yielding of the PT steel and another was the use of PT strands in lieu of PT bars as strands had a higher ultimate strength.

A total of six specimens were tested in Phase II. Four of these specimens were designed similarly to the monolithic Zone 4 specimens and two to the monolithic Zone 2 specimens. The tests of the Zone 2 precast specimens was felt necessary and useful by the advisory committee due to concerns of the possibility of an occurrence of a major earthquake in the eastern United States. Specimens, C-P-Z4 and D-P-Z4, were identical to the Phase I specimens, A-P-Z4 and B-P-Z4, with the only difference being the location of the post-tensioning bars (Fig. 3). Two other specimens, E-P-Z4 and F-P-Z4, were post-tensioned with fully bonded strands. The two precast Zone 2 specimens, A-P-Z2 and B-P-Z2, were post-tensioned with fully bonded strands. The details of the Phase II beams are given in Fig. 3.

2.1.4 Phase III Tests

A concern which arose from the Phase I and II tests was the formation of a slip zone in which the joint exhibited effectively zero stiffness upon load reversal (Figs. 21 - 22) of the precast specimens during the latter stages of the tests. This slip was felt to be caused by yielding of the PT steel. A suggested method to eliminate this slip was the use of partially bonded tendons. By using partially bonded tendons, a reduction of the tendon strains was expected and thereby, an approximate bilinear elastic behavior was predicted as shown in Fig. 4 [Priestley and Tao 1993]. As a result, Phase III specimens, G-P-Z4 and H-P-Z4 (Fig. 3), were identical to the Phase II specimens, E-P-Z4 and F-P-Z4, with the exception that the tendons in the Phase III specimens were unbonded through the column and for 381 mm on either side of the column. A total of two specimens was tested in this phase.

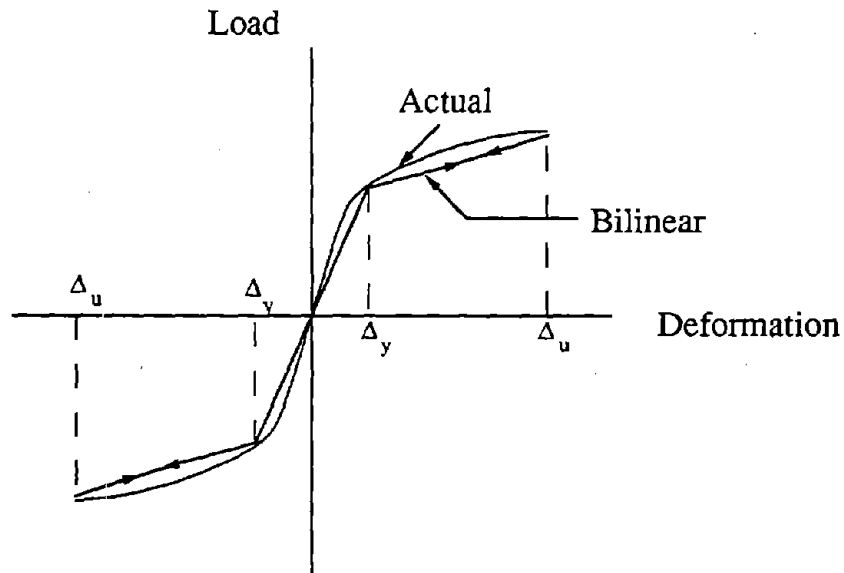


Figure 4. Predicted Bilinear Elastic Behavior for Phase III Specimens [Priestley and Tao 1993].

High compression strains were anticipated in the beam hinge region and confinement of the beam was felt to be necessary. Therefore, in the beam hinge region, interlocking spirals (2 adjacent spirals with a slight overlap) were used to confine the concrete.

A summary of all the model precast specimens is given in Table 1. The design concrete strength was 34 MPa and the steel reinforcement consisted of grade 60 ($f_y = 414$ MPa, where f_y is the yield stress) bars. The prestressing strands used were 7-wire strands, Grade

270 ($f_{pu} = 1862$ MPa, where f_{pu} is the ultimate tensile stress) meeting A416-87a [ASTM, 1988] specifications and the high-strength bars had an ultimate stress of 1033 MPa meeting A722-86 [ASTM, 1988] specifications.

Table 1. NIST Specimens^a.

Test Phase	Specimen Names	Seismic Zone	Type ^b	PT Steel		Bar dist. from extreme fiber	Length of debonded PT Steel	Mild Steel	
				Type ^c	Bond ^d			Area (mm ²)	Bond ^d
I	A-M-Z2 B-M-Z2	2	M	---	---	---	---	568	F
I	A-M-Z4 B-M-Z4	4	M	---	---	---	---	613	F
I	A-P-Z4 B-P-Z4	4	P	B	F	89 mm	---	---	---
II	A-P-Z2 B-P-Z2	2	P	S	F	63 mm	---	---	---
II	C-P-Z4 D-P-Z4	4	P	B	F	135 mm	---	---	---
II	E-P-Z4 F-P-Z4	4	P	S	F	102 mm	---	---	---
III	G-P-Z4 H-P-Z4	4	P	S	P	102 mm	1219 mm	---	---
IV A	I-P-Z4 K-P-Z4	4	P	S	F	254 mm	---	142	F
IV A	J-P-Z4	4	P	B	U	51 mm	914 mm	213	F
IV A	L-P-Z4 A	4	P	S	U	40 mm	914 mm	---	---
IV A	L-P-Z4 B	4	P	B	U	40 mm	914 mm	---	---
IV A	L-P-Z4 C	4	P	S	U	40 mm	914 mm	186	U

a Phase IV-B Parametric Specimens not included.

b M = Monolithic; P = Precast

c B = Post-tensioning bars; S = Prestressing strands

d F = Fully grouted; P = Partially grouted; U = Unbonded

Note: 25.4 mm = 1 in.

2.2 Phase IV A Tests

2.2.1 Introduction

The results of the previous NIST precast beam-column tests showed that both the connection strength and drift capacity of a precast connection matched and/or exceeded the performance of a monolithic connection. However, the energy dissipation characteristics of the precast specimens with post-tensioning alone was not comparable to that of the monolithic specimens. Therefore, the main goal of the Phase IV-A tests was to improve the energy dissipation characteristics of the precast connection through the use of energy dissipators.

The premise of the hybrid connections is that the PT steel would clamp the precast elements together and the low strength steel would dissipate the energy through yielding. The clamping force provides the necessary resistance to the applied loads through friction developed between the beam-column interface. To maintain the clamping force, it is necessary to keep the PT steel in the elastic range.

Through collaborative work with Dr. John Stanton at the University of Washington and Mr. Dave Seagren of Charles Pankow Builders, Ltd., three experimental hybrid beam-column precast connections were designed. The first design uses fully bonded mild steel located in the top and bottom of the beam with fully bonded strands in the middle of the beam. In this design, the potential of yielding of the PT steel is minimized by locating it in the middle of the beam.

A second design calls for the use of fully bonded mild steel and unbonded PT steel located at the top and bottom on the beam. As the PT steel is located at the top and bottom of the beam (the region of highest flexural strain), the delay in yielding of the PT steels is accomplished through the use of unbonded PT steel.

The third design is based on the concept of using replaceable steel. The ability to repair a structure instead of condemning it after an earthquake is economically attractive. The design calls for the use of unbonded low strength steel and PT steel located at the top and bottom of the beam. As with the second design, the strains in the PT steel are reduced by using unbonded PT steel.

The first design uses PT strands that would run the entire length of the building whereas the second and third designs use short lengths of PT steel, which is tensioned on a column-by-column basis. The advantage of the using full length PT is that it requires fewer anchorages and reduces labor.

2.2.2 Prototype Structure

The details of the Phase IV A specimens were different from those of the previous specimens because the design was supplied by a precast contractor for a prototype building under consideration. The dimensions and details were based on joint forces obtained using UBC (ICBO, 1988) seismic Zone 4 criteria for a 12-story moment resisting frame office structure with 6 x 12 bays in each direction. The center-to-center spacing of the columns was 5.49 m and the story height was 3.96 m.

The required moment capacity of the column, M_u , was 2929 kN-m ($6/5 * \text{Beam moment}$, [ICBO, 1988]) based on a nominal moment, M_n , capacity of 2440 kN-m of a 457 mm x 1219 mm beam with 4 - #11 and 3 - #10 top and bottom ($\phi = 0.9$, $f_y = 414$ MPa). This moment capacity is comparable to that for the prototype beam used in Phases I to III which was 2304 kN-m. A maximum moment of 3241 kN-m was obtained for $\phi=1$ and $f_y = 517$ MPa (1.25 factor applied to f_y). Based on a moment of 3241 kN-m, the shear force at the column face including dead load was 1557 kN. The dimensions of the prototype column were 914 mm x 914 mm with 28 - #14 longitudinal bars. The nominal capacity of the prototype column was 4419 kN-m for an axial load of 17,792 kN.

Currently, there is no accepted procedure for the design of a precast beam-column connection with mild and PT steel as proposed in this test program. Therefore, a simple computer program, B6.FOR, was developed to aid in the determination of the necessary amounts of mild steel and PT steel to meet the required moment and shear. The program is written in Lahey Fortran and runs on a personal computer. It computes the moments of an arbitrary section for imposed beam rotations. The strain in the unbonded part of the PT tendon was assumed to be equal over the entire unbonded length. The concrete compressive force was computed based on a triangular stress distribution for steel strains less than or equal to yield and on the equivalent Whitney stress block for steel strains greater than yield. More detailed information is presented in Appendix E.

The required beam moment was set at 2712 kN-m (2440 kN-m / 0.9). The factor of 1.25 applied to f_y was not used as the program uses representative stress-strain curves for the reinforcement and these curves are carried out to bar fracture which include strain hardening. The minimum required area of PT steel was based on the friction force needed to resist beam shear at the column face and was determined by:

$$\mu \times A_{ps} \times f_{ps} + 0.4 A_s \times f_y \geq 1557 \text{ kN} \quad (2-1)$$

where:

$$\begin{aligned} \mu &= 0.6 \lambda && \text{ACI 11.7.4.3 [ACI, 1989]} \\ \lambda &= 1.0 \text{ for normal weight concrete.} \\ A_{ps} &= \text{Area of PT steel.} \\ f_{ps} &= \text{Nominal stress of PT steel.} \end{aligned}$$

A_s = Area of mild steel.
 f_y = Yield stress of mild steel.

The value of μ used was conservative as the concrete surfaces on the beam and column were intentionally roughened and therefore, a value of μ equal to 1 would have been permissible by ACI criteria. The PT steel area necessary to provide the design moment strength of the beam generally exceeds the minimum value required by Eq. (2-1) above.

The beams in the Phase IV A specimens had "dogbones" - over and under expanded flanges measuring 51 mm (I-P-Z4 and K-P-Z4) and 68 mm (J-P-Z4 and L-P-Z4 A-C) high and 305 mm long (model dimensions) - which made the beams deeper at the column faces. They are shown in Fig. 5. The mild steel -- used for energy dissipation -- in the Phase IV specimens extended from one end of the beam dogbone flanges through the column to the end of the second beam dogbone. A horizontal failure plane occurring across the base of dogbone was a possibility due to the high shearing stress. Therefore, additional transverse reinforcement was included in the dogbone regions to prevent this mode of failure. The design of the reinforcement was based on that for corbels. In addition to the increased transverse reinforcement in specimen J-P-Z4, steel angles were located at the ends of the dogbones, as shown in Fig.7. These angles were considered necessary to provide confinement of the dogbone region as the PT steel in specimens J-P-Z4 and L-P-Z4 was also located in this section. Shear studs were welded to the angles farthest from the column face to prevent rotation of the angles. Also, #3 bars, 178 mm long, were welded to the angles closest to the column face to anchor the angles.

2.2.3 I-P-Z4 and K-P-Z4 Specimen Details

Specimens I-P-Z4 and K-P-Z4 were constructed based on the first design concept: fully bonded low strength steel located in the dogbones with fully bonded PT steel in the middle of the beam. The fully bonded PT provided resistance to corrosion and to progressive collapse. The central location of the PT reduced the strains in the PT steel.

The low strength steel in specimen I-P-Z4 consisted of two #3, grade 40 ($f_y = 276$ MPa) reinforcing bars. Grade 40 ($f_y = 276$ MPa) bars were used instead of grade 60 ($f_y = 414$ MPa) for reasons of enhanced ductility. In practice their yield strengths were much higher than the specified 276 MPa.

Specimen K-P-Z4 was identical to specimen I-P-Z4 with the only difference being the use of grade 60 ($f_y = 414$ MPa) reinforcing bars instead of grade 40 ($f_y = 276$ MPa). Specimen K-P-Z4 was a retest of specimen I-P-Z4. This was done because of premature failure of I-P-Z4 due to bond failure of the mild steel as described in Section 3.1. The fully bonded prestressing tendons, 3 - 13 mm diameter 7-wire strands, in specimens I-P-Z4 and K-P-Z4 were located in the middle of the beam so that the tendons would experience low strains and would therefore not exhibit loss of stiffness due to yielding as observed in the earlier

specimens. The initial axial beam prestress was 5.0 MPa for specimens I-P-Z4 and K-P-Z4 (Section A-A, Fig. 5). The initial stress in the strands after losses was approximately $0.65 f_{pu}$.

All dimensions in mm
25.4 mm = 1 in.

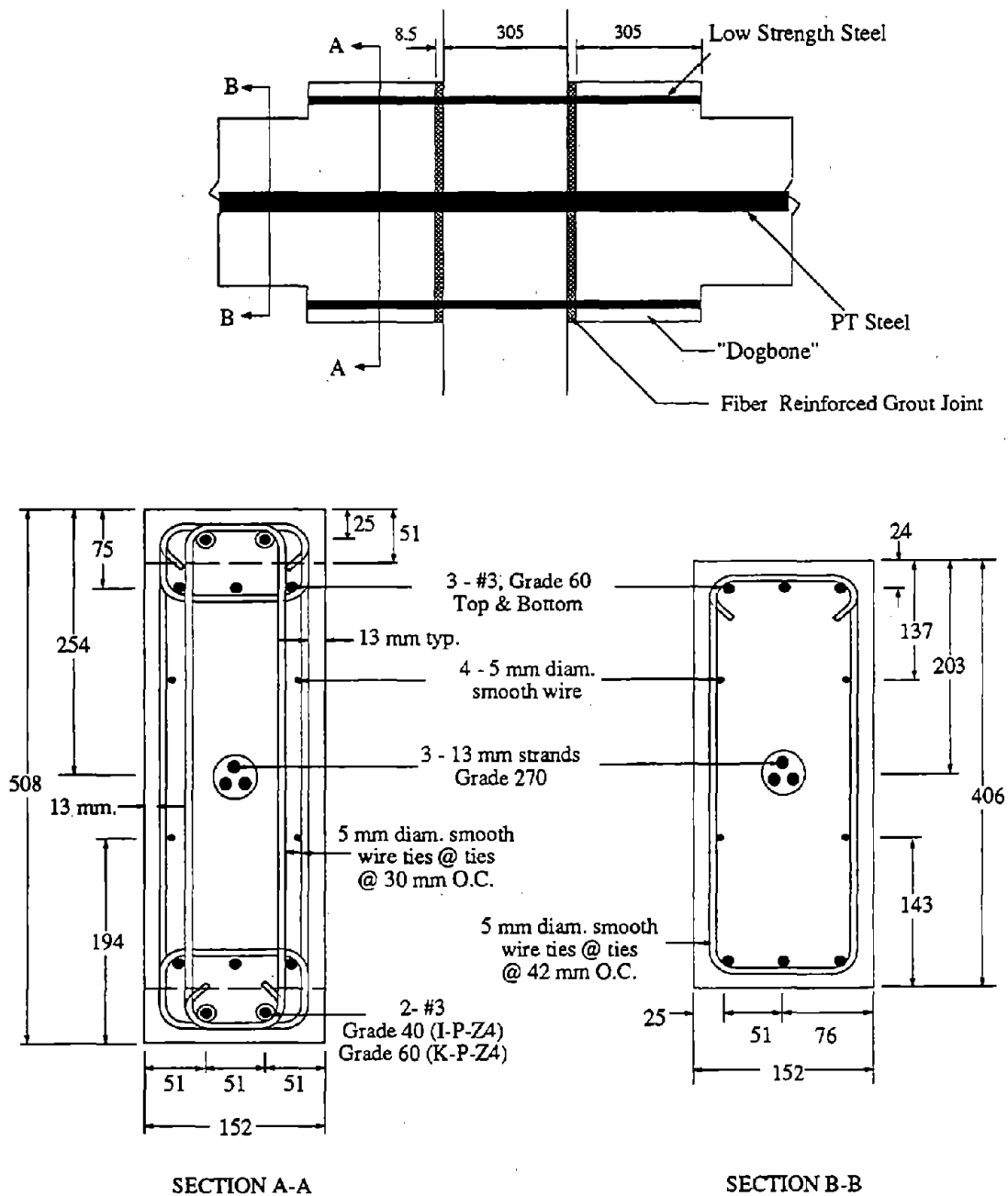


Figure 5. Model Beam Cross Sections for Phase IV A Specimens I-P-Z4 & K-P-Z4.

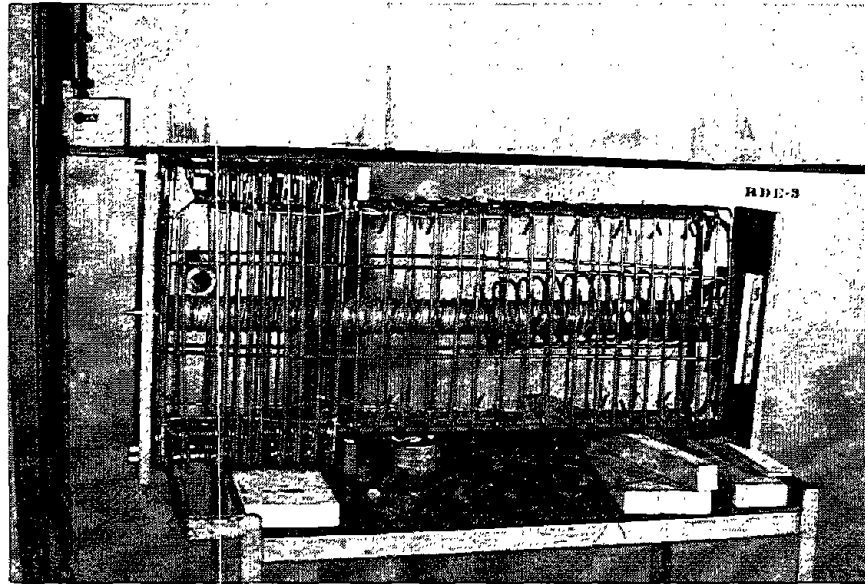


Figure 6. Steel cage for specimen I-P-Z4.

2.2.5 J-P-Z4 Specimen Details

Specimen J-P-Z4 was constructed based on the second design: unbonded PT and fully bonded low strength steels located in the dogbones. This design allows for construction to proceed on column by column basis.

The high strength bars were 16 mm diameter Dywidag bars machined as shown in Fig. B18 (Appendix B) to obtain the required area. The mild steel in this specimen was comprised of three #3 grade 60 ($f_y = 414$ MPa) bars. The argument for using grade 60 ($f_y = 414$ MPa) instead of grade 40 ($f_y = 276$ MPa) is the greater availability of grade 60 ($f_y = 414$ MPa) bars and that the real yield stress of a grade 40 ($f_y = 276$ MPa) bar is often closer to 414 MPa. The initial axial beam prestress was 3.2 MPa for specimen J-P-Z4. The initial stress in the high strength bars after losses was approximately $0.65 f_{pu}$.

All dimensions in mm
25.4 mm = 1 in.

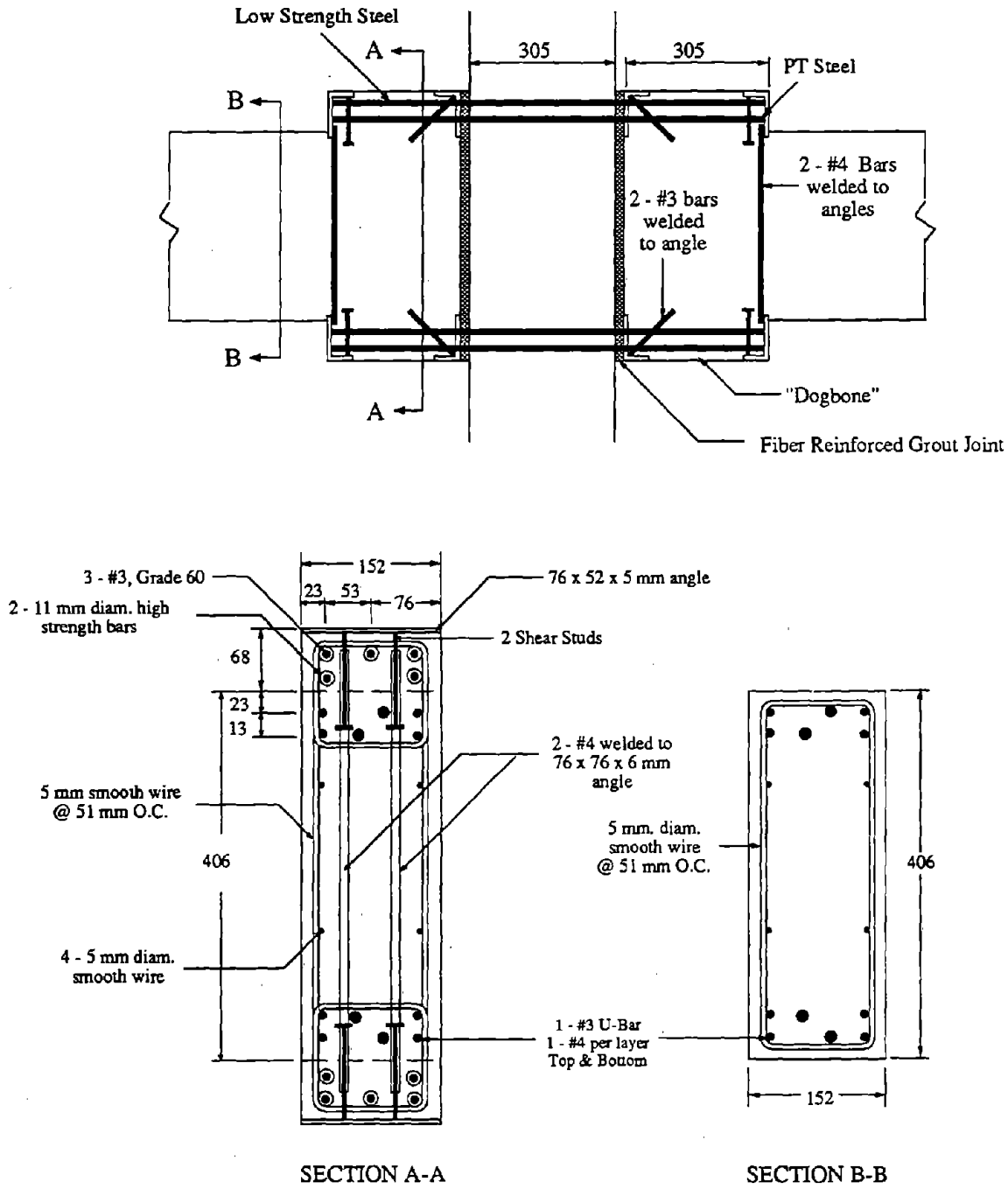


Figure 7. Model Beam Cross Sections for Phase IV A Specimen J-P-Z4.

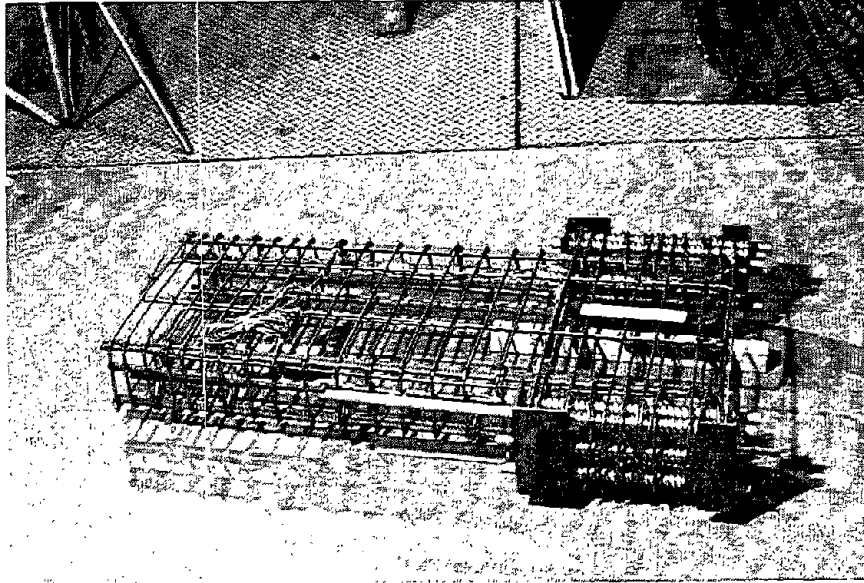


Figure 8. Steel Cage for Specimen J-P-Z4.

2.2.6 L-P-Z4 Specimen Details

Specimen L-P-Z4 was constructed based on the third design: A replaceable system with unbonded PT and low strength steels in the dogbones. Again, the design allows for the construction to proceed on a column by column basis. In order for the low strength steel to carry both tensile and compressive loads, the steel has to be anchored to the beam as shown in Fig. 10. This detail is complex and the cost of this detail may outweigh the economical benefits of repairing a damaged structure.

Specimens L-P-Z4 A - C were the same specimen tested using three variations of mild and PT steels. The ability to replace both the mild and PT steels made the additional two tests possible. Specimen L-P-Z4 A was post-tensioned with 2 - 11 mm diameter 7-wire strands, grade 270 (1862 MPa) top and bottom and contained no mild steel. After the testing of L-P-Z4 A, the specimen was reassembled as L-P-Z4 B with 11 mm diameter Dywidag bars ($f_{pu} = 1034$ MPa) replacing the strands with no mild steel included. The moment capacity of the section post-tensioned with 2 - 10 mm diameter strands ($f_{pu} = 1862$ MPa) is comparable to that of a section post-tensioned with 2 - 11 mm PT bars ($f_{pu} = 1034$ MPa). However, due to the availability of the 11 mm diameter strands, the larger diameter strands were used instead. From these two tests, it was decided that the use strands instead of bars for the third specimen, L-P-Z4 C, was the better choice as the bars yielded at a lower drift level than the strands.

For the third specimen (LPZ4-C), tubing made of 1026 steel (ASTM 513-91a, ASTM, 1992) was used as the mild steel and the PT steel was located concentrically inside the tubing as shown in Figs 9-11. Two - 10 mm diameter 7-wire strands, grade 270 top and bottom, were used to post-tension this specimen. The tubing was threaded at the ends and the cross section between the threaded ends was reduced to ensure that yielding occurred away from the threaded ends. This was necessary to assure easy removal of the tubes. The tubing was machined so that the reduced section had an outer diameter of 20 mm and an inner diameter of 17 mm (Fig. B17). This type of tubing with upset threaded ends is readily available commercially as J-55 tubing and is commonly used in the oil industry. As the J-55 tubing was not available in the required size, 1026 tubing was used instead in the model specimen L-P-Z4 C. The selection of 1026 steel tubing was based on the need to duplicate the stress-strain curve for the J-55 tubing which would be used in a prototype specimen.

During the assembly of the specimen, the tube was threaded into a coupler embedded into the middle of the column. At the end of the dogbone it was locked into place by two nuts as shown in Fig. 10. The use of two nuts allowed the tube to carry both tensile and compressive forces. The PT steel for specimen L-P-Z4 A-C was stressed to an initial value of $0.4 f_{py}$. The lower initial stress was used to increase the story drift at yield of the PT steel.

In the original design of specimen L-P-Z4, six reinforcing bars were to be welded to the plates located at the ends of the dogbones. This was necessary to allow the mild steel tubes to carry tensile forces. The reinforcing bars were to transfer the force from the front plate to the back angle thereby anchoring the plate to the dogbone when the tube was subjected to compression. However, a T-section was used in the final 1/3-scale model due to congestion in the block-out which would have made installation of the nuts and ring impossible. The use of the T-section introduced a potential horizontal failure plane between the flange of the T-section and the beam. This is so because the resistance to shear at the interface between the steel and concrete is much less than if the interface was monolithically cast concrete. To reduce the chances of this type of failure, 4 - #4 bars 178 mm long were welded to the top of the flange to act as shear studs. Two of these bars were bent at 90 degrees while the other two were straight.

All dimensions in mm
25.4 mm = 1 in.

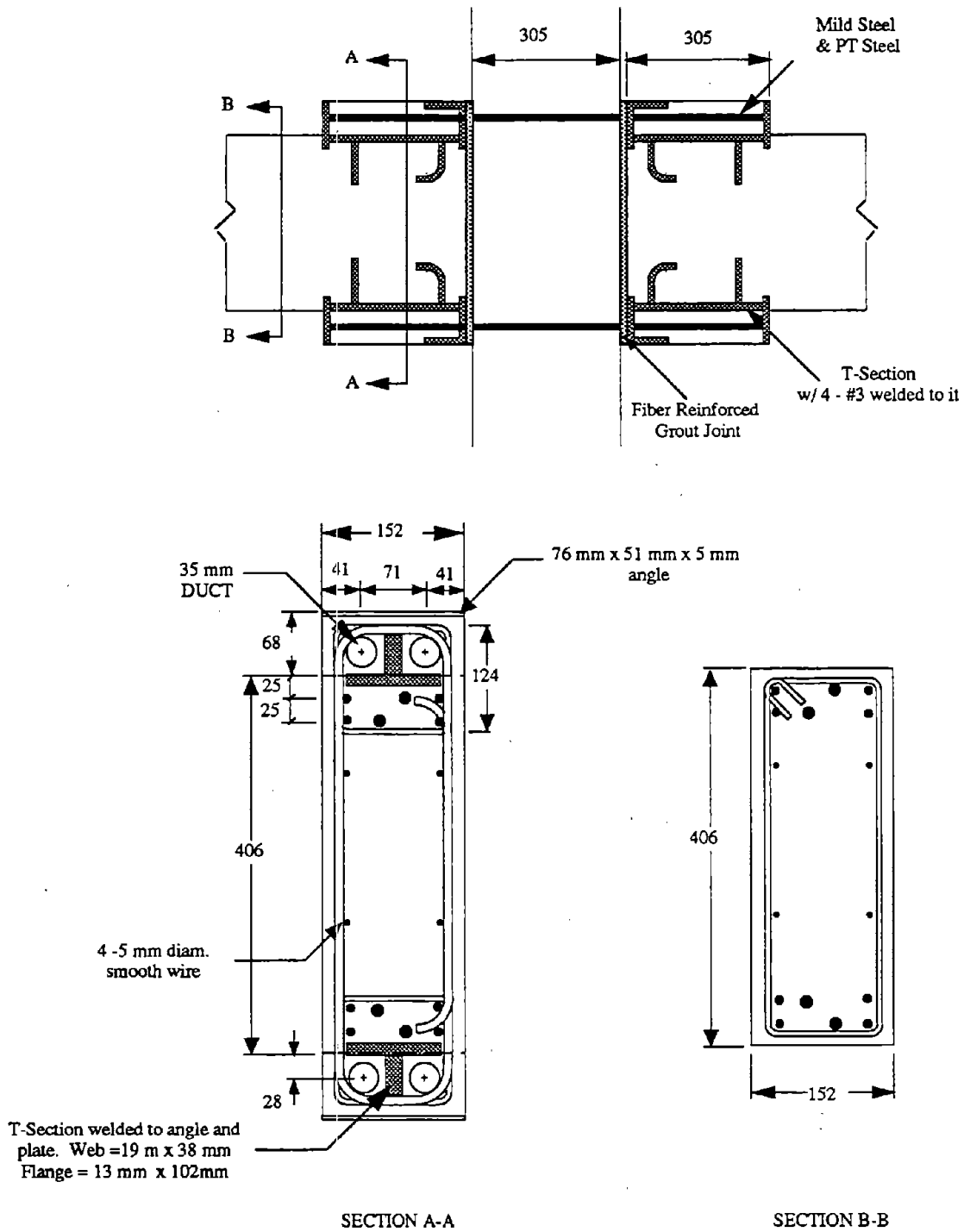


Figure 9. Model Beam Cross Sections for Phase IV A Specimens L-P-Z4 A-C.

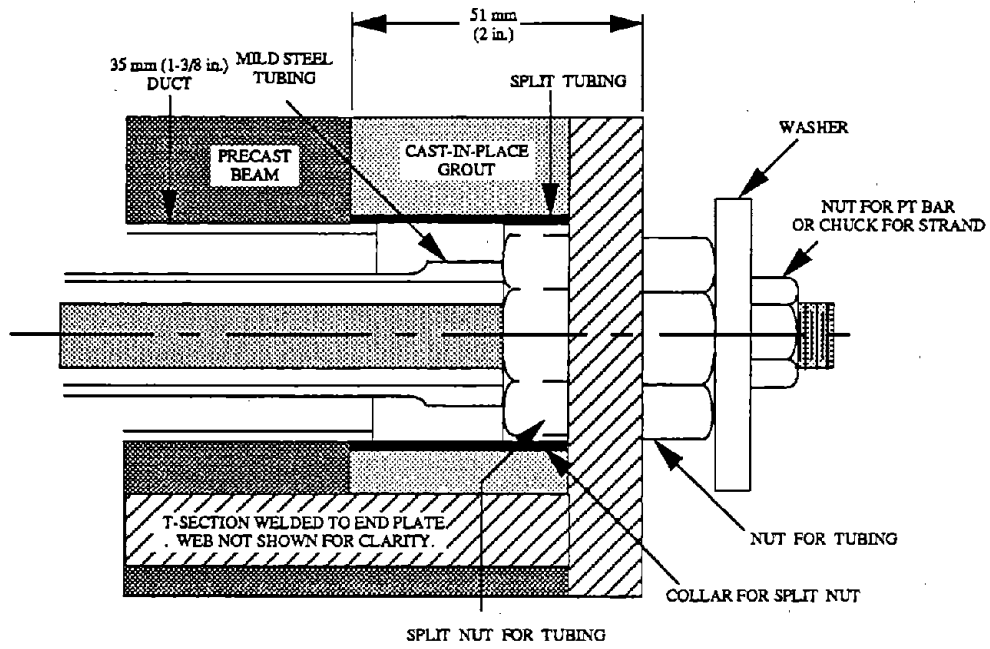


Figure 10. Details of the Block-out in Specimens L-P-Z4 C.

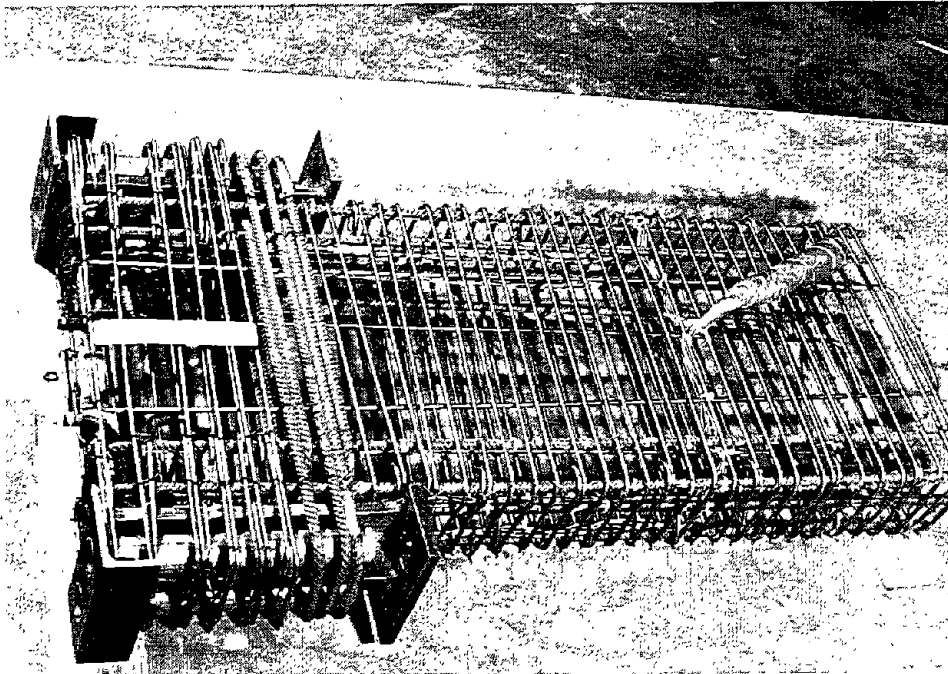


Figure 11. Steel Cage for Specimen L-P-Z4.

2.3 Grouting Process of Phase IV A Specimens

The ducts used in the specimens for the mild steel were 13 mm ID electrical conduit (sheathing for BX cable). Corrugated ducts regularly used in concrete construction were not available in the required size. Due to the presence of strain gages on the mild steel, which increased the diameter of the bars, the ducts in the beams and columns had to be removed to allow the bars to pass through the ducts. This was possible as the conduit could be unwound and removed.

The grout used in the construction joint between the precast beams and columns for all specimens was fiber reinforced. The joint widths in the Phases I - III specimens were 25 mm and the fibers were 19 mm straight steel fibers. The construction joint widths in Phase IV specimens were 8 mm. Construction joint width was reduced as a prototype joint width of 25 mm was felt to be more typical. Due to the small joint width and a desire to prevent corrosion of the fibers, nylon fibers, 12 mm long, were used. The fibers used were Caprolan-RC fibers with a diameter of 584 μm and a specific density of 1.16. The amount of nylon fibers used was 8.7 kg/m^3 of concrete. The strength of the nylon fiber reinforced grout was shown to be comparable to the grout with steel fibers, and the workability of the nylon reinforced grout was better.

A neat cement grout with a water-cement ratio of 0.35 was used to grout the bars in specimen I-P-Z4. Celbex 208, a gelling agent and a dispersant, was added to improve the pumpability of the grout. However, this specimen experienced premature bond failure of the mild steel as discussed in Section 3.1.1. Although the neat cement grout was not the cause of the failure, it was felt that the use of a commercially available grout would be more representative of field conditions. Therefore, a cable grout (Masterflow 816 cable grout) containing fine sand was used to grout the bars and strands for specimens J-P-Z4 through L-P-Z4.

The concrete and grout strengths and the stress-strain curves for the different steels are given in Appendix C. Drawings for the specimens used to construct the Phase IV specimens are given in Appendix B.

2.4 Discussion of Specimen Design

The descriptions in the previous sections show that the specimens in the four different phases were intended to perform in somewhat different ways, and this should be kept in mind when the results are evaluated.

The monolithic specimens in Phase I were conventionally reinforced concrete specimens containing only grade 60 ($f_y = 414 \text{ MPa}$) reinforcing bars. Therefore, all the steel was intended to yield so that these specimens were expected to exhibit significant energy

dissipation. However, the absence of post-tensioning meant that no clamping force existed across the interface and the specimen did not return to zero displacement on unloading.

The precast specimens in Phases I through III contained only post-tensioning steel through the joint. This provided the necessary clamping force but only if the post-tensioning did not undergo extensive yield. Thus, with only one type of reinforcing, maintenance of the clamping force is possible at the expense of energy dissipation capacity and vice versa. Whereas the traditional objective is to maximize energy dissipation, some recent studies [Priestley and Tao, 1993] suggest that global displacements may in fact be controlled very nearly as well by the dissipation of only some energy provided that the other aspects of the behavior such as joint and member degradation and drift are controlled. Some energy is dissipated by crushing of the concrete which is relatively undesirable because of the need for subsequent repairs and some by debonding of the steel. However, these sources do not dissipate much energy.

In the Phase III specimens, the PT steel was debonded through the column and a certain distance on either side of the column to reduce the amount of yielding. By doing this, the reduction in the clamping force is minimized but so too is the potential energy dissipation.

The Phase IV specimens were intended to take advantage of both clamping force action and energy dissipation. The post-tensioned steel was either unbonded or located in the center of the beam to avoid yielding and thereby maintain the clamping force. Energy dissipation was to be attained by yielding of the mild steel. The use of these two different types of reinforcement allows the two objectives (maintenance of the clamping force and energy dissipation) to be met simultaneously.

2.5 Test Procedure

The boundary conditions and basic loading history (except for specimens L-P-Z4 A-C) are shown in Fig. 12. Boundary conditions for the test specimens were as follows: pinned at the column bottom and roller supported at the column top and beam ends. Slight deviations from this basic load history were used in the actual tests: a third cycle at a particular displacement ductility was added if a significant loss in the peak lateral load occurred in the second cycle.

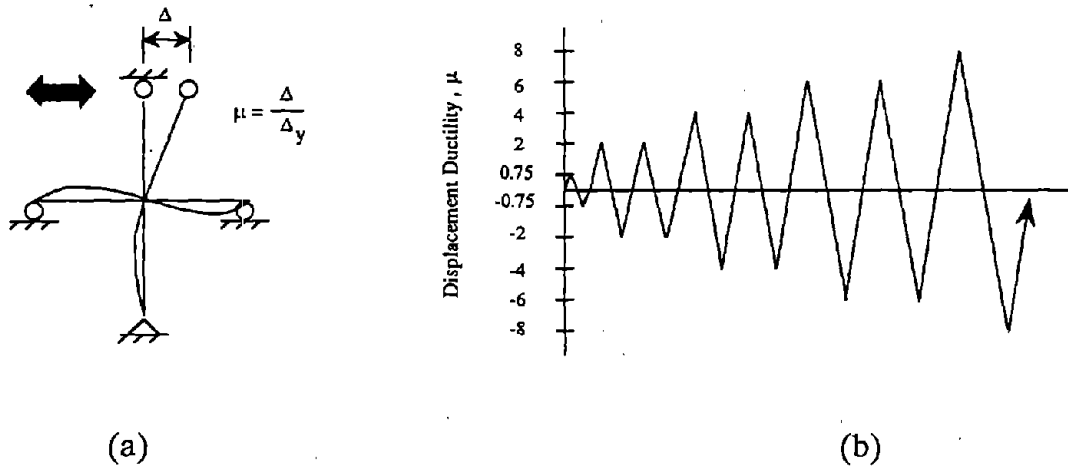


Figure 12. Boundary Conditions and Loading History.

The load history shown in Fig. 12b is similar to that used by other researchers [French, 1989] for cyclic testing and was chosen for the NIST tests so that comparisons could be made with these other tests. Failure was considered to have occurred when the lateral load during a cycle dropped below 80% of the maximum load that was achieved in the first cycle at $2 \Delta_y$. All columns were subjected to an axial load. However, the axial load imposed on the Phases I - III specimens was equal to $0.1 f'_c A_g$ while the axial load for the Phase IV specimens was approximately equal to $0.4 f'_c A_g$. The higher axial load was specified in the design provided by the precast contractor.

The load history used for specimens L-P-Z4 A-C (Fig. 13.) was based on story drift and is the one used in the PREcast Seismic Structural Systems (PRESSSS) Program [Priestley, 1992]. The change in the loading history was made so that comparisons with other PRESSSS specimens could be made more easily. The following drift levels were used: 0.001, 0.0015, 0.002, 0.0025, 0.0035, 0.005, 0.0075, 0.01, 0.015, 0.02, 0.025, 0.03. Three cycles were completed at each drift level followed by an intermediate elastic cycle. In the elastic cycle, the specimen was loaded to approximately 30% of the peak load in the preceding three cycles. This load history will be used in Phase IV B but with the drift level beginning at 0.002 as the cycles at lower drift levels are not necessary for ductile systems. The specimen is considered to have failed if the lateral load at the column top falls below 80% of the maximum load achieved by the specimen. The testing of specimens L-P-Z4 A & B was stopped at a drift level of 0.015 to prevent significant damage to the specimens, since some components were needed for subsequent testing.

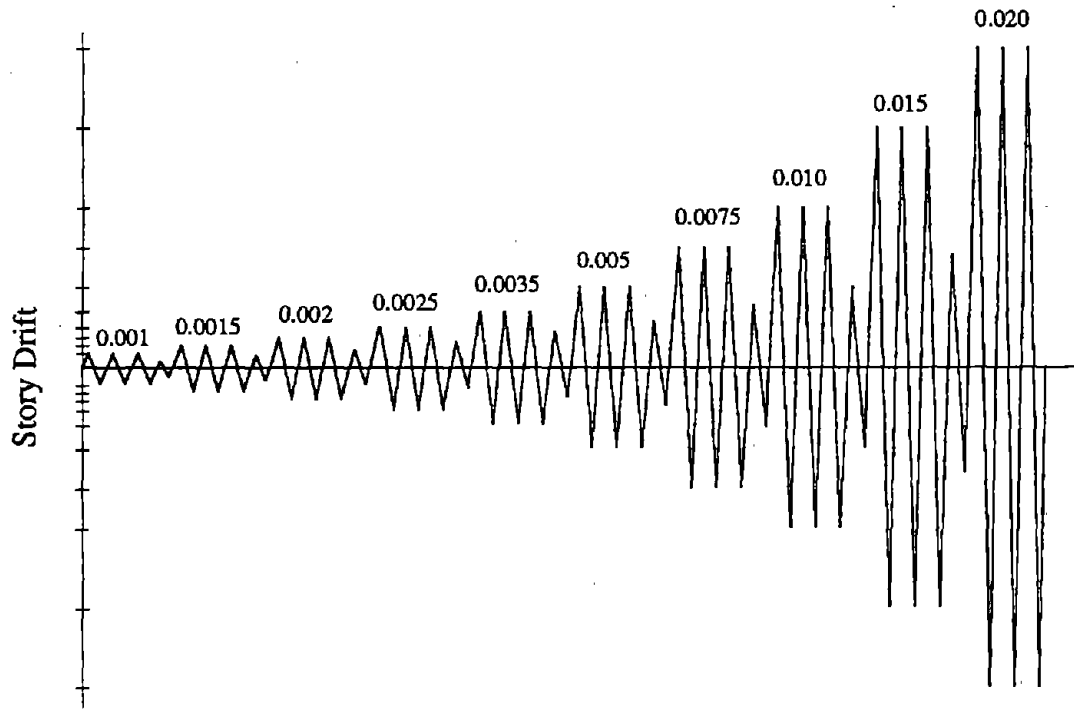


Figure 13. Load History for Specimens L-P-Z4 A-C.

Concentrated loads simulating gravity loads on the beams were applied to all Phase IV specimens. A load of approximately 20 kN was applied to each beam at approximately 89 mm from the column face. The load was equivalent to a uniform dead load of 5.3 kPa and live load of 2.4 kPa. The loads on the beams were maintained constant throughout the tests.

3.0 DISCUSSION OF TEST RESULTS

3.1 Failure Mode

3.1.1 Phase I-III Specimens

A brief description of the failure modes of the previous specimens is provided for purposes of comparison. The monolithic Zone 4 specimens failed due to beam hinging and deterioration. The flexural reinforcement did not fracture in the monolithic specimens.

All the Phase I-III precast specimens that were tested to failure exhibited the same failure mode. The PT steel yielded and the concrete crushed, which resulted in a gap opening at the construction joint between the beam and column.

The partially bonded precast specimen tests were stopped before failure because no strength degradation had occurred in these specimens by a story drift of 6%. Fine cracks developed in the column joint, but otherwise no significant damage occurred in this region. The width of the opening, at a given story drift, at the beam-column joint increased as the post-tensioning steel was placed closer to the beam centroid. The fiber reinforced grout in the joints held together very well throughout the tests.

Unlike the monolithic Zone 2 specimens which failed predominantly in shear in the column joint region, the precast Zone 2 specimens did not experience severe joint distress. The failures of the monolithic Zone 2 specimens resulted from insufficient joint reinforcement in these specimens despite being designed in accordance with UBC requirements [ICBO, 1985]. However, the drift levels that these specimens were subjected are unlikely to occur in a region classified as Zone 2.

3.1.2 Phase IV A: Fully Bonded Mild and PT Steels [I-P-Z4 & K-P-Z4]

Specimen I-P-Z4 failed prematurely due to bond failure of the mild steel at a story drift of approximately 1.7%. The bond failure occurred only in the dogbone part of the beams.

The development length provided (305 mm, the length of the dogbone) was considered to be adequate to fully develop the #3 bars in accordance with UBC 2612 (c) and (d) [UBC, 1988]. However, the bars were bonded by grouting into a rough duct rather than by being cast into concrete, as assumed in UBC, so it was considered of interest to obtain the strain profile along the mild steel. To accomplish this, a total of 7 strain gages were installed on the mild steel bars over a length of 914 mm. In the dogbone regions, 6 gages were installed on the mild steel bars (3 per 305 mm length), and one gage was located in the column at the column centerline. Failure of the specimen was attributed to the presence of the strain gages and their coatings on the mild steel which eliminated approximately 40% of the available bond length and divided the remaining bond length into several short sections.

This was confirmed by subsequent pullout tests with identical ducts, grout, and mild steel bars. As a result, the mild steel bars in the other Phase IV specimens were not instrumented.

Figure 14 shows specimen I-P-Z4 at failure at 2.7% story drift. As seen in Fig. 14, the specimen was not severely cracked, but crushing of the beam corners at the column face did occur. Due to the lack of significant damage to the column, the column was salvaged and used in specimen K-P-Z4; new beams were constructed. As a result of the bond failure, the bars slid in and out of the ducts as the specimen was displaced. Figure 15 shows the mild steel bar extending out of the duct at a story drift of 4.6%.

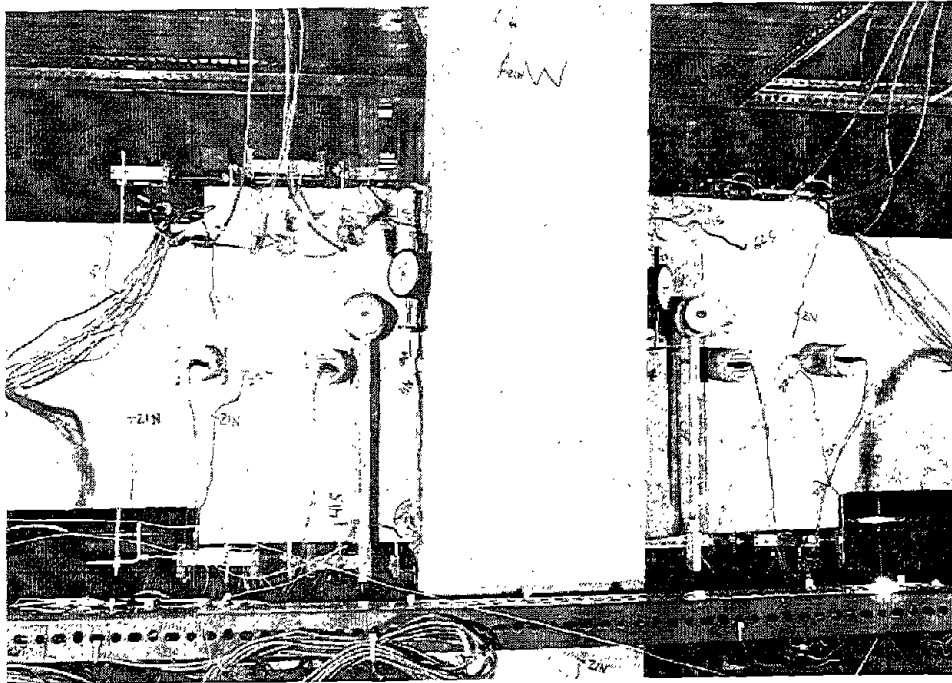


Figure 14. Specimen I-P-Z4 at Failure - 2.7% Story Drift.

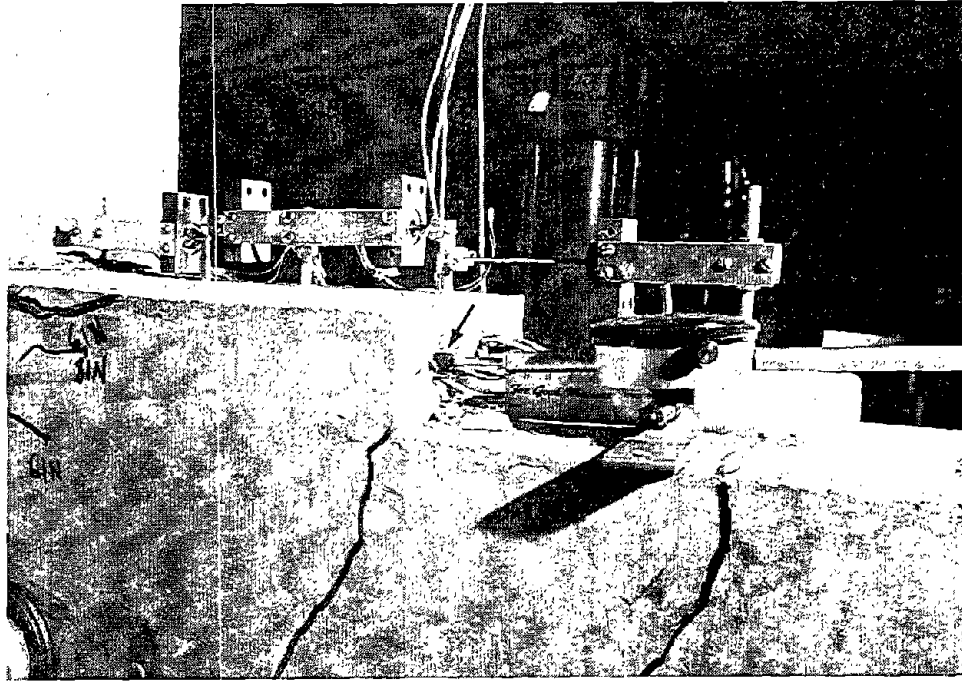


Figure 15. Mild Steel Bars Sliding Out of Duct at 4.6% Drift - I-P-Z4.

Specimen K-P-Z4, the replacement specimen, failed due to fracture of the mild steel. Figure 16 shows specimen K-P-Z4 at failure at a story drift of 3.1%. This failure mode differed from that for the monolithic Zone 4 specimens which was plastic hinging of the beams with no bar fracture. This is likely a result of greater mild steel strains in the precast specimen due to concentration of the beam rotation at the column face whereas the beam rotation in the monolithic specimen was distributed over the plastic hinge length.

The column joint region in specimen K-P-Z4 (Fig. 16) sustained more cracking than did the column joint region in specimen I-P-Z4 (Fig. 14). This is likely due to the debonding of the mild steel bars in specimen I-P-Z4 which reduced the tension stress in this region.

Crushing of the beam corners occurred at a drift level of approximately 0.9%. The shape of the hysteresis curves (Fig. 27) indicates that the mild steel bars were close to yield or began to yield at this drift level. At a story drift of approximately 2.0%, the concrete around the mild steel bars began to form a "pullout cone" and to pull out from the column. All four #3 bars fractured in one beam with no bar fracture occurring in the other beam. The first bar fracture occurred at 3.0% story drift with the subsequent three bar fractures occurring at story drifts of 3.9%, 4.5%, and 5.0%, respectively. Similar to the previous precast specimens, this specimen experienced extensive concrete crushing at the beam corners next to the joint. Significant spalling of the column concrete also occurred around the mild steel bars. The width of the joint opening at failure (3.1% story drift) was approximately 11 mm.

At the completion of the test, no vertical slip of the beams or bond failure of the mild steel was observed. Also, the beam crack widths were less than 1 mm.

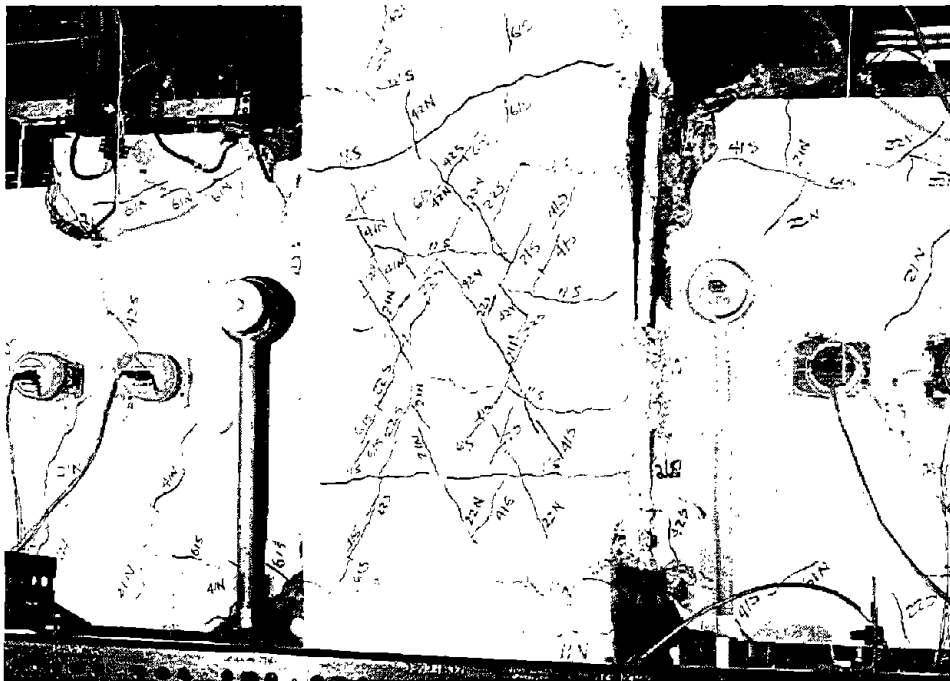


Figure 16. Specimen K-P-Z4 at failure - story drift = 3.1%.

3.1.3 Phase IV A: Bonded Mild Steel and Unbonded PT Steel [J-P-Z4]

Similar to specimen K-P-Z4, failure of specimen J-P-Z4 was caused by fracture of the mild steel bars. Figure 17 shows the specimen at failure at a story drift of 3.6%. A total of 6 bar fractures occurred with the first and second occurring at 3% story drift. The other 4 bar fractures occurred at a story drift of 3.6%. Identification as to which bar fractured when was not possible due to obstruction of the fracture location by the surrounding concrete.

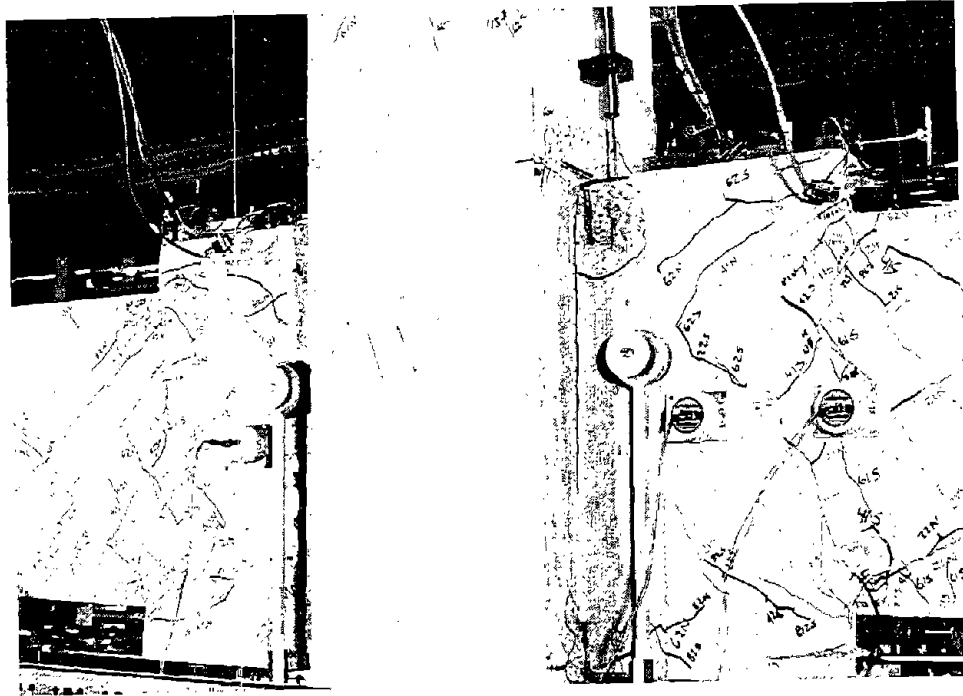


Figure 17. Specimen J-P-Z4 at failure - story drift = 3.6%.

Crushing of the beams at the corners initiated at approximately 1.0% story drift. The corners of the beams in specimen J-P-Z4 did not experience as much spalling as those in specimen K-P-Z4 due to the presence of the angles located at the ends of the dogbones in specimen J-P-Z4. Pullout of the concrete in the column around the mild steel bars began at about 2.0% story drift; there was no corresponding pullout cone in the beam, again due to the presence of the angles. At the conclusion of the test, these regions in the column had significant spalling.

The shape of the hysteresis curves (Fig. 26) indicates that the mild steel bars yielded at approximately 1% story drift. Readings from the load cells indicated that one of the PT bars yielded at 1.7% story drift and that while the other three PT bars were close to yielding, they did not yield.

The beams in specimen J-P-Z4 sustained more extensive shear cracking than did those of specimens I-P-Z4 and K-P-Z4. Several points are worth noting when comparing the specimen behaviors.

First, the absence of PT in the main part of the beam of J-P-Z4 lowered its total shear resistance and the load at which shear cracking started. The other two specimens contained PT in the beam.

Second, the area of shear reinforcement for this specimen was 20% less than for specimens I-P-Z4 and K-P-Z4. This was unintentional and was a result of their being designed by different agencies.

Third, the shear reinforcement was designed in accordance with UBC seismic provisions (ICBO, 1988), which are based on the largest shear force that could occur given the beam flexural strengths at its ends. The real stress in the mild steel flexural reinforcement at incipient fracture was higher than the $1.25 f_y$ anticipated by UBC, but the stress in the PT was lower than this value. The net result was that the real shear force was slightly higher than that allowed for in design.

Fourth, the shear strength was just sufficient, but the shear cracks were wide enough (about 2 mm) to have required extensive repair, had this been a real structure. Since one possible philosophy for the precast system, which would render it superior to an otherwise comparable monolithic system, is to concentrate the damage in the connection steel and thereby avoid potential costs of concrete repair, extensive shear cracking would be unacceptable. Thus there is a case for designing shear reinforcement not only for strength but also for crack control.

Finally, the specimen stirrups were made from smooth wire, which derives its anchorage largely from the bends around the main bars. Therefore the vertical legs probably slip more than their prototypical counterparts, and the specimen crack widths were probably greater than those to be expected in the field. This is true of the shear cracks in all the model specimens.

3.1.4 Phase IV A: Unbonded Mild and PT Steels (Replaceable System) [L-P-Z4, A, B, & C]

Specimens L-P-Z4 A & B were not tested to failure. These specimens had PT steel located at the top and bottom of the beams with no mild steel. The purpose was to determine which PT steel would behave best before testing the joint in its intended configuration of combined mild and PT steel. The specimens sustained fine shear cracks in the beams and very minimal crushing of the beam at the column face through a story drift of 1.5%. However, at a drift of 1.5%, the PT bars yielded in specimen L-P-Z4 B. Other than a few very minor cracks, the column in both tests did not experience any damage. At the end of

the test, the strands in specimen L-P-Z4 A had lost approximately 30% of their initial force while the bars in specimen L-P-Z4 B lost approximately 80% of their initial force. The reduction in force in the strands was likely due to the re-seating of the chucks as the strands were subjected to higher forces during the test than at seating and also to any crushing that occurred in the beams. The 30% force loss corresponds to a total change in length of only 1 mm. In a full scale prototype the change in length would still be the same, so the changes in strain, stress, and force would be significantly smaller. The force reduction in the PT bars was a result of the yielding of these bars and of crushing of the beams.

Failure of specimen L-P-Z4 C resulted from shear cracks that formed at the interface between the flange of the T-section and the beam in the dogbone region. Despite the bars welded to the T-section (Fig. 9) and the heavy shear reinforcement (Fig. 19) significant slip occurred along the failure plane before the required resistance developed. These cracks, approximately 3 mm in width, turned vertical at the column face and formed a sideways "U" shaped failure plane as shown in Figs. 18 and 19. Figures 18 and 19 show the same beam but the cracks on the face shown in Fig. 18 were not highlighted while the cracks on the face shown in Fig. 19 were highlighted for increased visibility. The specimen failed at 2% story drift. At this point, the vertical cracks that began as shear cracks at the T-section interface were approximately 4-5 mm wide. This undesirable mode of failure would likely not occur in the prototype specimen as reinforcing bars would be used instead of the T-section. As discussed in Section 2.2, the presence of the T-section introduced a potential failure plane between the T-section and the beam.

The mild steel tubes in Specimen L-P-Z4 C yielded at approximately 0.75% story drift as indicated by readings from strain gages and by the shape of the hysteresis curves (Fig. 30). The predicted story drift at yield due to deformation of the joint system alone is approximately 0.6%, suggesting that the additional 0.15% was attributable to beam and column deformations and column joint shear deformations. Beam crushing and spalling occurred at a story drift of 1.5%. Splitting cracks also formed at the bottom of the dogbones at this drift level. A maximum force equal to $0.75 f_{py}$ was observed in one of the PT strands at 2% story drift. Throughout the three tests, the column sustained only very minimal damage.

Due to the extent of the shear cracks observed in the beams of specimen J-P-Z4, the transverse reinforcement in specimen L-P-Z4 was increased by 100%. However, this increase in the amount of transverse reinforcement did not significantly reduce the amount of shear cracks in specimen L-P-Z4. This is not surprising because all the additional strength came from reinforcement, but the concrete must crack before the steel strains can reach yield.

Comparison of the performance of specimen K-P-Z4 (central PT) with that of specimen J-P-Z4 and L-P-Z4 (PT top and bottom in dogbone) indicates that the presence of a post-tensioning force throughout the entire beam is more effective in reducing shear cracking in the beams than an increased amount of transverse reinforcement.

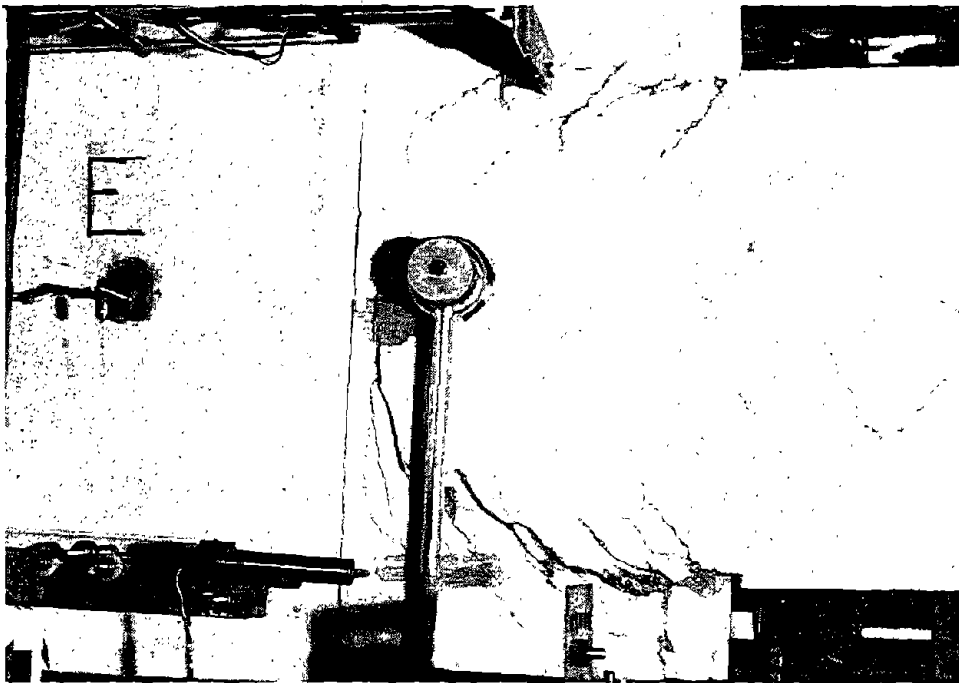


Figure 18. Specimen L-P-Z4 C at story drift of 2%.

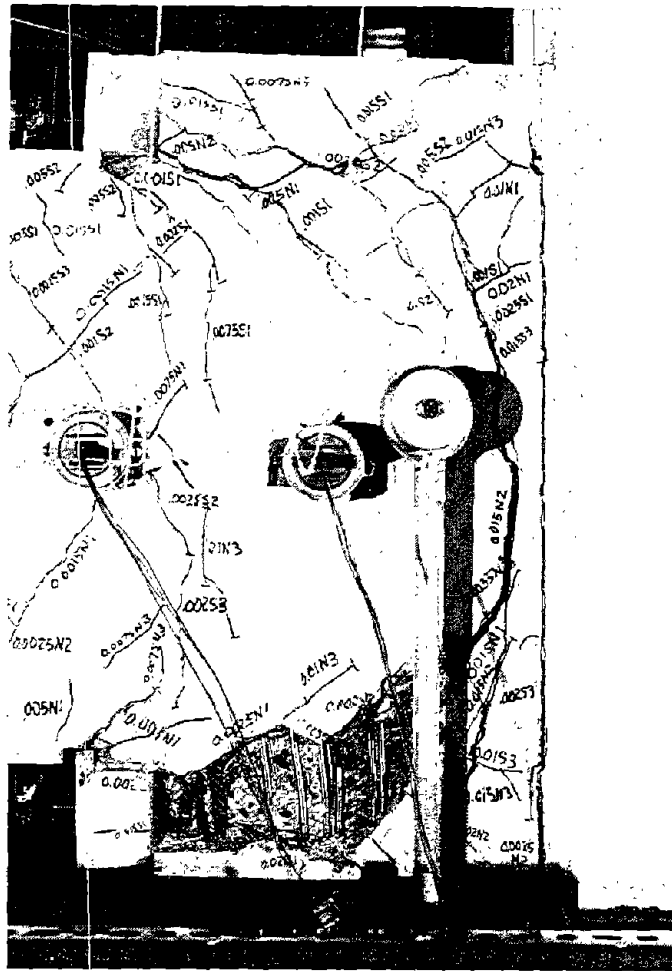


Figure 19. Specimen L-P-Z4 C at story drift of 2%.

3.2 Story Drift

The experimental story drifts at failure are given in Table 2. An attempt was made to predict the story drifts using program B6.FOR [Appendix E], but the drifts are not included in Table 2 for the following reasons:

1. The program imposes a rotation on the beam at the column face and computes the corresponding moment. As a result, the joint shear deformations, elastic and inelastic column rotations, etc. are not taken into account.

2. The specimens with fully bonded mild steel and/or PT steel were treated as such in the program. However, debonding of these steels was observed during the actual tests. Therefore, the strains in these steels for a given drift would have been reduced resulting in a higher drift capacity at yield.
3. Crushing of the beams resulted in axial shortening and therefore a reduction in the strains in the mild and/or PT steels. Again, this would result in a higher story drift than predicted.

The hysteresis plots for representative tests of the Zone 4 specimens are given in Figs. 20 - 30. The low drift for precast specimen I-P-Z4 is due to premature bond failure of the mild steel as discussed in Section 3.1.1. Specimen J-P-Z4 (Fig. 26) underwent smaller increases of story drifts than did specimen K-P-Z4 at each new load level. This was due to an incorrect assumption used when calculating the predicted maximum moment for specimen J-P-Z4 leading to a lower value. As the yield displacement was based on this maximum moment, the imposed displacements in the subsequent cycles which were multiples of the yield displacement were therefore lower. It is for reasons such as this that drift-based loading histories are being used for seismic testing.

In general, the precast Zone 4 specimens were more ductile than the monolithic specimens and achieved higher story drifts at failure. The specimens with unbonded or partially bonded PT steel behaved in an approximately bilinear-elastic manner, as predicted, with little energy dissipation and increased ductility. Specimen L-P-Z4 C achieved a low story drift at failure as a result of shear failure in the beams.

Table 2. Connection Strengths and Story Drifts.

Specimen Name	Moment (kN-m)		Experimental Story Drifts @ Failure (%)
	Predicted	Experimental	
A-M-Z2 & B-M-Z2	68	80 / 75	4.1 / 4.3
A-P-Z2 & B-P-Z2	49 ^a	54 / 54	2.6 / 2.5
A-M-Z4 & B-M-Z4	132	148 / 153	3.0 / 3.4
A-P-Z4 & B-P-Z4	160 ^a	186 / 186	3.1 / 3.4
C-P-Z4 & D-P-Z4	159 ^a	171 / 169	4.8 / 4.9
E-P-Z4 & F-P-Z4	113 ^a	138 / 146	5.2 / 5.0
G-P-Z4 ^b & H-P-Z4 ^b	111 ^a	123 / 132	3.9 / 3.6
I-P-Z4 ^d	133 ^a	138	2.7
J-P-Z4	153 ^a	152	3.6
K-P-Z4	139 ^a	151	3.1
L-P-Z4 A ^b	126 ^a	105	1.5
L-P-Z4 B ^b	98 ^a	82	1.5
L-P-Z4 C ^e	141 ^a	117	2.0

- a Moments obtained from an analysis program with calculates the moments for a section given an imposed beam rotation.
- b These specimens were not tested to failure.
- c Maximum drift allowed by analysis program.
- d Bond Failure of mild steel.
- e Shear failure in beam.

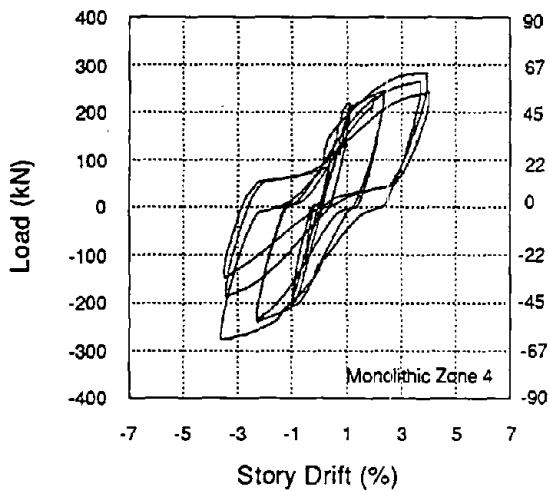


Figure 20. Hysteresis curves for A-M-Z4.

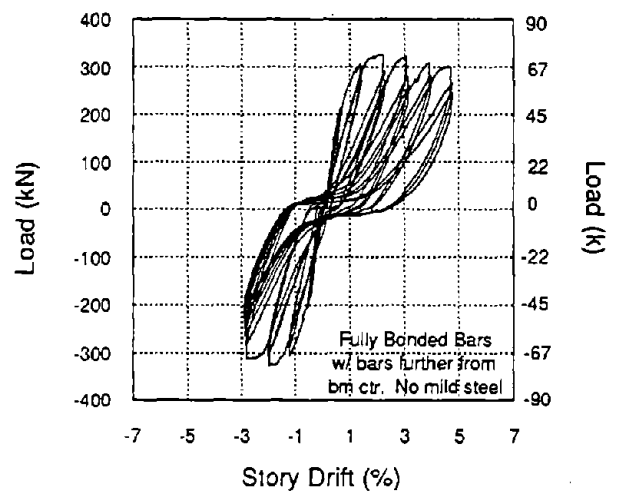


Figure 21. Hysteresis curves for A-P-Z4.

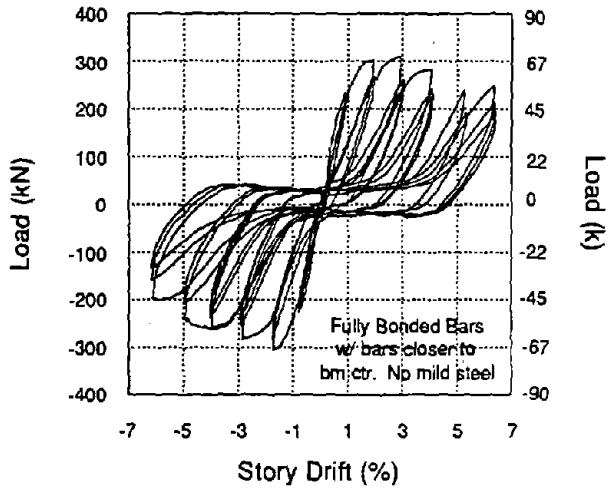


Figure 22. Hysteresis curves for C-P-Z4.

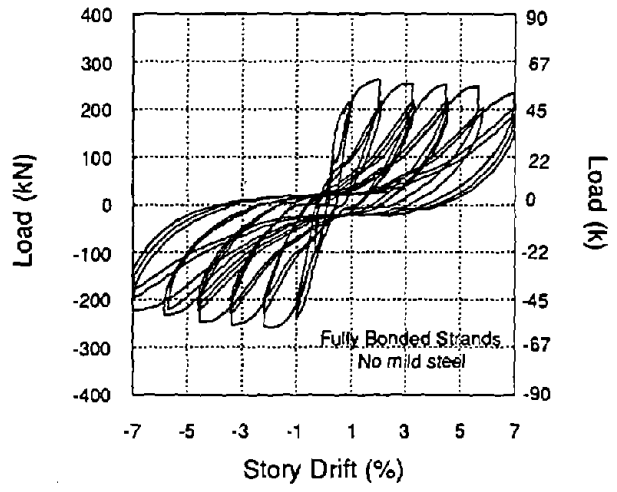


Figure 23. Hysteresis curves for E-P-Z4.

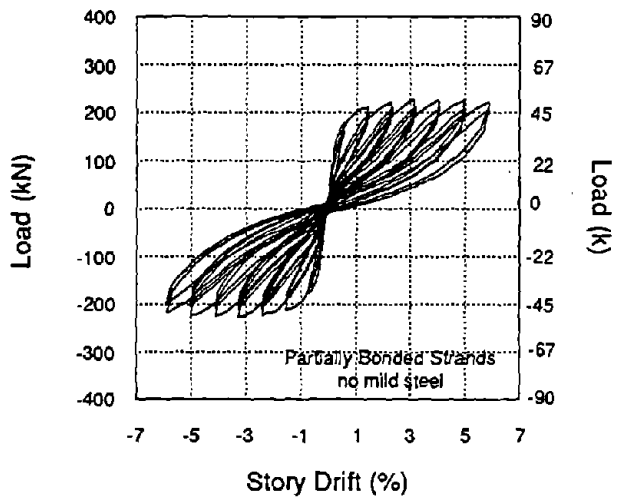


Figure 24. Hysteresis curves for G-P-Z4.

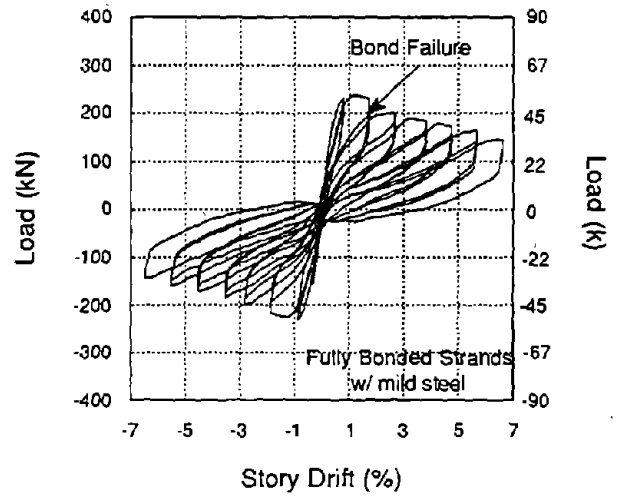


Figure 25. Hysteresis curves for I-P-Z4.

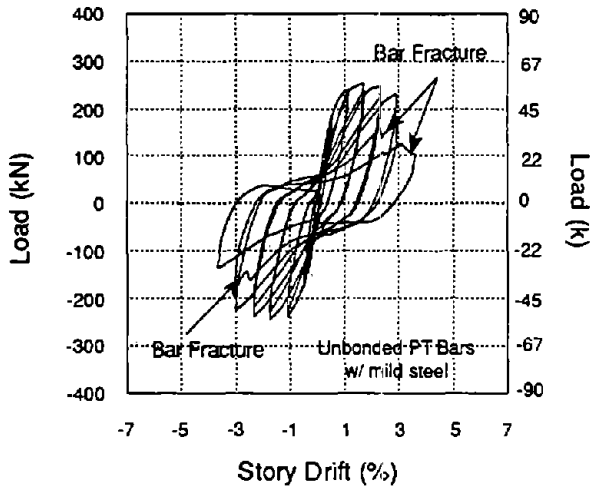


Figure 26. Hysteresis curves for J-P-Z4.

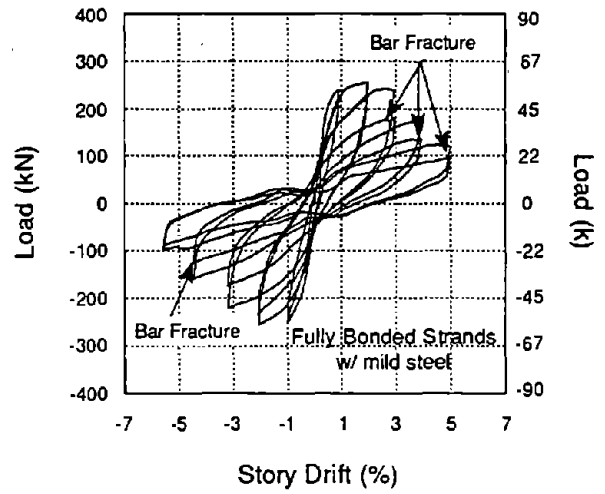


Figure 27. Hysteresis curves for K-P-Z4.

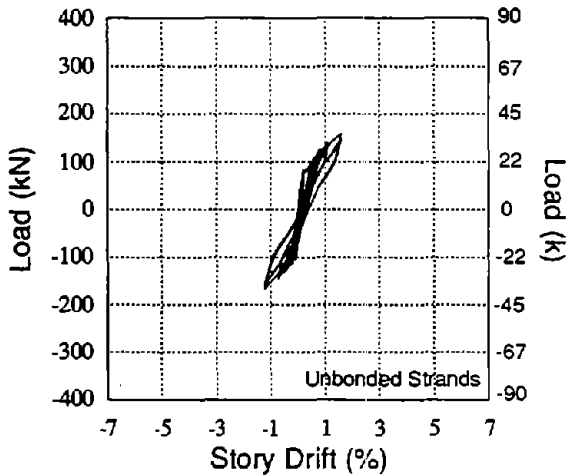


Figure 28. Hysteresis curves for L-P-Z4 A.

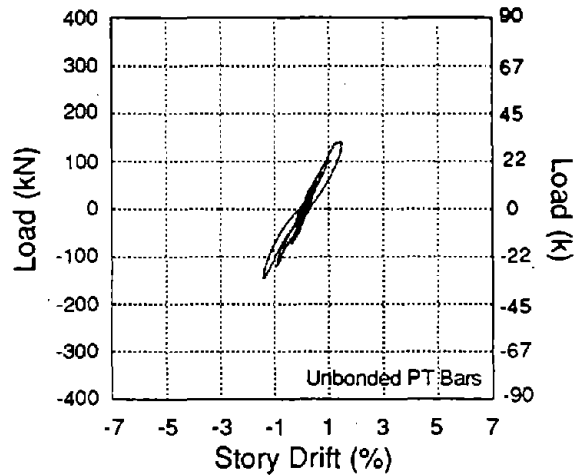


Figure 29. Hysteresis curves for L-P-Z4 B.

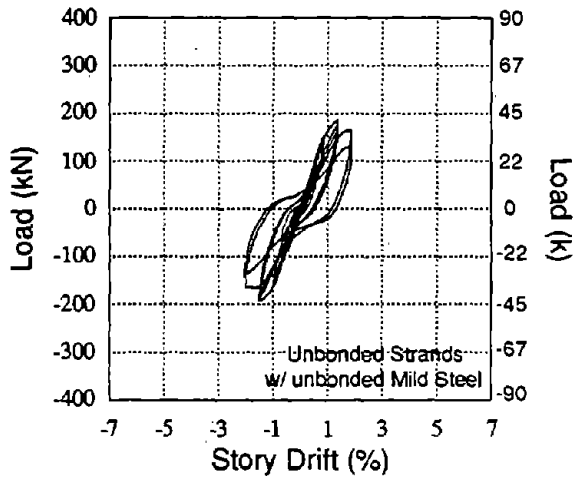


Figure 30. Hysteresis curves for L-P-Z4 C.

3.3 Connection Strength

The maximum experimental moments for all the precast specimens exceeded the predicted values. Except for the two cases where the failure mode was unanticipated [Sections 3.1.1 and 3.1.3], the precast specimens performed as well as the monolithic specimens in terms of connection strength. These moments for the monolithic specimens were calculated based on the actual yield stress of the steel with a factor of 1.25 applied to it to account for steel strain hardening, the 28-day concrete compressive strength and an ultimate concrete strain of 0.003. The moments for the precast specimens were calculated using program B6.FOR [Appendix E]. Steel strain hardening is accounted for in the program as the stress-strain curves used in the program for the given steel include values through bar fracture. The concrete compression force was computed based on a triangular stress distribution up to steel yield and on the Whitney stress block thereafter.

As seen in Table 2, the experimental moments obtained for the monolithic specimens were on average 14% greater than the calculated moments. For the precast specimens, excluding specimens I-P-Z4 and L-P-Z4 A-C which failed prematurely, the experimental moments were on average 12% higher than the calculated moments. Placement of the post-tensioning bars closer to the beam centroid does not effect the connection strength.

3.4 Energy Dissipation

Due to the different yield displacements and concrete strengths for the specimens, it was felt that the most practical means to compare the energy dissipation was to plot the dimensionless cyclic energy dissipated against the story drift. The dimensionless quantity of cyclic energy dissipated was determined by dividing the energy dissipated per cycle by the product of the maximum predicted moment and the story drift (percent) for that cycle. In Fig. 31, the normalized cyclic energy is plotted against the story drift and a best-fit curve is drawn through these points.

As shown in Fig. 31, increased cyclic energy dissipation can be achieved by having mild steel and PT steel in the connection. The precast specimens (J-P-Z4, K-P-Z4 and L-P-Z4 C) in Phase IV A matched the behavior of the monolithic specimen up to approximately 1.5% story drift when failure was about to occur (J-P-Z4 and K-P-Z4) or had occurred (L-P-Z4 C). Specimen K-P-Z4 with PT steel in the center and mild steel top and bottom of the beam, and specimen J-P-Z4 with PT steel and one-third more mild steel at the beam top and bottom had similar cyclic energy dissipation. It appears that locating the PT steel in the center of the beam improved the cyclic energy dissipation characteristics. Also, after fracture of the mild steel, the drop in cyclic energy dissipation was greater for specimen J-P-Z4 than for specimen K-P-Z4 likely due to a higher loss of the PT force in specimen J-P-Z4. As seen in Fig. 31, after fracture of the mild steel bars in specimen K-P-Z4, the normalized cyclic energy dissipation curve followed those of the other precast specimens with PT steel only. The implications of this behavior are that even if seismic induced strains exceed the fracture strain for the energy dissipative steel, a fail-safe residual strength level will be provided by the PT steel.

As mentioned in Sections 3.1.1 and 3.1.2, failure of specimens J-P-Z4 and K-P-Z4 resulted from fracture of the mild steel. Therefore, matching of monolithic behavior in terms of normalized cyclic energy dissipation to higher drift levels would be possible if fracture of the mild steel bars could be delayed. This is discussed in Section 4.2.

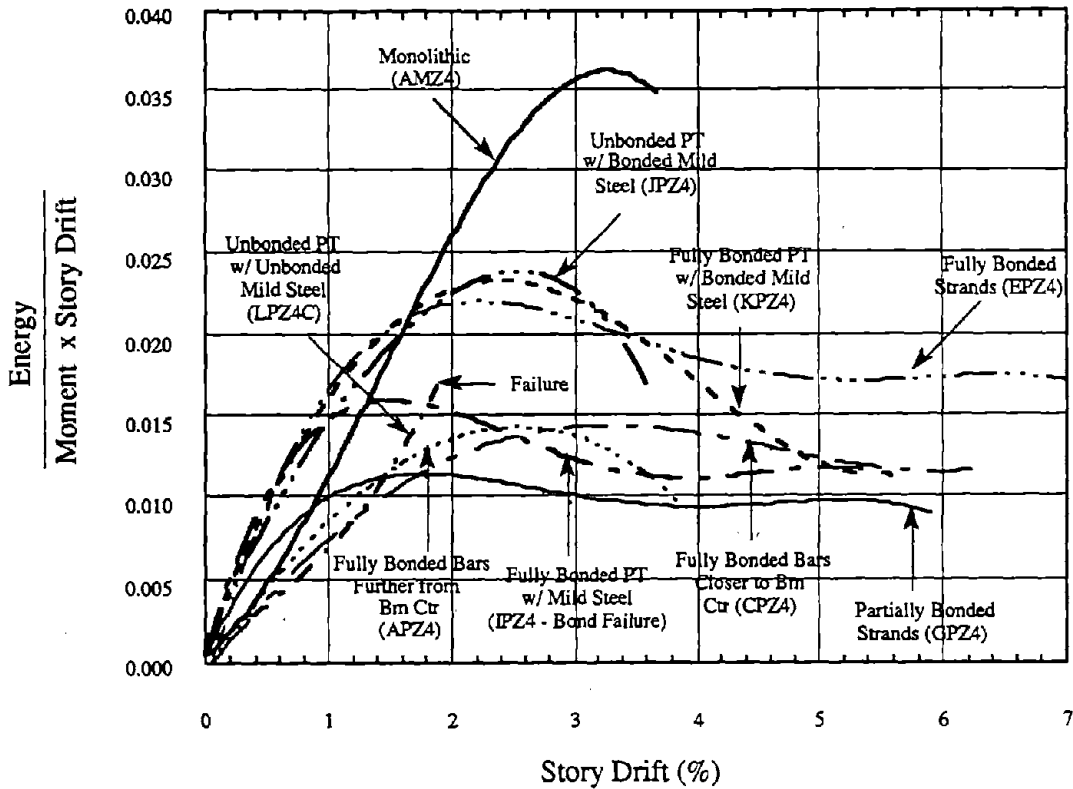


Figure 31. Comparison of the Normalized Cyclic Energy and Story Drift.

The normalized cyclic energy dissipated by precast specimen I-P-Z4, the first specimen tested in Phase IV, was similar to that for the monolithic specimen until about 1% story drift when suspected debonding occurred. The curves for this specimen and specimen K-P-Z4 are similar at the stage after fracture of the mild steel bars occurred in K-P-Z4. This is expected as both of these specimens are essentially identical at this point with only the PT steel holding the connection together.

The performance of the specimen E-P-Z4 (Fig. 31), fully bonded PT steel only, also performed as well as these specimens in terms of energy dissipation. This specimen had approximately 50% more PT steel than specimen K-P-Z4. This gives an indication of the effectiveness of using dissipators which will, in general, be more economical, in terms of \$/kg, than PT steel.

With the exception of specimen E-P-Z4, the cyclic energy dissipated by the precast specimens in Phases I - III was much less than that for the monolithic specimens as can be seen in Figs. 20 - 24. The normalized cyclic energy dissipated by the partially bonded specimen, G-P-Z4 (Fig. 31), is approximately half that of the fully bonded specimen, E-P-Z4.

A comparison of the normalized cumulative energy dissipated is shown in Fig. 32. The normalized cumulative energy dissipated is defined as the summation of the cyclic energy to failure divided by the product of the predicted maximum moment and a story drift of 1.5%. The normalized cumulative energy dissipated to failure by precast Zone 4 specimens C-P-Z4 through H-P-Z4 was greater than the cumulative energy dissipated by the monolithic Zone 4 specimens. This is a result of the higher story drifts achieved by these precast specimens. The normalized cumulative energy dissipated was higher for specimen J-P-Z4 than K-P-Z4 due to J-P-Z4 having a slightly higher story drift at failure and undergoing more cycles prior to failure as explained in Section 3.2.

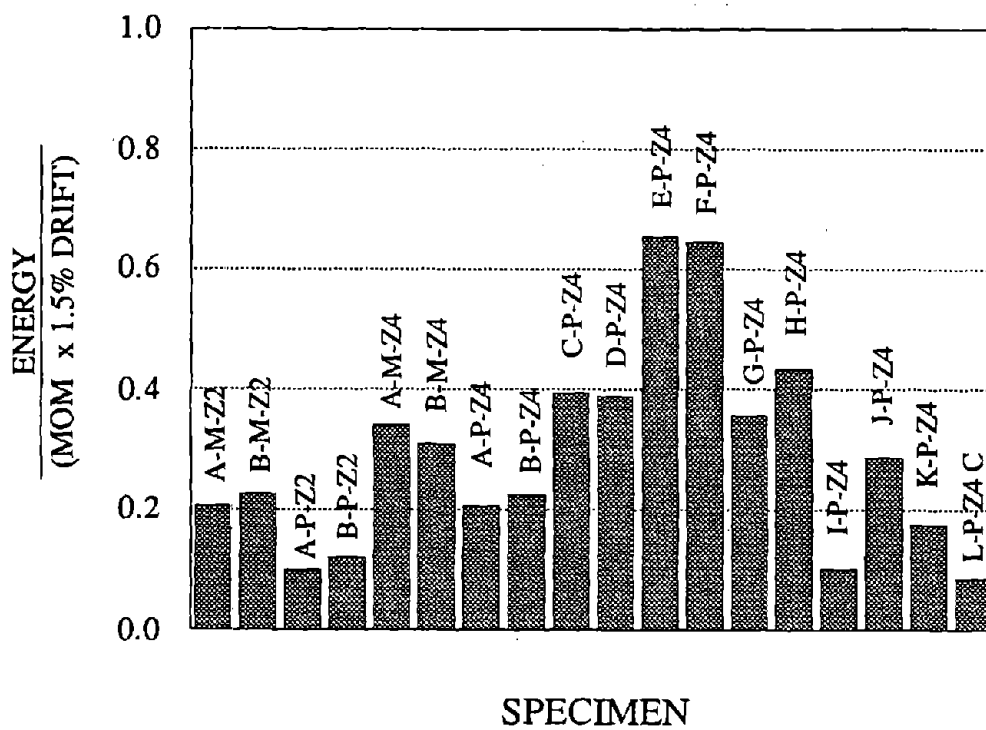


Figure 32. Normalized Cumulative Energy Dissipated.

3.5 General Discussion

Several points are worth discussing at this stage. First, the experimental data indicate that the envelope curve for the Phase III specimens can be approximated by a bilinear elastic relationship. However, a certain amount of damage was sustained by this joint detail during testing which lead to reduced stiffness during subsequent cycles to greater displacement ductilities. Significant spalling also occurred at the extreme compression fibers of the beams.

Nonetheless, there was almost no reduction in strength at the conclusion of the tests ($\approx 6\%$ story drift) which were stopped due to stroke limitations of the test facility.

The use of partially bonded tendons eliminates the slip zone (Fig. 24) at the zero displacement crossing that was characteristic of the Phase I and II specimens. However, the partially bonded precast specimens also dissipated significantly less energy per cycle than the fully bonded specimens - approximately 50% less. The issue here is not strength capacity but one of drift limitation. In this sense the Phase III joints should prove viable and robust, where site-specific time history analyses indicate that drift will not be a problem. Generally, one can expect this to be the case for high rise (long period) buildings founded on bedrock. Where hysteretic damping is to be relied upon (i.e. large energy dissipation per cycle) for drift limitation, then the Phase III connection detail should not be used.

Secondly, the results of the Phase IV specimens (J-P-Z4 and K-P-Z4) indicated comparable energy dissipation performance with monolithic joint details through approximately 2% drift which is very promising. Also, displacement instrumentation indicated no vertical slip of the precast beams with respect to the column at the beam-column joint throughout these tests. This indicates that slip due to dead load shear is not a factor and that the previous test results (NIST) are not compromised. However, for the sake of further verification, gravity loads will be applied to the specimens in the Phase IV B tests.

As can be seen in Figs. 5 and 7, the specimens I-P-Z4/K-P-Z4 and J-P-Z4 were designed with substantial reinforcement across the potential horizontal failure plane between the dogbone and the beam to prevent shearing off of the dogbone. Observations made during the tests suggest that the reinforcement provided was sufficient to prevent the shearing off of the dogbone. In fact, it would appear that the amount of reinforcement may be reduced, but the determination of the amount of reduction is beyond the scope of this project.

Strain readings in the #4 bars located at the end of the dogbone furthest away from the column face indicated that these bars yielded in specimen J-P-Z4. These bars were welded to the angles located at the top and bottom of the dogbone and the purpose of these bars was to act as tension ties in a region where tensile forces were anticipated. From the observations, it would appear that the assumption of large tensile forces in this region was correct and the presence of these ties was warranted. A simple truss model shows the need for them. However, the forces are much smaller if the PT acts at the center of the beam rather than being anchored in the dog-bone, in which case the tension forces can probably be resisted by the full-depth ties distributed along the dog-bone. This hypothesis was born out by the test results.

Finally, the objective of the precast design is not to emulate the behavior of a monolithic design. The damage in these frames is typically distributed in a plastic hinge zone about a beam depth long on either side of the columns. In the precast specimens, it is possible to keep the beams and columns essentially free from damage and to concentrate the inelastic action in the connection steel. This approach has the benefit of reducing, and in small to moderate earthquakes eliminating, structural repair costs.

However, because of the current perceived need to match monolithic performance in all aspects, the best chances of getting approval for a "new" type of design by building officials would be if it were shown that the "new" design can meet or exceed monolithic performance in terms of strength, energy dissipation, and story drift capacity. The procedure involving proof testing is expensive and the acceptance process is time consuming. Therefore, to encourage innovation and competitiveness, it would be beneficial if the acceptance process of new concepts and ideas could be expedited. A method to do so is presented in Appendix A.

4.0 CONCLUSIONS AND FUTURE RESEARCH

4.1 Conclusions

Post-tensioned precast concrete beam-column connections have been shown in this study to perform as well as or better than an equivalent monolithic specimen in terms of connection strength and drift capacity. The precast specimens which contained both post-tensioning steel and mild steel showed promise for being able to meet or exceed monolithic connection performance in terms of energy dissipation, strength and drift capacity.

Post-tensioned precast connections do not require corbels or shear keys because the friction between the precast beams and column developed from the post-tensioning force can resist the applied shear and gravity loads.

From the results of these tests (Phases I - IV A), improved energy dissipation per cycle can be achieved by: a) including low strength steel through the joint region near the top and bottom of the beams; b) locating the PT steel closer to the beam centroid; and c) having fully bonded PT steel (if no mild steel is included). However, the latter arrangement risks loss of shear capacity if the PT yields at large story drifts.

4.2 Future Research at NIST

Due to steel congestion in the dogbone regions, simplification of the Phase IV A designs was necessary before the commencement of the production type testing. In addition to ways of simplifying the details, other variables that merited further investigation included:

1. The amount of mild steel needed to match or exceed monolithic joint performance
2. The optimal amount of post-tensioning steel
3. Effects of type of mild steel/ PT steel
4. Use of higher strength concrete

Only four specimens will be tested in the production phase, Phase IV B. This number of test specimens will clearly not allow all the variables listed above to be examined. The last variable, use of higher strength concrete, will not be studied in Phase IV B.

From the results of the Phase IV A tests, it was decided that the Phase IV B specimens should be post-tensioned with strands located in the middle of the beam and the mild steel located at the top and bottom of the beam similar to the configuration used in specimens I-P-Z4 and K-P-Z4. The use of strands that run the full length of the building would reduce the construction costs as the number of anchorages and labor involved with the use of shorter tendons is reduced. The placement of the PT steel in the middle of the beam reduces the seismic strains in the PT steel and allows for more efficient use of the steel in terms of cyclic energy dissipation as discussed in Section 3.4.

In addition to locating the tendons in the middle of the beam, the post-tensioning steel will be partially bonded to reduce the strains in the tendons and thereby maximizing the chances of the tendons remaining elastic. In a prototype structure, the tendons will be unbonded through the column and on either side of the column. The unbonded length of the tendons in the beams will be determined by the required development length of the tendons. Therefore, bonding of the tendons will occur in mid-span of the beam. The use of partially bonded tendons will lessen the risks of a progressive collapse.

For ease of construction and from a standpoint of acceptance by the architectural and precast community, the dogbones in the beams have been eliminated. In place of the dogbones, a "trough" beam will be used. The trough will be located in the middle of the beam at the top and bottom and will begin at a distance of 914 mm (prototype) from the column face. This trough will allow the mild steel to be dropped into the trough and to be pushed through ducts in the beams and columns while maintaining a uniform rectangular external profile. Figs. 33 - 34 show the proposed beam cross sections for the Phase IV B specimens.

Based upon the observation that deviation from monolithic behavior for the NIST hybrid specimens initiated upon fracture of the mild steel energy dissipators, AISI (American Iron and Steel Institute) 304 stainless steel rods will be used in one of the Phase IV B specimens. These rods will be deformed. It is expected that the enhanced fatigue and strain capacity of a 304 stainless steel dissipator (greater than 5 times the capacity of a typical reinforcing bar) will significantly enhance energy dissipation at higher drift levels with the benefit of lower reinforcement ratios. Also, the use of angles at the corners of the beams is felt necessary to reduce crushing damage in these regions.

All dimensions in mm
25.4 mm = 1 in.

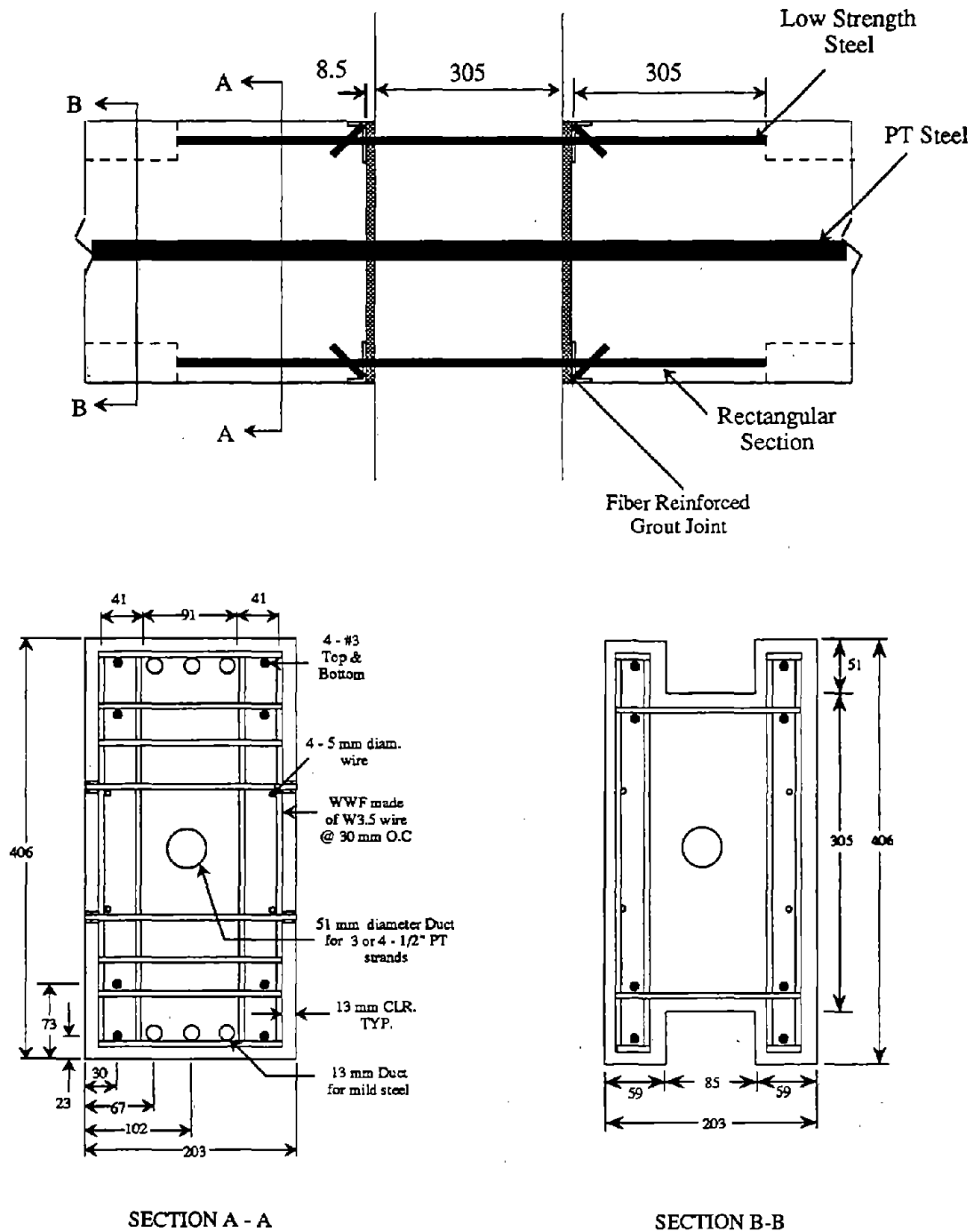


Figure 33. Generic Beam Details for Phase IV, B Production Specimens.

All dimensions in mm
25.4 mm = 1 in.

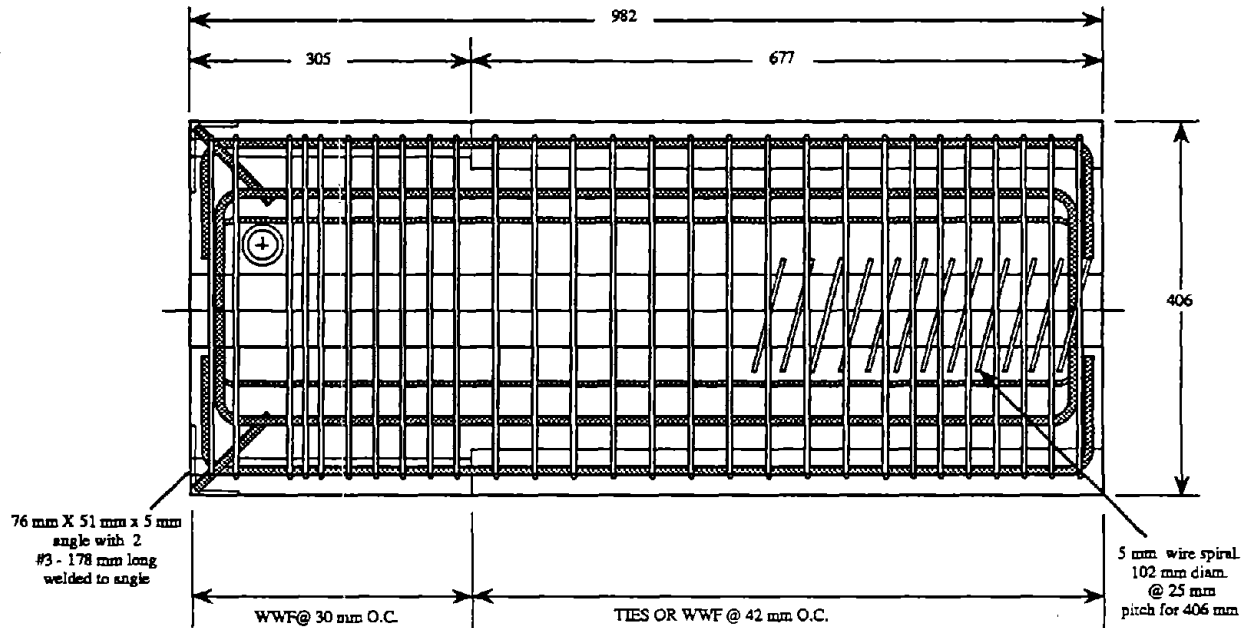


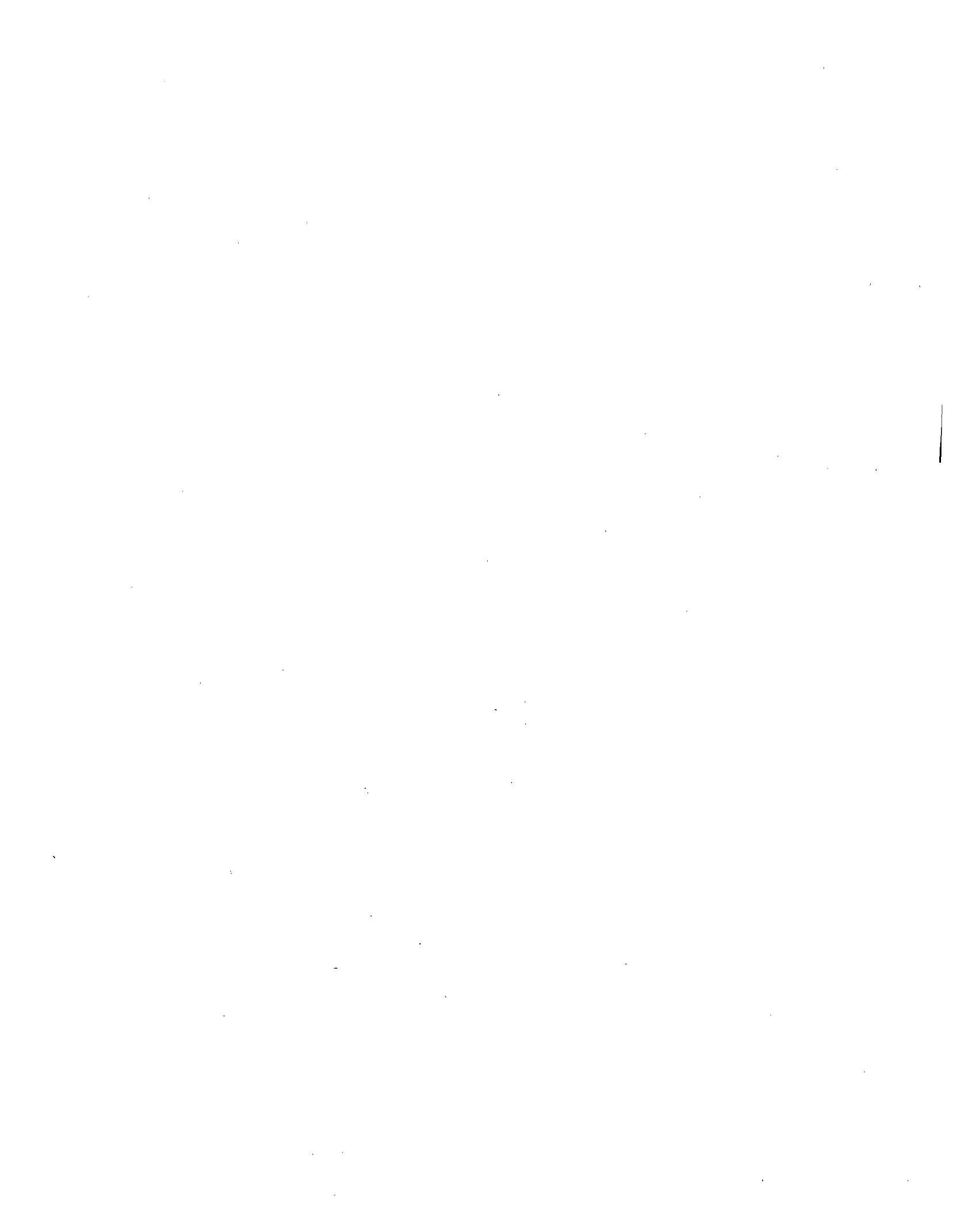
Figure 34. Elevation View of Phase IV, B Production Specimens.

The results from these and previous NIST specimens combined with the results from the PRESS program will provide a basis from which hysteretic failure model parameters may be determined. Using these parameters to characterize the connection behavior, the inelastic dynamic behavior of a precast connection may be studied for a series of earthquakes.

ACKNOWLEDGEMENTS

The assistance of Mr. Frank Rankin, Mr. Max Peltz, Mr. Jim Little, and Mr. Erik Anderson of the Structures Division laboratory staff is gratefully acknowledged. Their willingness to work extended hours and weekends is very much appreciated. Special thanks are extended to Mr. Dean Stephan, Mr. Dave Seagren, and Dr. John Stanton for their invaluable support, advice and insight in the Phase IV tests.

The authors would also like to extend their thanks for the technical support from the following individuals: Dr. Robert Englekirk, Dr. Cathy French, Dr. S. K. Ghosh, Mr. Jacob Grossman, Dr. Grant Halverson, Mr. Dan Jenny, Mr. Paul Johal, Mr. Bob Mast, Ms. Suzanne Nakaki, Mr. Courtney Phillips, Dr. Nigel Priestley, Mr. Barry Schindler, and Mr. Norm Scott. The support and/or donations of materials from Charles Pankow Builders, Ltd., Concrete Research and Education Foundation of the American Concrete Institute, Dywidag Systems International, and Allied Fibers are gratefully acknowledged.



REFERENCES

- Allahabadi, Rakesh (1987), "Drain-2DX, Seismic Response and Damage Assessment for 2D Structures," Department of Civil Engineering, University of California, Berkeley, March, 1987.
- American Concrete Institute (1989), "Building Code Requirements for Reinforced Concrete (ACI 318-89) and Commentary (ACI 318R-89)," Detroit, MI, November, 1989.
- American Society of Testing and Materials (1988), "Annual Book of ASTM Standards", Vol. 01.04, ASTM, Philadelphia, PA, 1988.
- American Society of Testing and Materials (1992), "Annual Book of ASTM Standards", Vol. 01.01**, ASTM, Philadelphia, PA, 1992.
- Cheok, G. and Lew, H. S. (1990), "Performance of 1/3-Scale Model Precast Concrete Beam-Column Connections Subjected to Cyclic Inelastic Loads," NISTIR 4433, NIST, Gaithersburg, MD, October, 1990.
- Cheok, G. and Lew, H. S. (1991), "Performance of 1/3-Scale Model Precast Concrete Beam-Column Connections Subjected to Cyclic Inelastic Loads - Report No. 2," NISTIR 4589, NIST, Gaithersburg, MD, June, 1991.
- Cheok, G., Stone, W., and Lew, H. S. (1992), "Partially Prestressed and Debonded Precast Concrete Beam-Column Joints", Proc. of the 3rd Meeting of the U.S. - Japan Joint Technology Coordinating Committee on Precast Seismic Structures Systems, November, 1992.
- Cheok, G. and Lew, H. S. (1993), "Model Precast Concrete Beam-to-Column Connections Subject to Cyclic Loading," paper submitted to PCI Journal for publication.
- El-Borgi, S., Stone, W.C., White, R.N., and Gergely, P. (1992), "Analytical Study on Seismic Behavior of Lightly Reinforced Concrete Frame Buildings," NIST Project 50SBNB1C6543, Report #3, School of Civil and Environmental Engineering, Cornell University, Ithaca, NY 14853, September 15, 1992.
- French, C., Amu, O., Tarzikh, C. (1989), "Connections Between Precast Elements - Failure Within Connection Region," ASCE Structural Journal, New York, NY, February, 1989, pp. 3171 -3192.
- International Conference of Building Officials (1985, 1988), Uniform Building Code, Whittier, CA, 1985 & 1988.
- Hart, G.C. (1992), "Design Criteria for Precast Concrete Structures: Foundation of a New Direction," Report on the Third U.S. PRESSS Coordinating Meeting, Report No. PRESSS-92/02, Dept. of Applied Mechanics & Engineering Sciences, UCSD, La Jolla, CA, August, 1992.
- Idriss, I.M. (1993), "Procedures for Selecting Earthquake Ground Motions at Rock Sites," Report to the Structures Division of the Building and Fire Research Laboratory, NIST, Gaithersburg, MD, February, 1993.
- Park, Y.J., Reinhorn, A.M., and Kunnath, S.K. (1987), "IDARC: Inelastic Damage Analysis of Reinforced Concrete Frame-Shearwall Structures, (1987)", Technical Report NCEER-87-0008, Department of Civil Engineering, State University of New York at Buffalo, Buffalo, NY, July 20, 1987.

- Phan, L.T., Todd, D.R., and Lew, H.S. (1993), "Strengthening Methodology for Lightly Reinforced Concrete Frames-I," NISTIR-5128, National Institute of Standards and Technology, Gaithersburg, MD, February, 1993.**
- Priestley, M.J.N, Ed. (1992), Report on the Third U.S. PRESSS Coordinating Meeting, Report No. PRESSS-92/02, Dept. of Applied Mechanics & Engineering Sciences, UCSD, La Jolla, CA, August, 1992, p 12-16.**
- Priestley, M. J. N. and Tao, J. R. (1993), "Seismic Response of Precast Prestressed Concrete Frames with Partially Debonded Tendons," PCI Journal, Vol. 38, No. 1, Jan/Feb 1993, pp. 58-69.**
- Stone, W.C., and Taylor, A.W. (1993), "Seismic Performance of Circular Bridge Columns Designed in Accordance With AASHTO/CALTRANS Standards," BSS-170, National Institute of Standards and Technology, Gaithersburg, MD, February 1993.**
- Stone, W.C., and Taylor, A.W. (1992), "A Predictive Model for Hysteretic Failure Parameters," Proceedings of the 10th World Conference on Earthquake Engineering, July 19-24, 1992, Madrid, Spain, A.A. Balkema, Rotterdam, 1992, pp. 2575-2580.**
- Taylor, A.W., and Stone, W.C. (1991), Selecting Bedrock Motions for the Seismic Design of Bridges," U.S. - Japan Workshop on Earthquake Protective Systems for Bridges, National Center for Earthquake Engineering Research (NCEER), State University of New York, Buffalo, September 4-5, 1991.**

APPENDIX A: DEVELOPMENT OF CODE CRITERIA

Work at NIST, at universities and industry involved with the PRESSS program, and elsewhere have investigated (or are investigating) a number of precast moment resisting frame joint details that fall into the following seven categories:

1. Fully bonded PT strand, no mild steel (NIST)
2. Fully bonded PT strand, bonded mild steel (NIST)
3. Fully bonded PT bars, no mild steel (NIST)
4. Partially debonded PT strand, no mild steel (NIST)
5. Fully debonded PT strand, no mild steel (U. C San Diego)
6. Unbonded PT bars, bonded mild steel (NIST)
7. No PT, fully bonded mild steel (U. MN, U. TX, Austin)
8. Unbonded PT bars, unbonded mild steel (NIST)

From the data obtained thus far, there is clear evidence that precast moment resisting frames can be designed to meet the strength requirements of the UBC. For the range of specimens tested, the NIST and UCSD test programs have also shown that corbels may be eliminated from such designs and that friction developed at the interface between the beam and column via axial post-tensioning can be designed to handle gravity loads and seismic shear loads without any slip.

In almost all configurations tested, strength was maintained in the precast frames to story drifts levels of as much as 5% which is far in excess of the 1-1/2% allowed. This indicates substantial reserve deformation capacity in the precast details which in many cases exceeds that of monolithic comparison tests.

In some designs tested, there was a significant slip zone in the hysteresis curves that developed due to yielding of the post-tensioning steel. This could, under certain inertial loading conditions, cause large lateral displacements and lead to unacceptable residual drift. Likewise, some designs exhibited nearly bi-linear elastic behavior. These latter two cases (slip-dominated and bi-linear elastic) require special design consideration from a drift limitation standpoint that would not be required of a joint detail matching or exceeding monolithic performance. However, as will be detailed below, it is felt that the use of more sophisticated design tools in these special cases will enable them to be safely used and permit a wide latitude of design freedom to the structural engineer.

From a design standpoint the following issues remain:

1. **ISSUE #1:** What details allow a precast joint to match or exceed monolithic performance in terms of strength, energy dissipation, and drift capacity? Present work at NIST (see Fig. 31) has shown that hybrid joints (containing unbonded or bonded PT and mild steel) can achieve story drift limits beyond those allowed by the code. Other details are scheduled to be tested in NIST Phase IV B and in

PRESSS Phase II. The mild steel in these tests serves as the energy dissipator while efforts must be taken at the same time to insure near elastic behavior in the PT steel to prevent slip-type behavior and to maintain the prestress necessary for resisting the applied shear force and gravity loads. Thus: 1) how much prestressed and non-prestressed steel is necessary to achieve satisfactory behavior? and 2) could other materials be used more efficiently to perform the function of the existing components (i.e. deformed stainless steel or other special alloy bars)?

Again, the objective of the precast design is not to emulate the behavior of a monolithic design but to meet or exceed its performance in terms of strength, and drift capacity. It may be optionally desirable, but not required, to meet or exceed the monolithic energy dissipation characteristics depending on the local site conditions and anticipated seismic activity. The damage in monolithic frames is typically distributed in a plastic hinge zone about a beam depth long on either side of the columns. In the precast specimens, it is possible to keep the beams and columns essentially free from damage and to concentrate the inelastic action in the connection steel. This approach has the benefit of reducing, and in small to moderate earthquakes eliminating, structural repair costs.

2. **ISSUE #2:** What about new details not covered in the current research areas? In order to encourage innovation on the part of the precast industry, a simplified acceptance procedure needs to be established for joint details which do not fall within the bounds of the existing knowledge base. Since the design procedures for strength (moment capacity) and shear are straightforward, the only remaining issues are those of energy dissipation characteristics and story drift limitations.

Work at NIST has shown that joint details have very specific energy dissipative "signatures", as manifested in a plot of normalized cyclic dissipated energy versus drift (see, e.g., Fig. 31). Recognizing this, the following method for the determination and rating of new joint details is proposed:

- A) Design the basic joint for moment and shear demand (both dead load and seismic load) using standard procedures.
- B) Conduct a minimum of one, and preferably two tests, model or full-scale, of the proposed joint (interior beam column joint) using the drift-based cyclic loading procedure presently being employed by PRESSS [Priestley, 1992].
- C) Plot the non-dimensionalized cyclic dissipated energy (as shown in Fig. 31) as a function of story drift for each cycle.
- D) The precast joint is accepted if:
 - (1) For drifts of 2% or less, the experimental energy curve falls within the band of one standard deviation of the monolithic curve in Fig. 31 (or

a similar, statistically derived curve based on experimental data for monolithic joint for other configurations).

- (2) The joint can sustain a drift level of approximately 3% prior to the onset of strength deterioration.

Otherwise, it will be subject to the more rigorous analysis procedures described below. This is a somewhat rigid definition but it may be useful as the basis for committee debate and parametric sensitivity studies to determine how much deviation from the empirical monolithic behavior may still be considered acceptable.

3. **Issue #3:** What design procedures are to be used for joint details not matching or exceeding monolithic performance? The use of such a design for a specific region or site will initially require the use of time history analyses and a hysteretic model, calibrated using experimental data, to determine the expected drift. However, with sufficient parametric analyses, it should be possible to develop design models that will employ higher safety factors and simplified equivalent static design procedures.

Initial code development work for precast moment resisting frames under PRESS [Hart, 1992] has identified three possible design procedures, distinguished by the level of required sophistication:

1. A simplified, equivalent static analysis which accounts for transient inelastic response through the use of conservative response modification factors in which allowable drift is severely restricted.
2. A design based on site specific response spectra involving essentially elastic analyses (with a limited amount of inelastic element response allowed) and story drift ratios limited to 1.5%.
3. A transient, non-linear dynamic analysis using maximum credible site specific time histories with residual interstory drifts being limited to 0.5% following inelastic excursions.

Commensurate with the more sophisticated design procedures is a greater degree of design freedom. What is lacking at this stage is specific guidance to bridge the gap between the experimental data that exist (and is being expanded in PRESS Phase II and NIST Phase IV B) on precast moment-resisting beam column joints and the design approaches described above. Before a time history analysis can yield valid design results, two critical components remain to be developed:

1. Hysteretic models must demonstrate a robustness to capture the seismic behavior of precast joints. System identification must then be carried out to characterize

hysteretic parameter coefficients, using the available test database. There are several possible analytical platforms which might be utilized (e.g., IDARC, DRAIN-2DX) for this operation, but the hysteretic models embedded in these codes vary widely in their abilities to capture precast joint behavior.

- 2) Relationships need to be developed by which hysteretic parameter coefficients can be determined *a priori* given only geometric and material properties for a proposed joint detail. This technique is reaching maturity at NIST in studies of RC bridge columns and cast-in-place shear wall structures [Stone and Taylor, 1993; Phan, Todd, and Lew, 1993].

At NIST the authors have adopted a 5-parameter hysteretic model which includes strength degradation, stiffness degradation, pinching, slip initiation, and slip length. This model has been embedded in IDARC 3.3 [Kunnath, et.al, 1993] as well as in the NIST graphics-based system identification package NIDENT 5.0 [Stone and Taylor, 1993]. A sample of the capabilities of this model is shown in Figs. A1 and A2 in which the load-displacement history of NIST specimen A-P-Z4 has been analytically generated given only the laboratory displacements as input. Other models, including differential equation based "smooth" models [e.g. El-Borgi et.al., 1992] could have been used. However, from the viewpoint of computational efficiency the 5-parameter linear model is superior and the loss in accuracy is negligible.

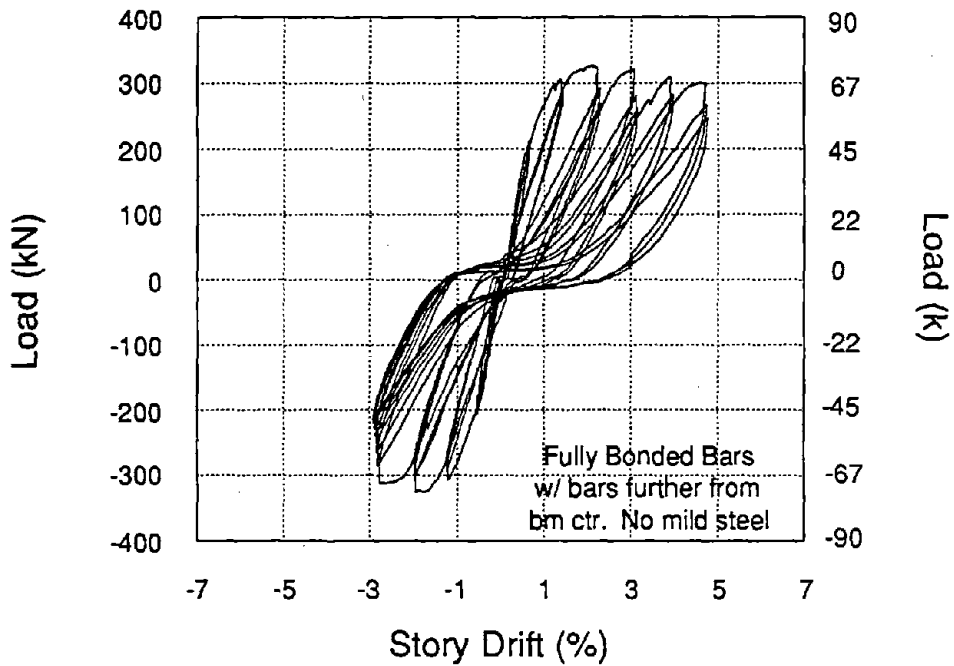


Figure A1. Experimental Hysteresis Curves for NIST Specimen A-P-Z4.

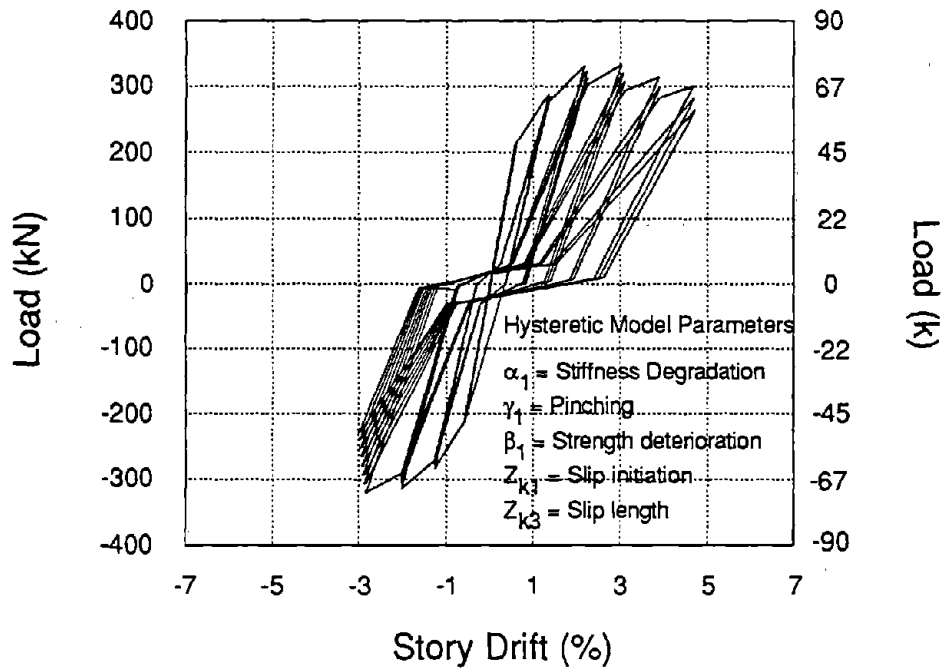


Figure A2. Predicted Hysteresis Curves Produced Using NIDENT 5.0 System Identification and IDARC 3.3 Inelastic Solution

Upon completion of laboratory parametric tests of the most promising of the hybrid connection designs, refinement of analytical methods for modeling the hysteretic behavior observed in the laboratory tests will be carried out. This work will be extended towards the development of a simplified (static equivalent, elastic) design criterion for precast moment resisting frames as follows:

1. A broad range of moment resisting 2-D precast frames will be designed which utilize the various precast joint details previously described (and for which hysteretic parameter coefficients have already been determined via system identification at NIST). These frames will be chosen in consultation with industry as being representative of the majority of commercial building designs that might be contemplated for this type of construction.
2. For each matrix of geometric (story height, number of stories, bay width, number of bays, beam and column dimensions and reinforcement details) and material (concrete and steel strengths and stress strain relations) characteristics corresponding to each type of precast system, computer models will be subjected to a series of design earthquake suites (5-10 records each) for varying epicentral distances and magnitudes. The inelastic transient behavior will be determined on the basis of interstory drift vs. time and the peak interstory drift for each run. Each analysis set will be repeated to represent the following conditions:
 - A. Zone 4 events (typical of California)
 - B. Zone 2 events (typical of eastern U.S.)
 - C. UBC/SEAOC soil types S1 - S4

An automated graphics-based program, EARTHGEN 1.0, for generation of bedrock earthquake ensembles has already been developed at NIST [Taylor and Stone, 1991] such that the massive number of analyses can be handled with relatively little effort. Historic records, scaled to match target response spectra generated via existing attenuation relationships [e.g. Idriss, 1993] will be used for Zone 4 analyses; synthetic generation techniques will be used for Zone 2. The output of EARTHGEN is compatible for direct input into ISDP the NIST Integrated Seismic Design Procedure [Stone and Taylor, 1993], an automated inelastic analysis package which accounts for soil type.

3. Elastic analyses will be conducted corresponding to Step 2 above using UBC/SEAOC simplified lateral load design criteria and determine peak interstory drifts.
4. On the basis of Steps 2 and 3 above, response modification factors (R_w) as a function of earthquake energy content (magnitude, distance) will be determined.

5. Based on Step 4, statistical analyses (step wise, linear regression) will be conducted to develop closed form equations defining R_w as a function of earthquake magnitude, epicentral distance, soil type, and seismic zone. Sensitivity analyses will then be used to determine the conditions in which a single value for R_w is appropriate.

In Step 5, at a certain energy content (as manifested by combinations of larger magnitude and shorter epicentral distances) unacceptable structural behavior may be exhibited, either in the form of excessive maximum drift, excessive residual drift, or high damage levels that might affect structural integrity. An initial performance-based design criterion, in which there is a sliding scale of permissible damage (or drift) directly tied to energy content, has been developed at NIST [Stone and Taylor, 1993]. What remains is for code-writing bodies to refine such an approach in parallel with (and eventually in lieu of) the "maximum credible earthquake." This would permit a rational link between simplified design procedures and with time history analyses, which presently does not exist.

APPENDIX B

SPECIMEN DRAWINGS

All dimensions in mm
25.4 mm = 1 in.

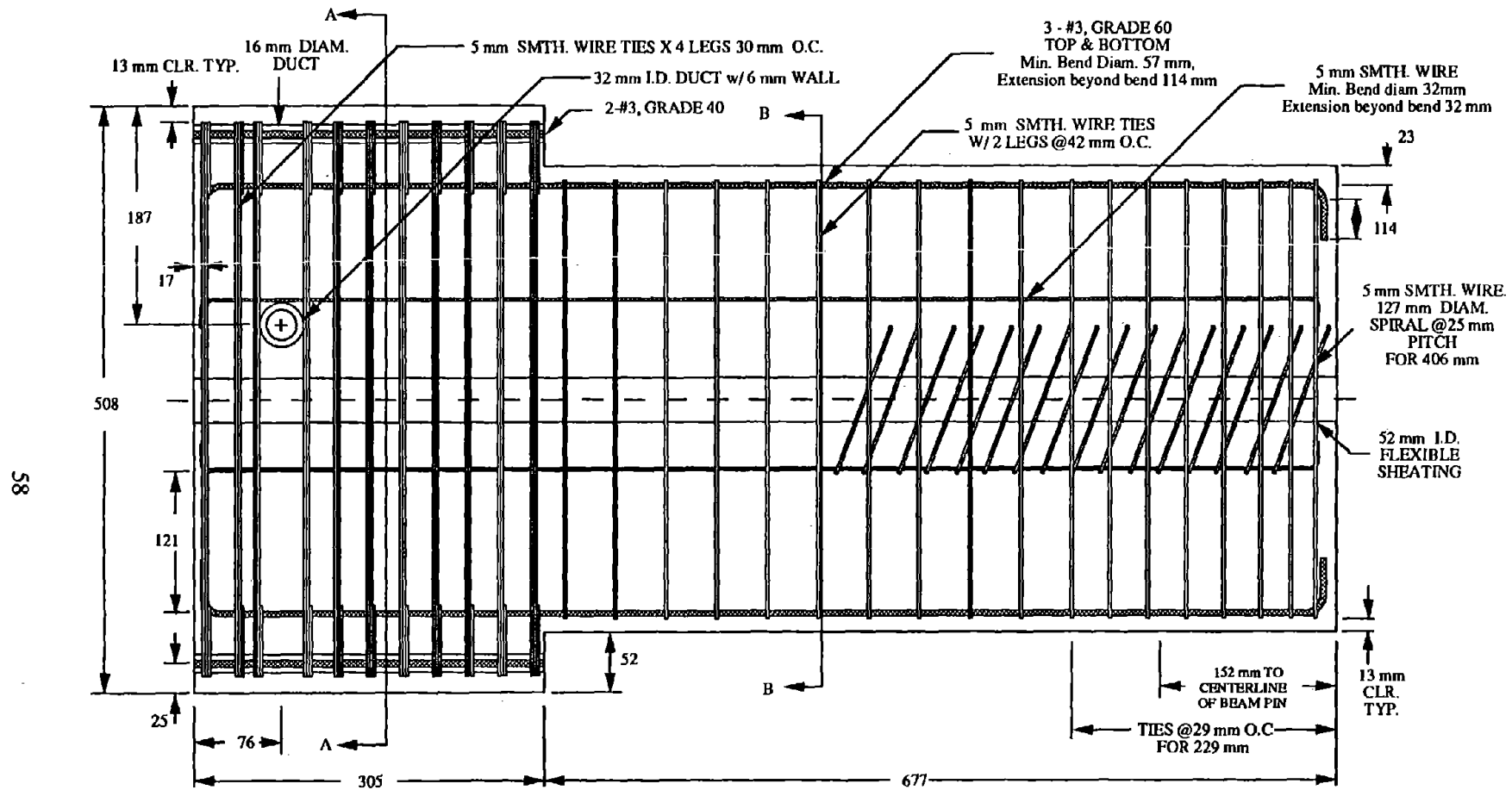


Figure B1. Elevation View of Beams - I and K P-Z4.

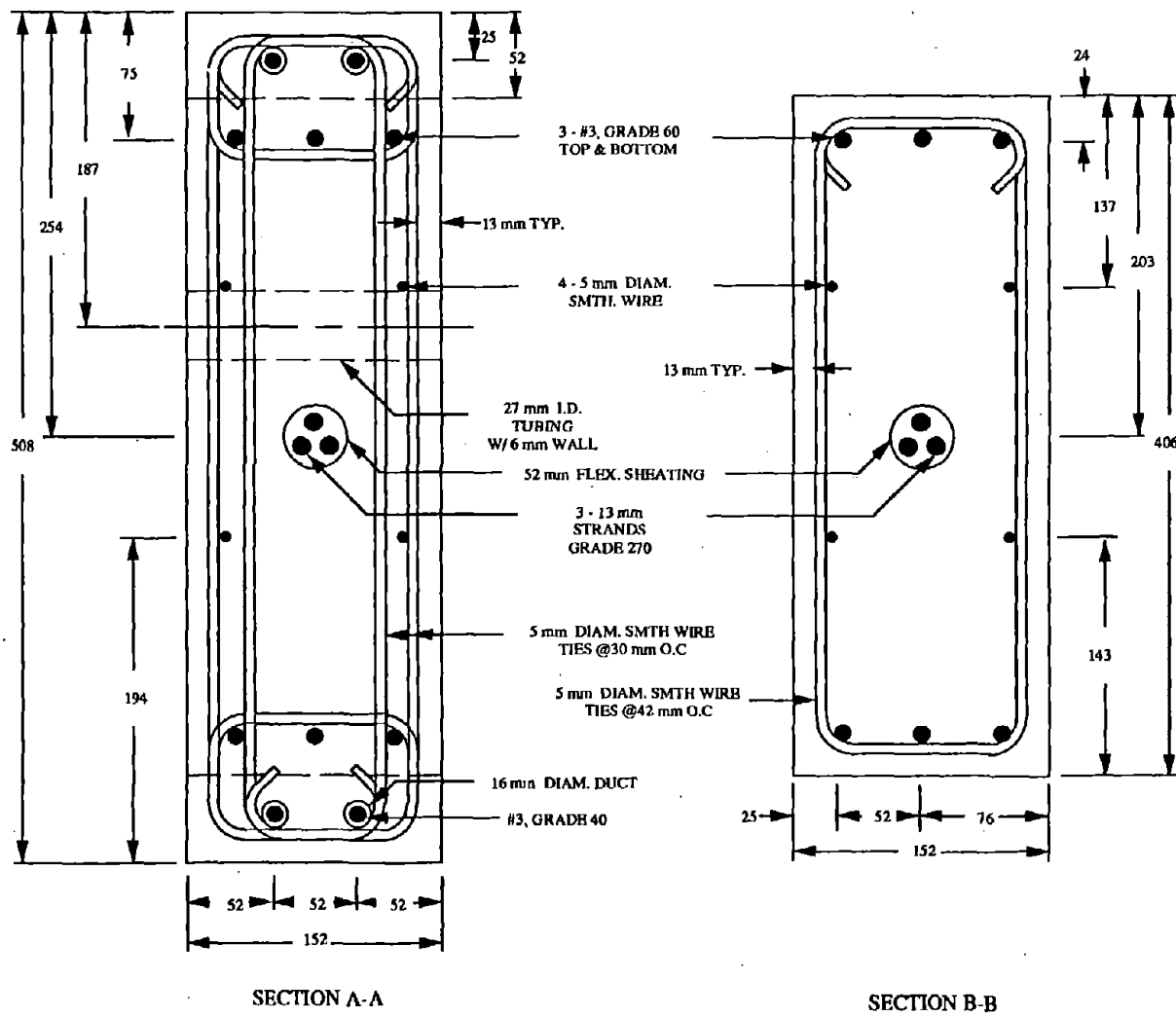
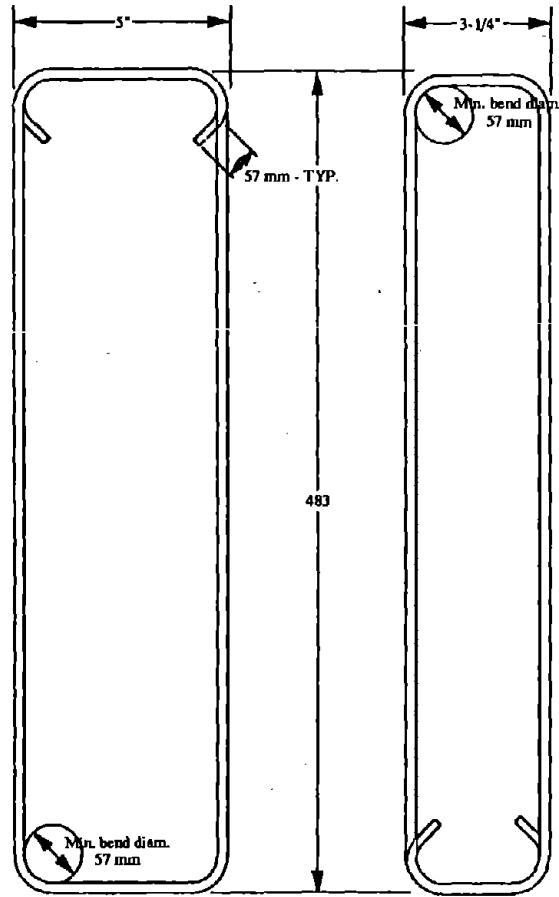
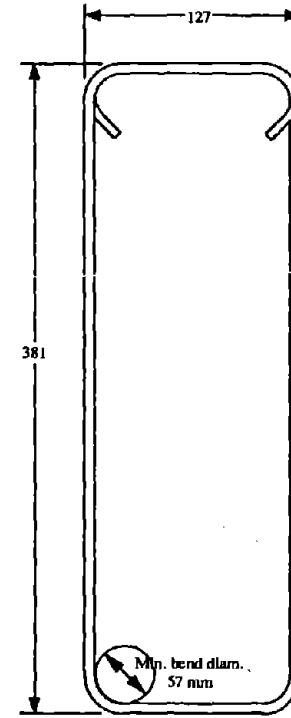
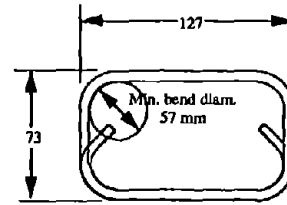


Figure B2. Beam Cross Sections - I and K P-Z4.

All dimensions in mm
25.4 mm = 1 in.



TIES FOR SECTION A-A



TIE FOR SECTION B-B

Figure B3. Beam Ties - I and K P-Z4.

All dimensions in mm
25.4 mm = 1 in.

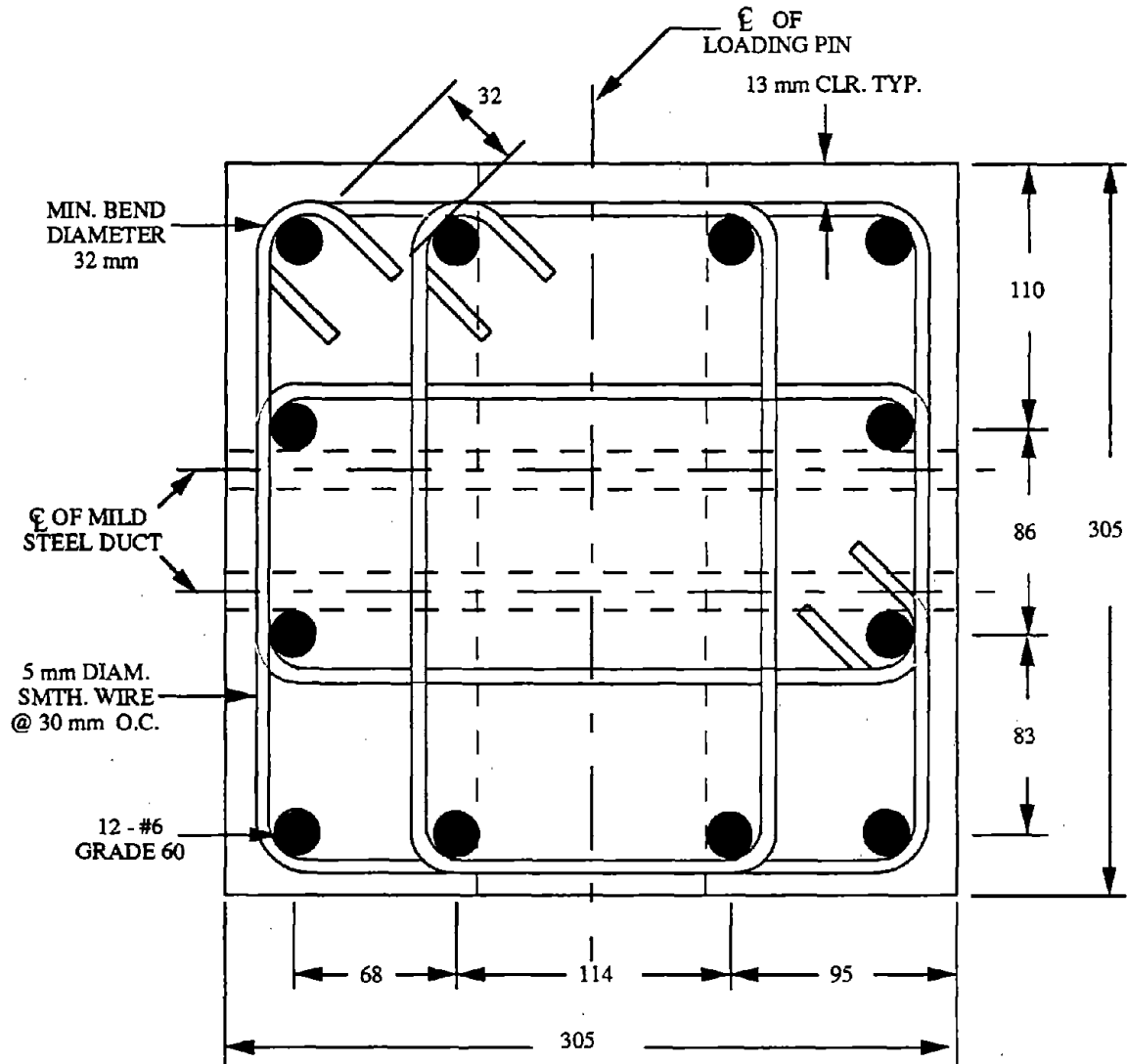
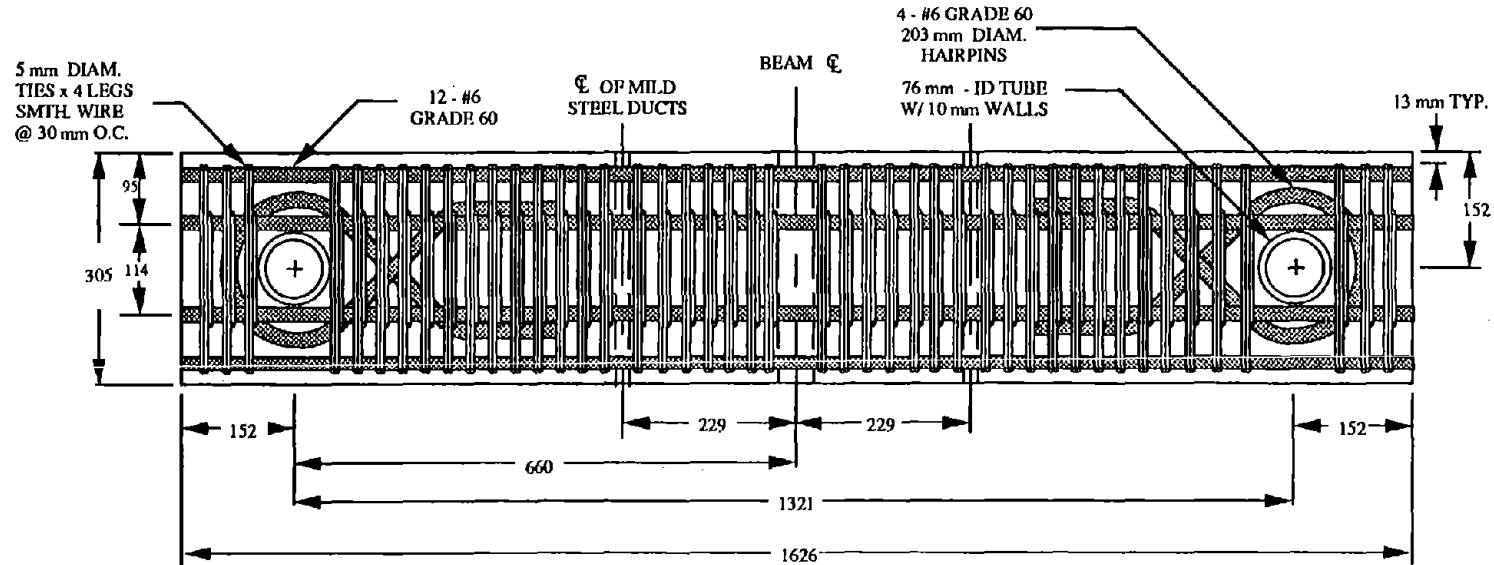
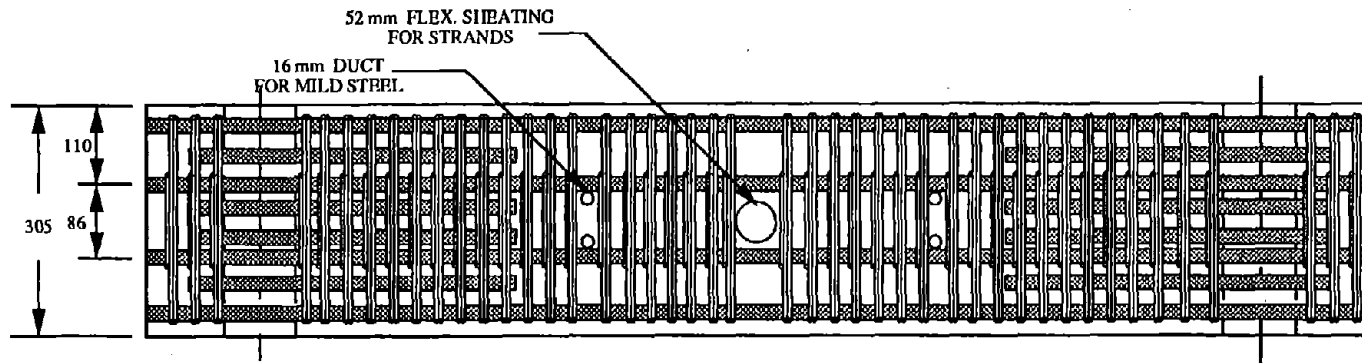


Figure B4. Column Cross Section - I and K P-Z4.

All dimensions in mm
25.4 mm = 1 in.



Top View



Elevation

Figure B5. Top and Elevation Views of Column - I and K P-Z4.

All dimensions
25.4 mm = 1 in.

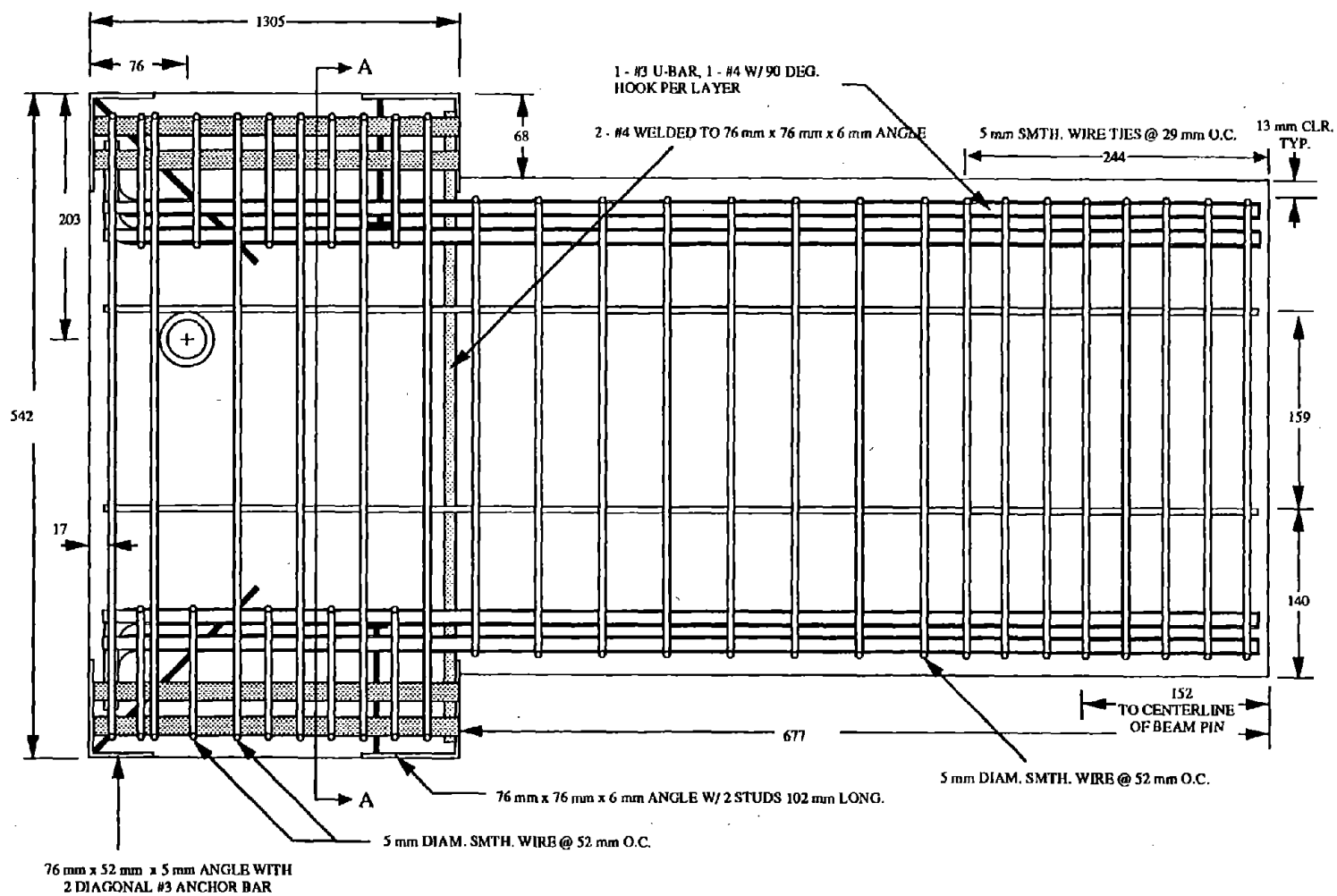


Figure B6. Elevation View of Beams - J-P-Z4.

All dimensions in mm
25.4 mm = 1 in.

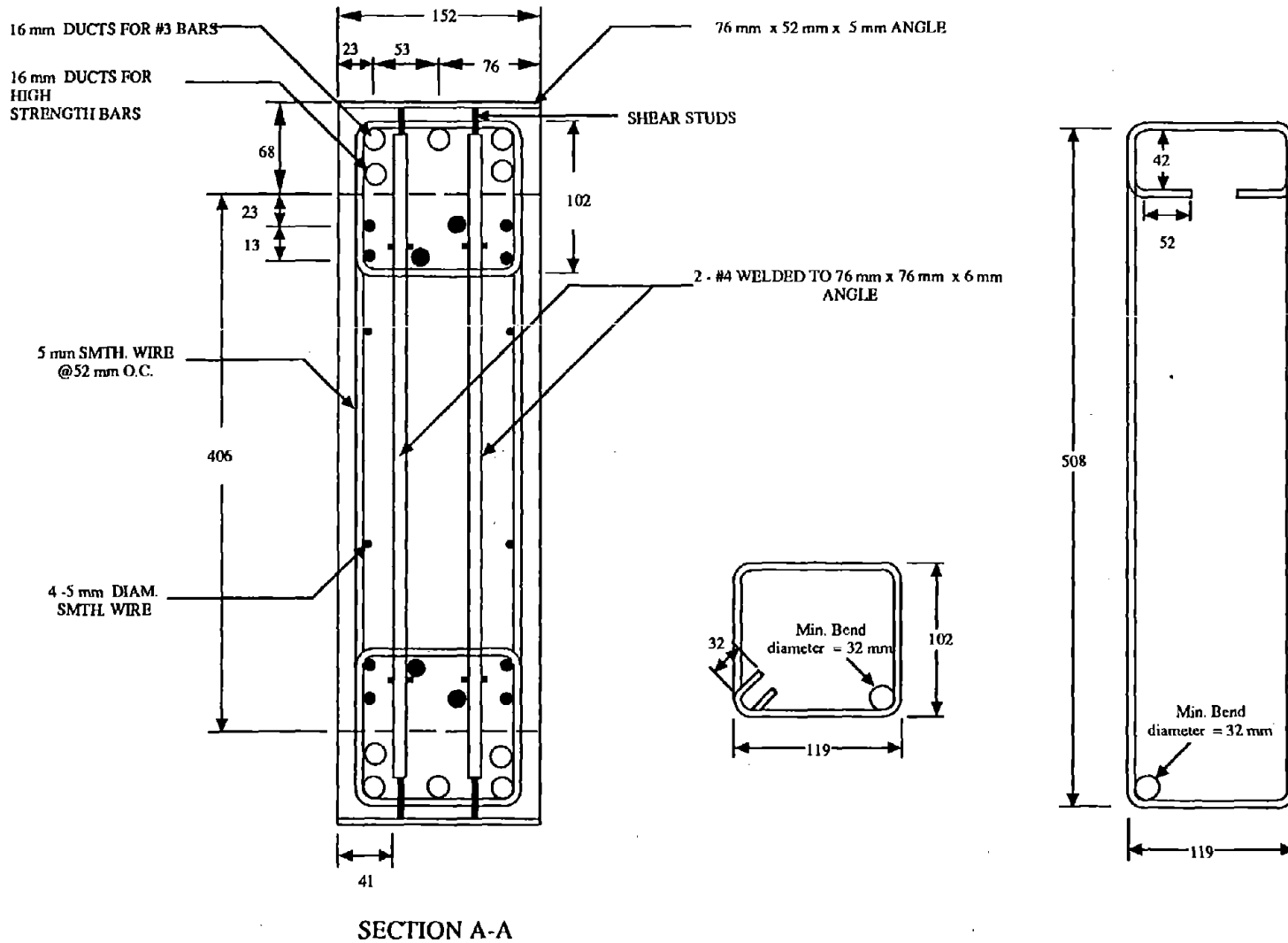
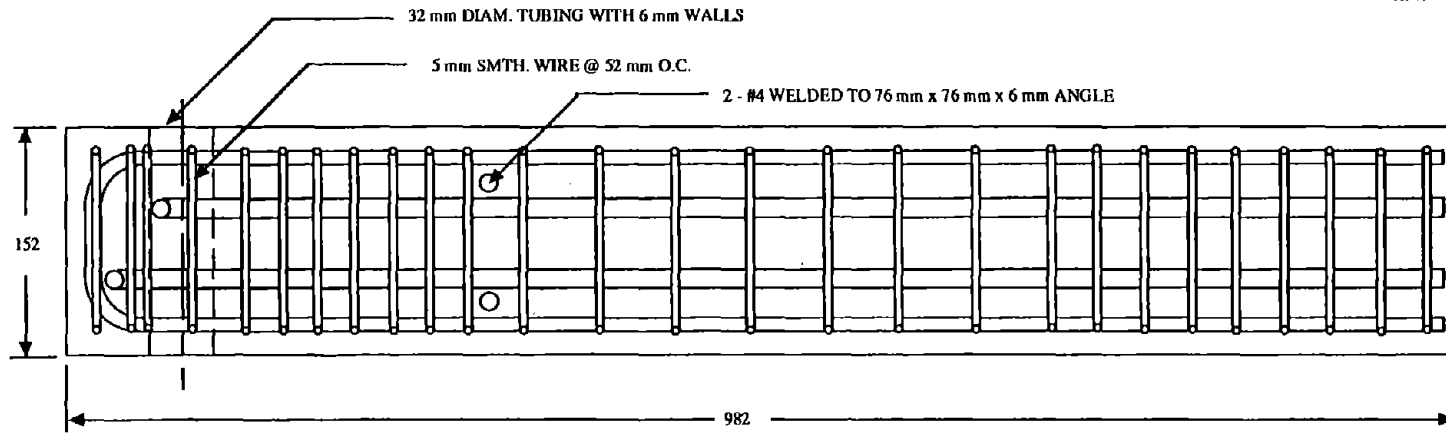
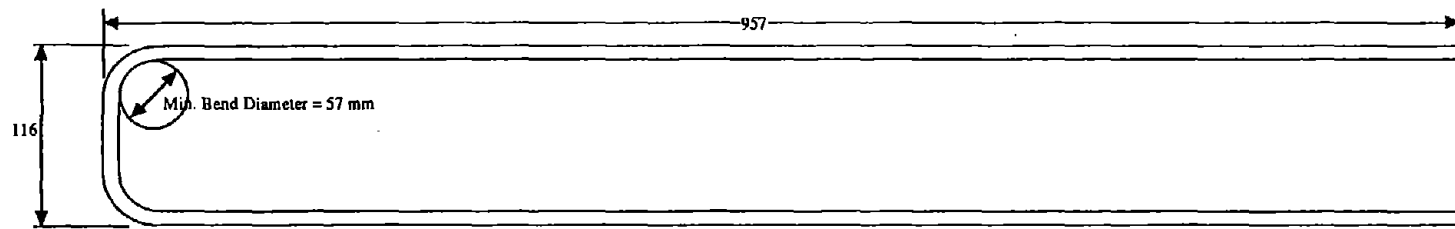


Figure B7. Beam Cross Sections - J-P-Z4.

All dimensions in mm
25.4 mm = 1 in.



TOP VIEW



#3 GRADE 60 U-BAR

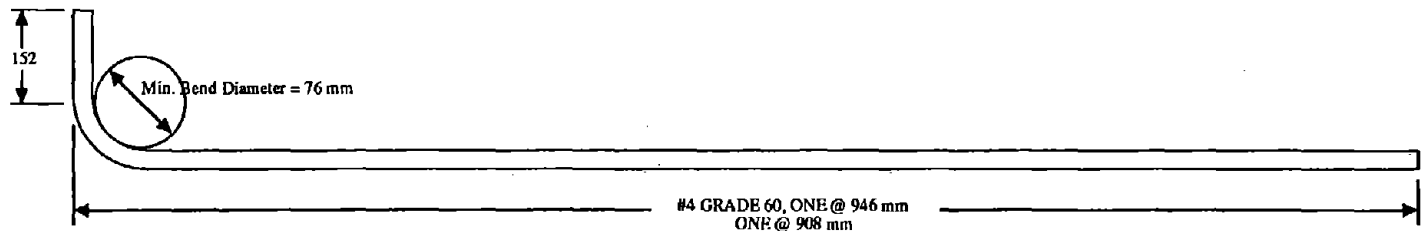


Figure B8. Beam Top View and Longitudinal Reinforcement - J-P-Z4.

All dimensions in mm
25.4 mm = 1 in.

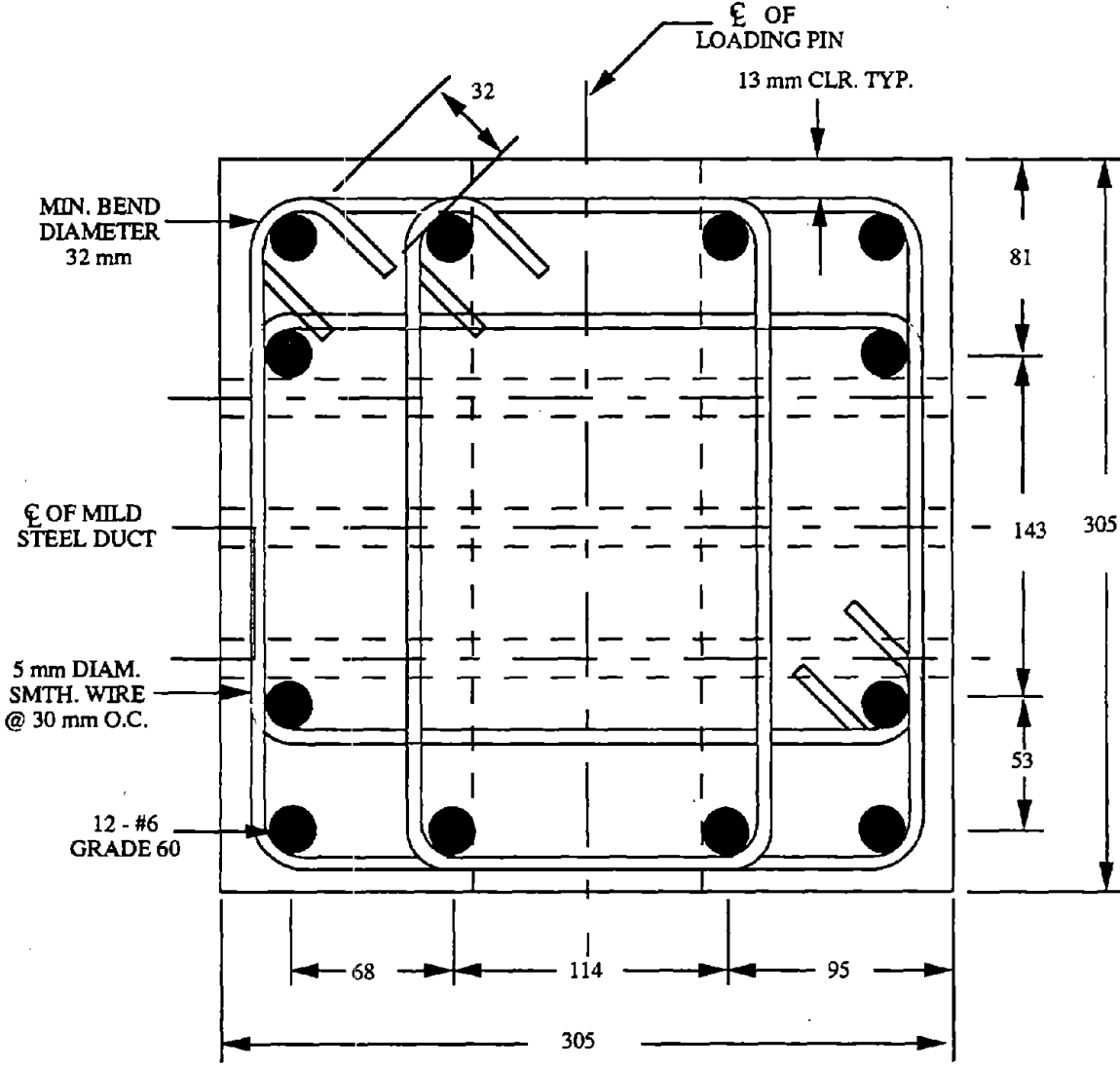
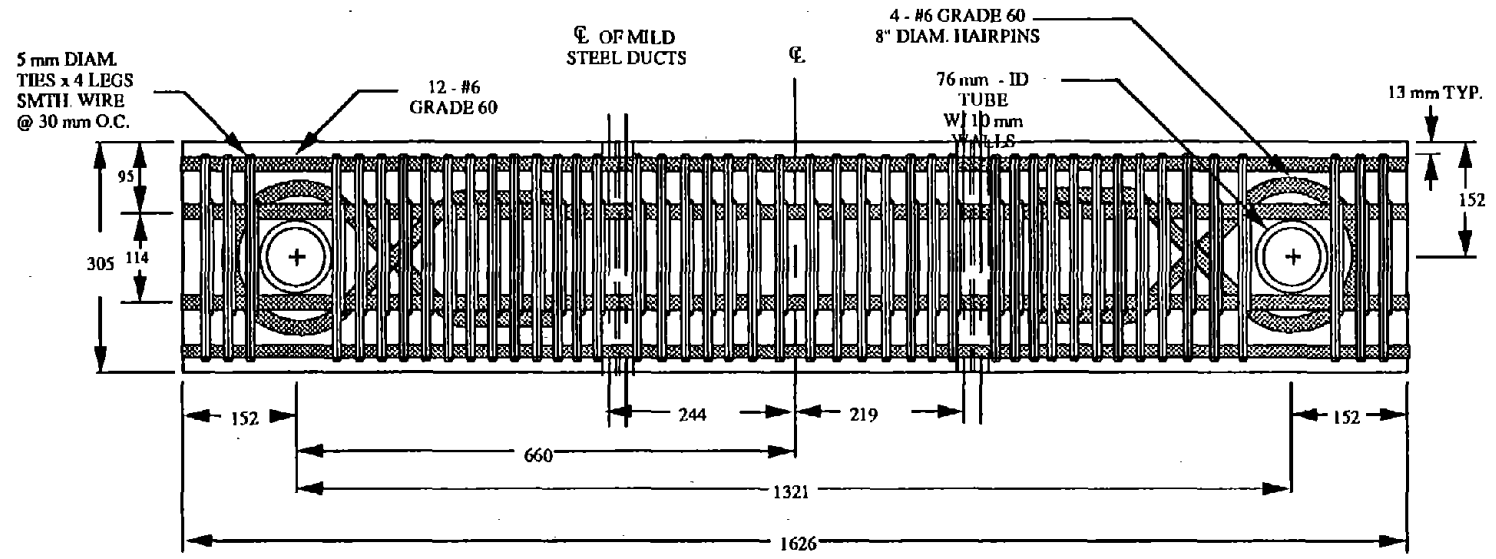
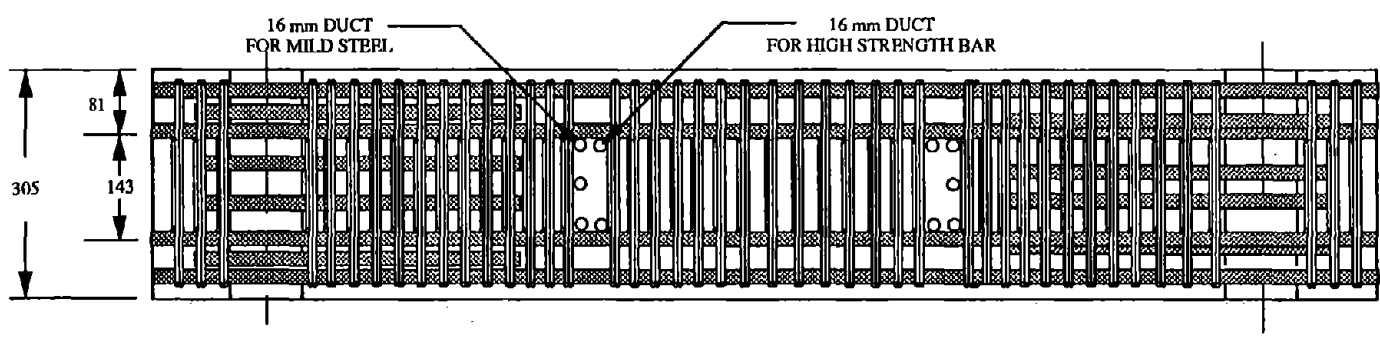


Figure B9. Column Cross Section - J-P-Z4.

All dimension in mm
25.4 mm = 1 in.



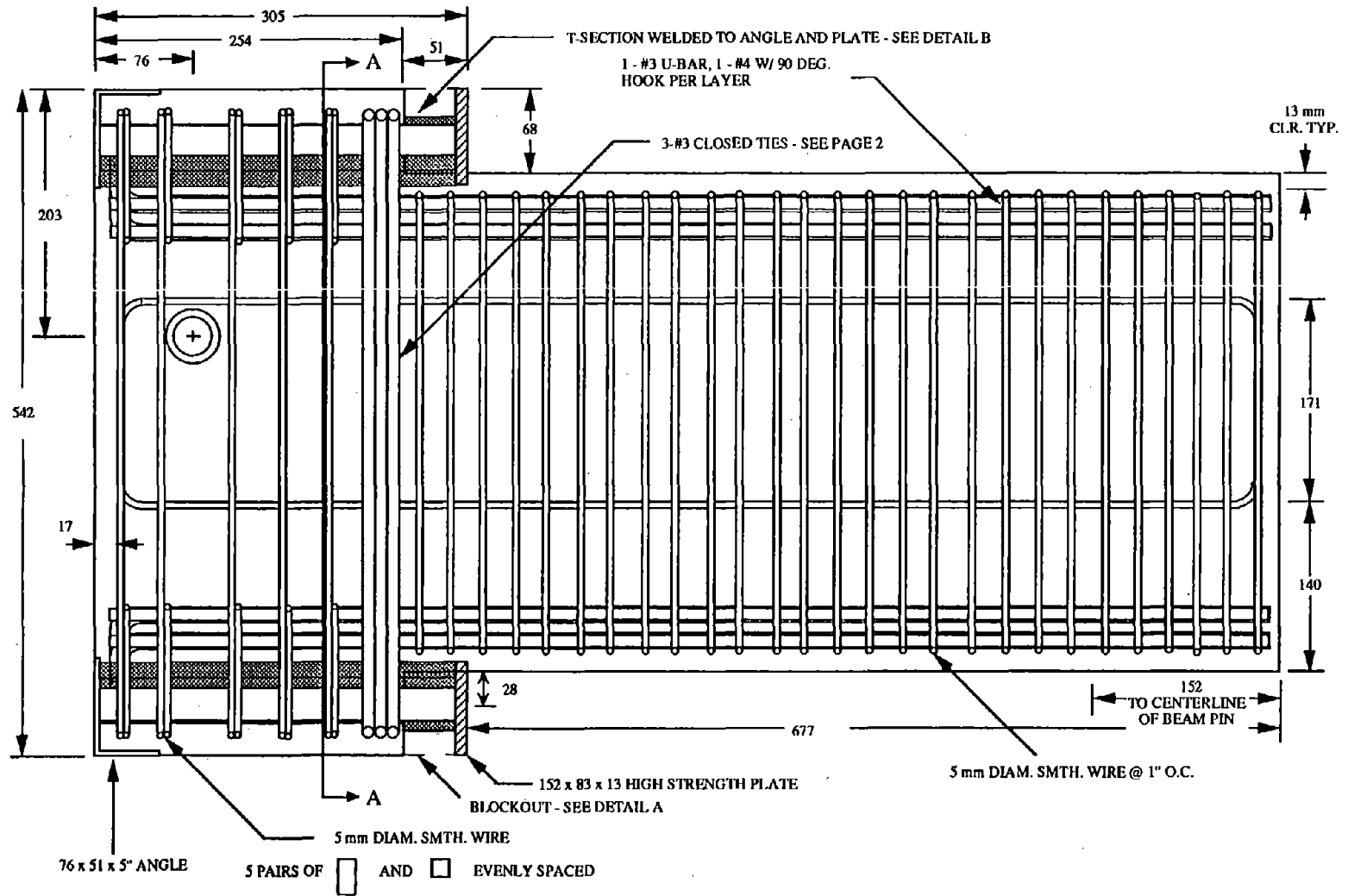
Top View



Elevation

Figure B10. Top and Elevation Views of Column - J-P-Z4.

All dimensions in mm
25.4 mm = 1 in.



88

Figure B11. Elevation View of Beams - L-P-Z4.

All dimensions in mm
25.4 mm = 1 in.

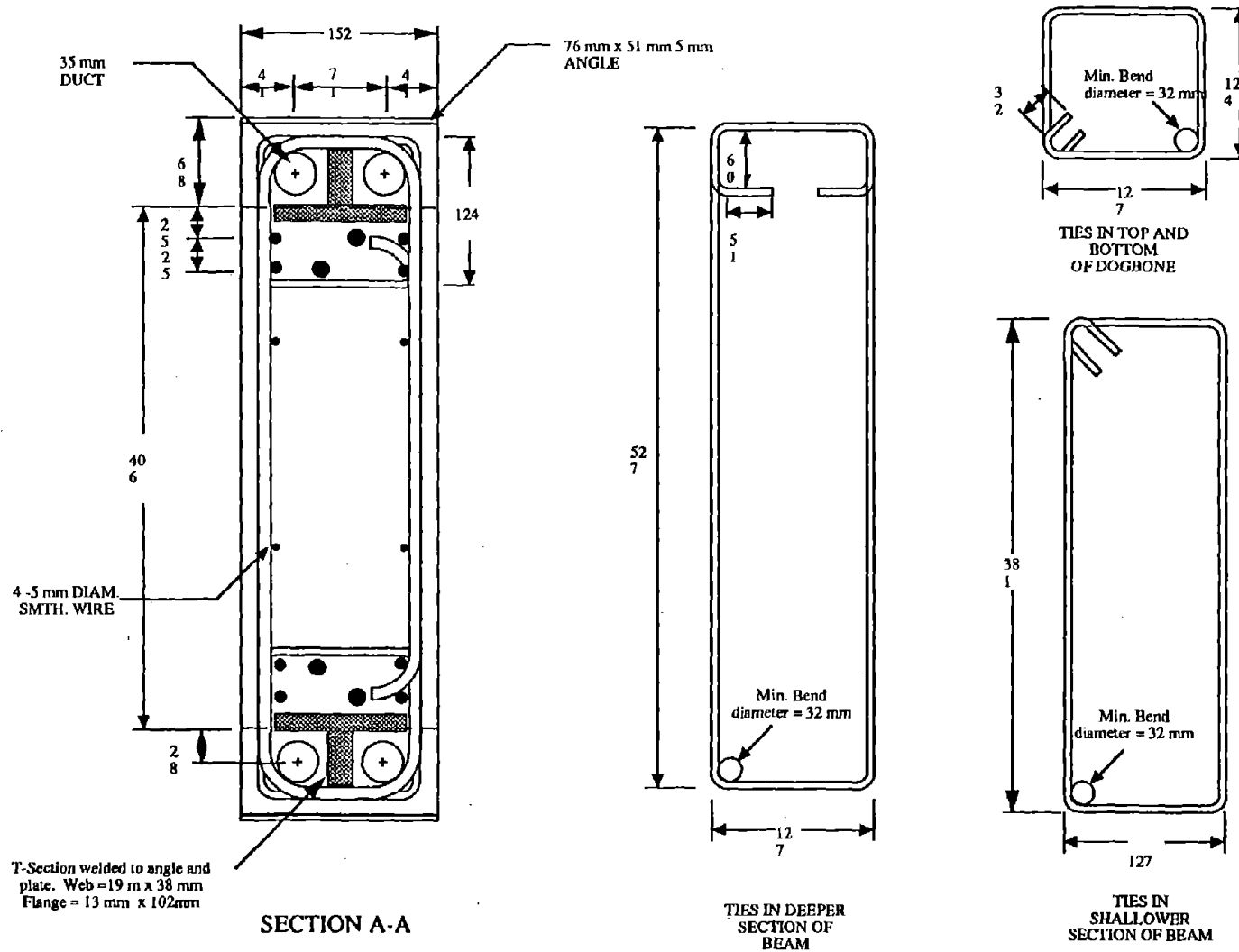
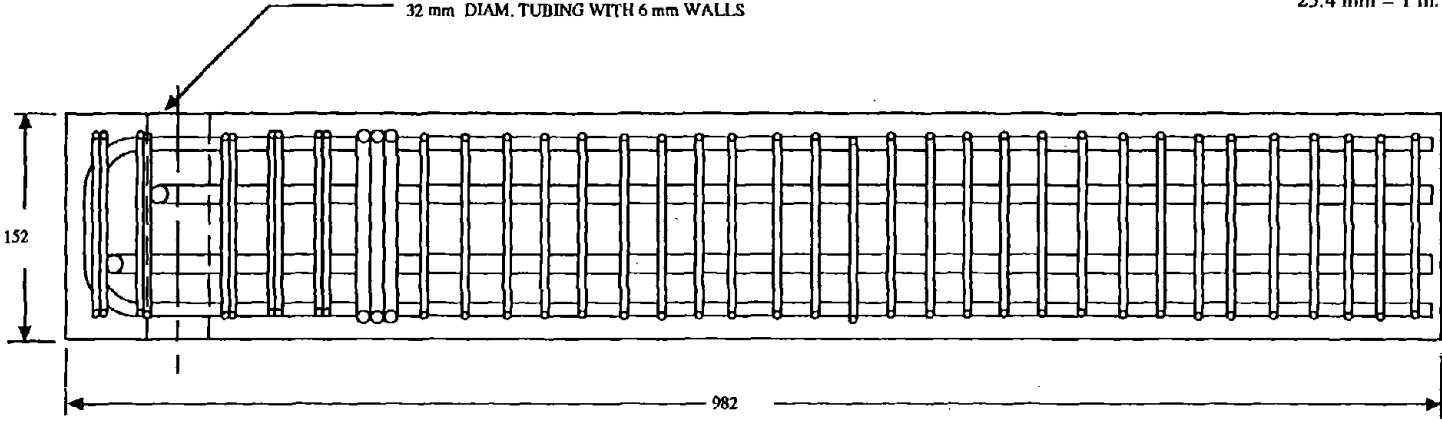
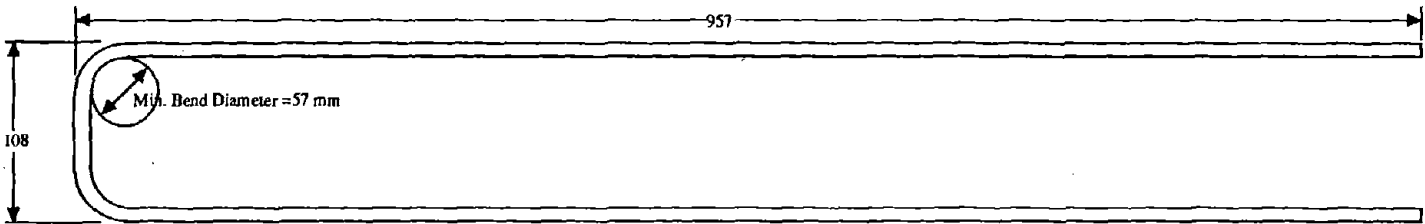


Figure B12. Beam Cross Section and Ties - L-P-Z4.

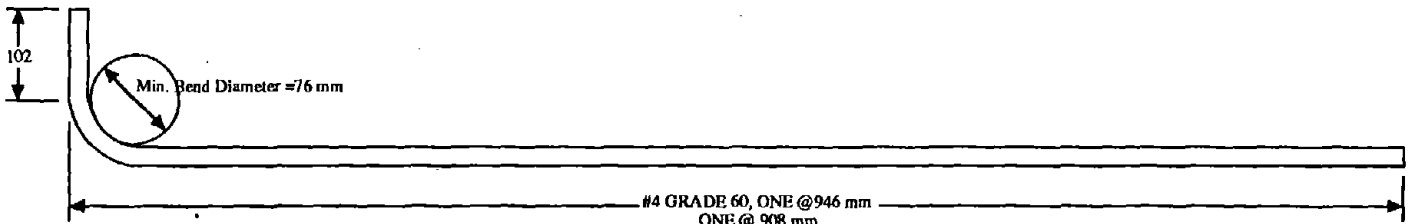
All dimensions in mm
25.4 mm = 1 in.



TOP VIEW



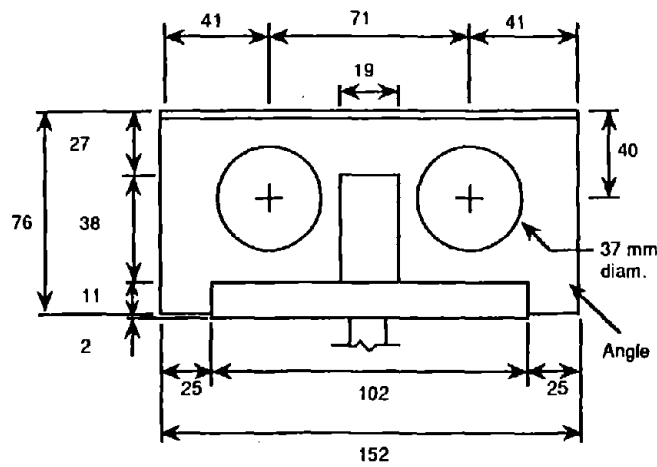
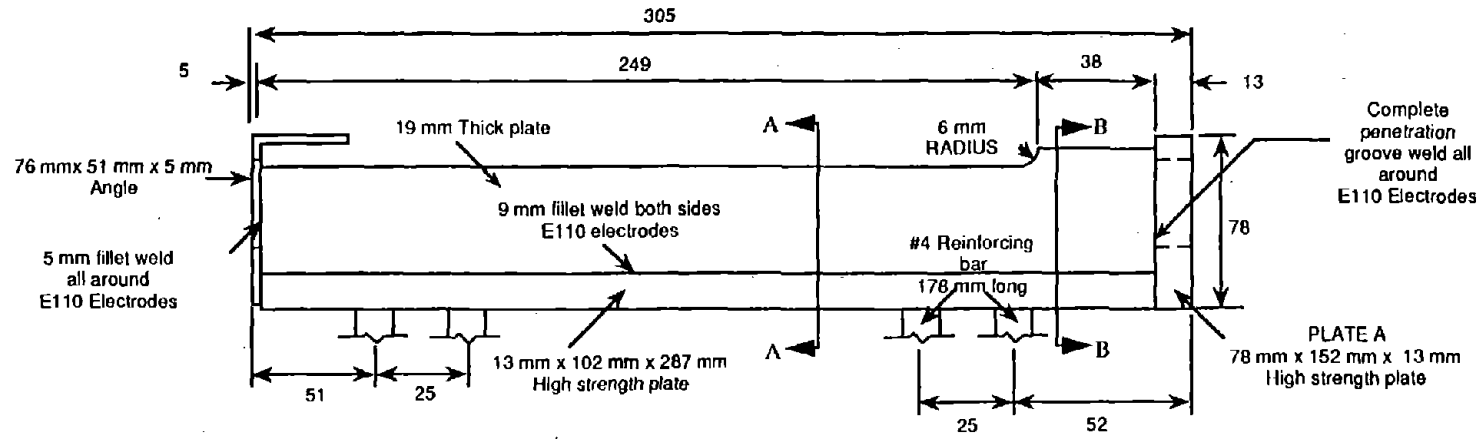
#3 GRADE 60 U-BAR



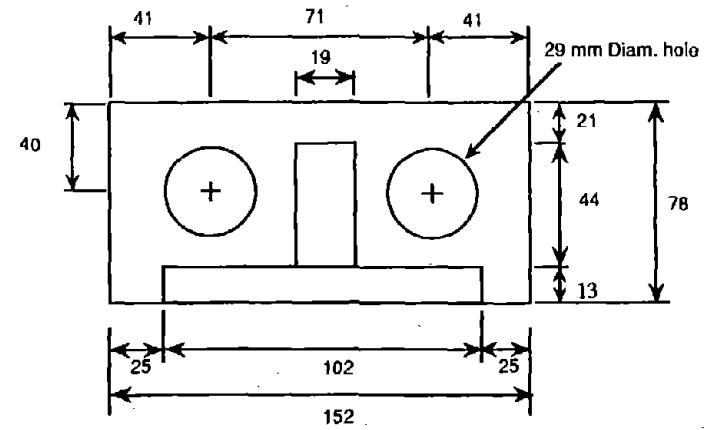
70

Figure B13. Beam Top View and Longitudinal Steel - L-P-Z4.

All dimensions in mm
25.4 mm = 1 in.



SECTION A-A



SECTION B-B

Figure B14. T-Section for L-P-Z4.

71

All dimensions in mm
25.4 mm = 1 in.

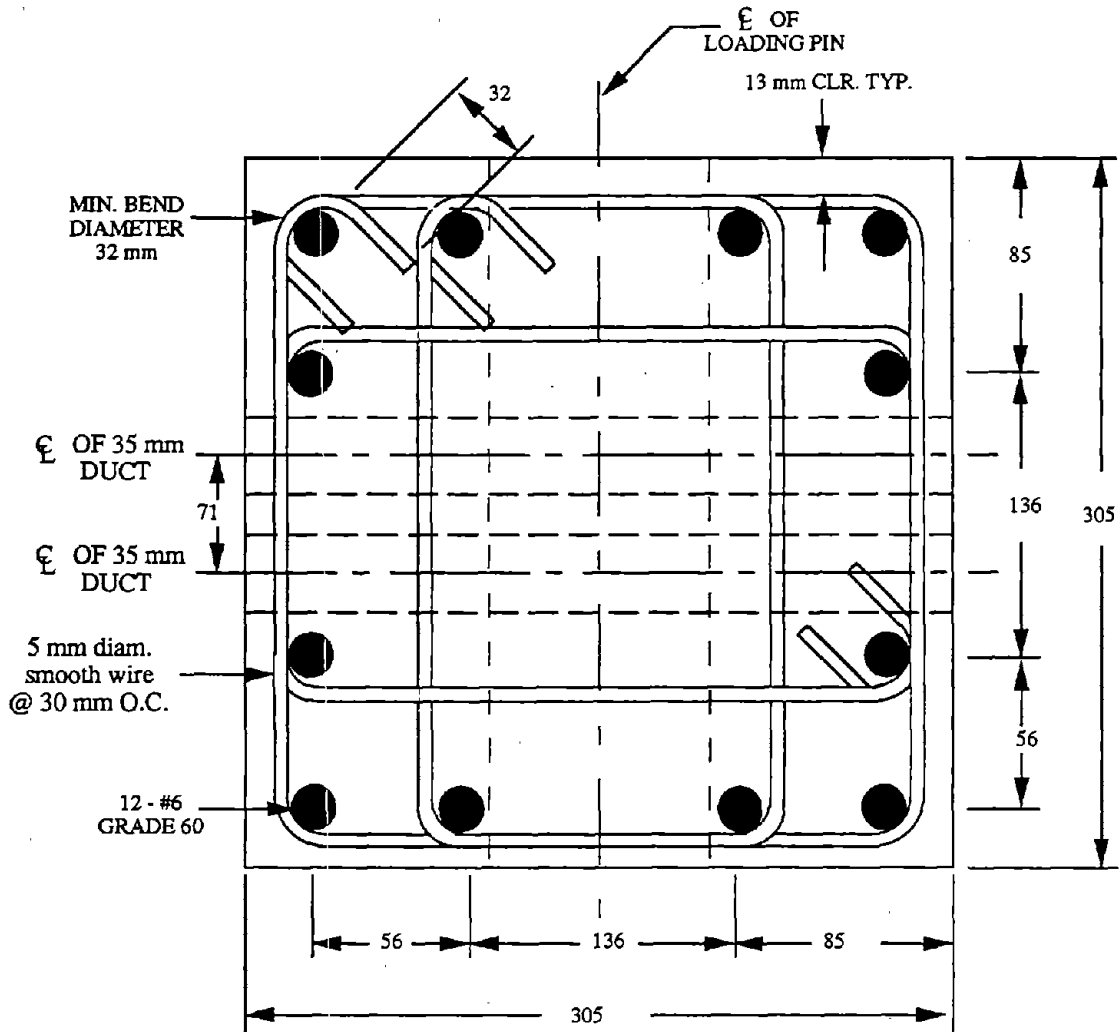
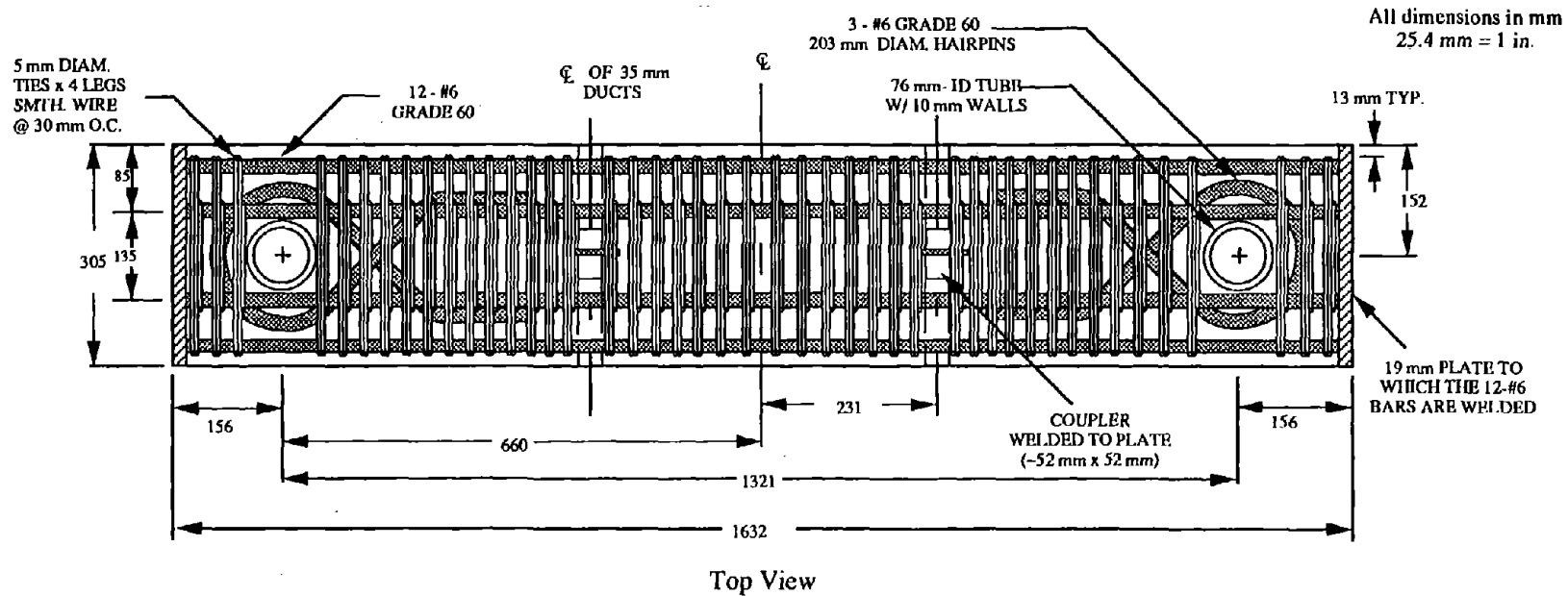


Figure B15. Column Cross Section - L-P-Z4.



73

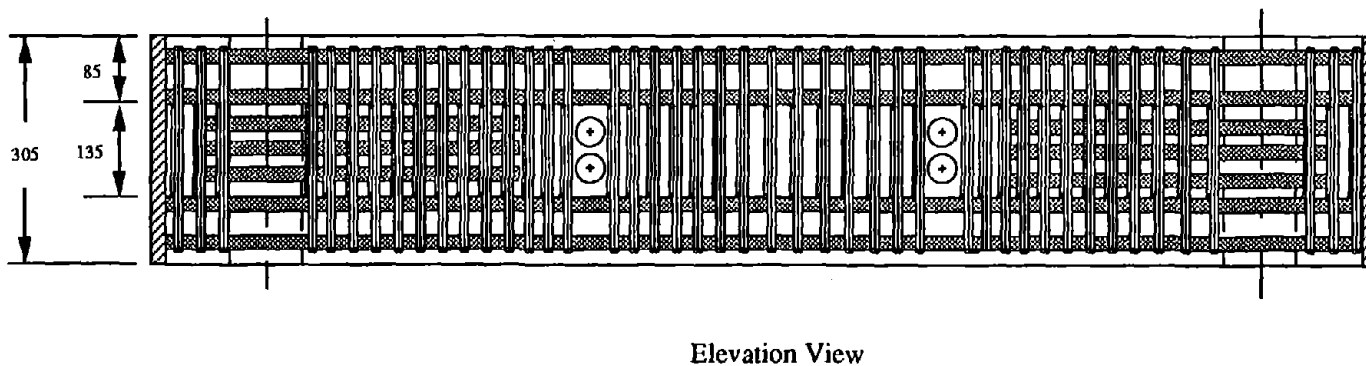
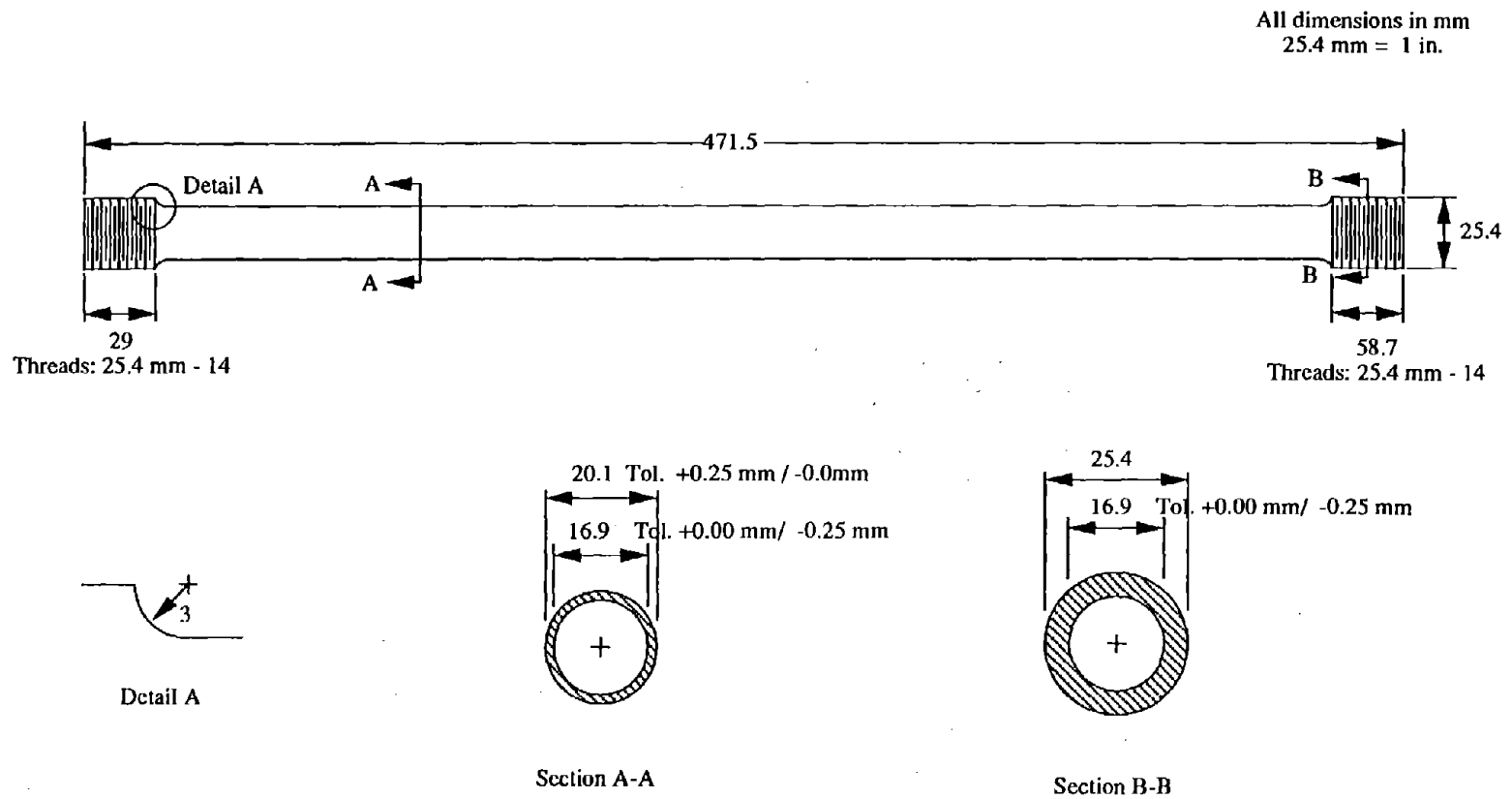


Figure B16. Top and Elevation Views of Column - L-P-Z4.



Material supplied is tube with 15.88 mm ID and 25.4 mm OD made of 1026 steel.

Make 8 pieces

Figure B17. Mild Steel Tube for Specimen L-P-Z4 C.

All dimensions in mm
25.4 mm = 1 in.

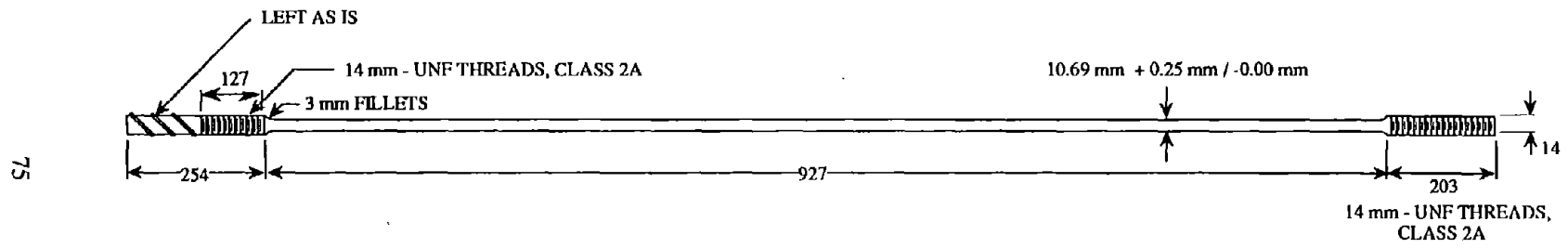


Figure B18. Modified Dywidag Bar.

APPENDIX C: MATERIAL PROPERTIES

Table C1. Concrete and Grout Strengths.

Specimen	Concrete Strength ^a (MPa)	Fiber Reinforced Grout ^a (MPa)	Duct Grout ^a (MPa)
A-M-Z2	43.5	---	---
B-M-Z2	41.1	---	---
A-P-Z2	34.0	87.4	68.3
B-P-Z2	36.4	88.3	70.2
A-M-Z4	30.7	---	---
B-M-Z4	32.2	---	---
A-P-Z4	40.6	73.6	59.9
B-P-Z4	44.5	78.9	65.8
C-P-Z4	46.8	92.1	77.9
D-P-Z4	44.9	88.6	82.0
E-P-Z4	29.2	97.3	78.8
F-P-Z4	27.7	101.4	83.2
G-P-Z4	30.1	84.5	74.7
H-P-Z4	32.3	90.5	86.3
I-P-Z4	40.9	89.6	69.0
J-P-Z4	43.5	77.8	82.1
K-P-Z4	36.6	71.5	64.3
L-P-Z4 A	34.7	62.5	---
L-P-Z4 B	35.8 ^b	71.7	---
L-P-Z4 C	38.0	71.7	---

^a Strengths obtained at day of test.

^b 28-day strength. Specimen was tested at 35 days.

1 MPa = 145 psi

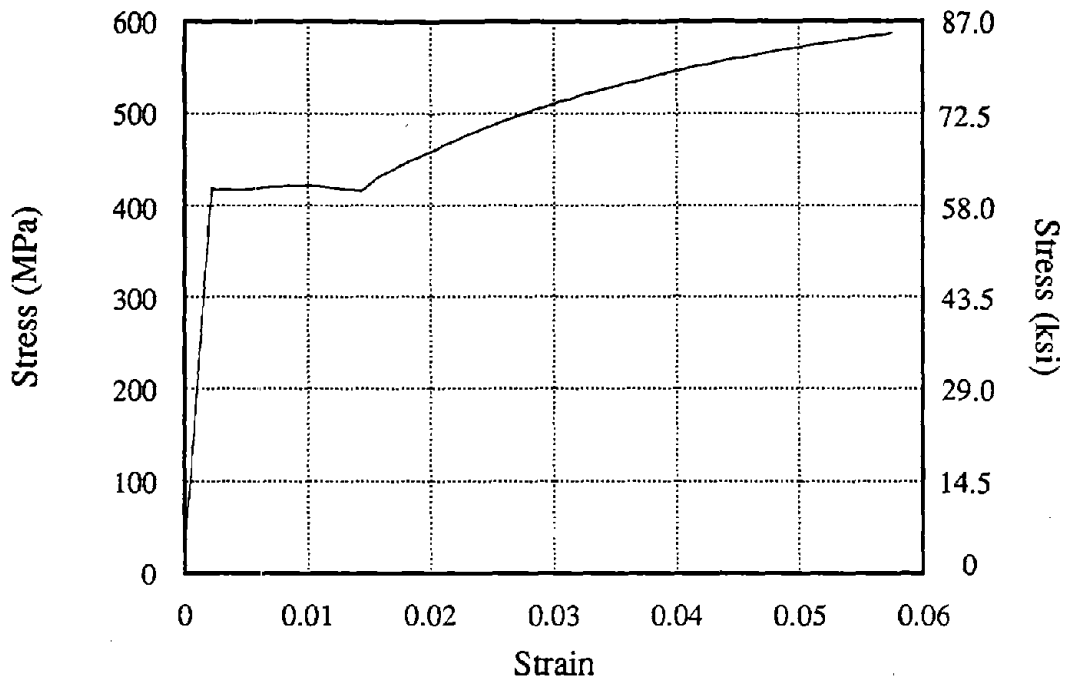


Figure C1. Stress-Strain Curve for #3, Grade 40 Reinforcing Bar.

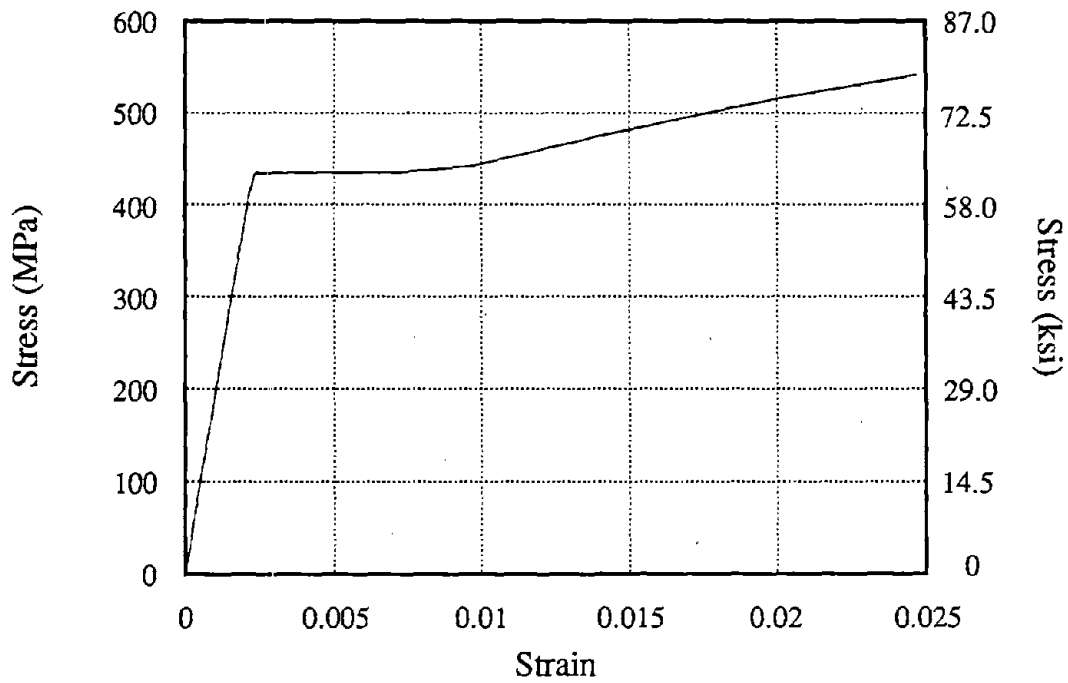


Figure C2. Stress-Strain Curve for #3, Grade 60 Reinforcing Bar.

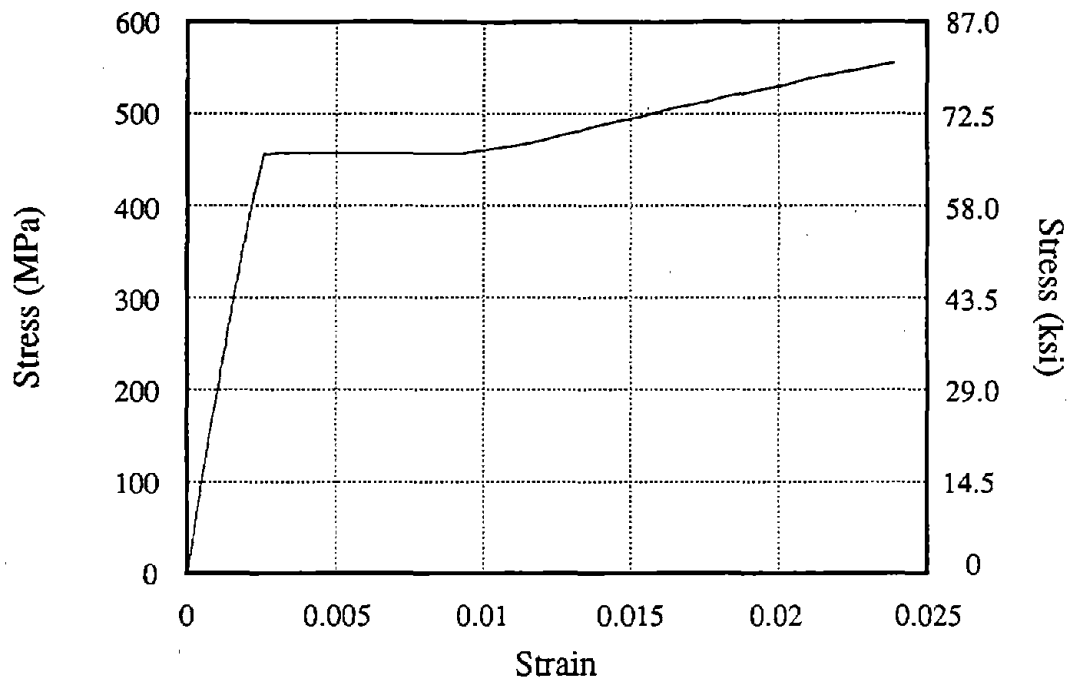


Figure C3. Stress-Strain Curve for #4, Grade 60 Reinforcing Bar.

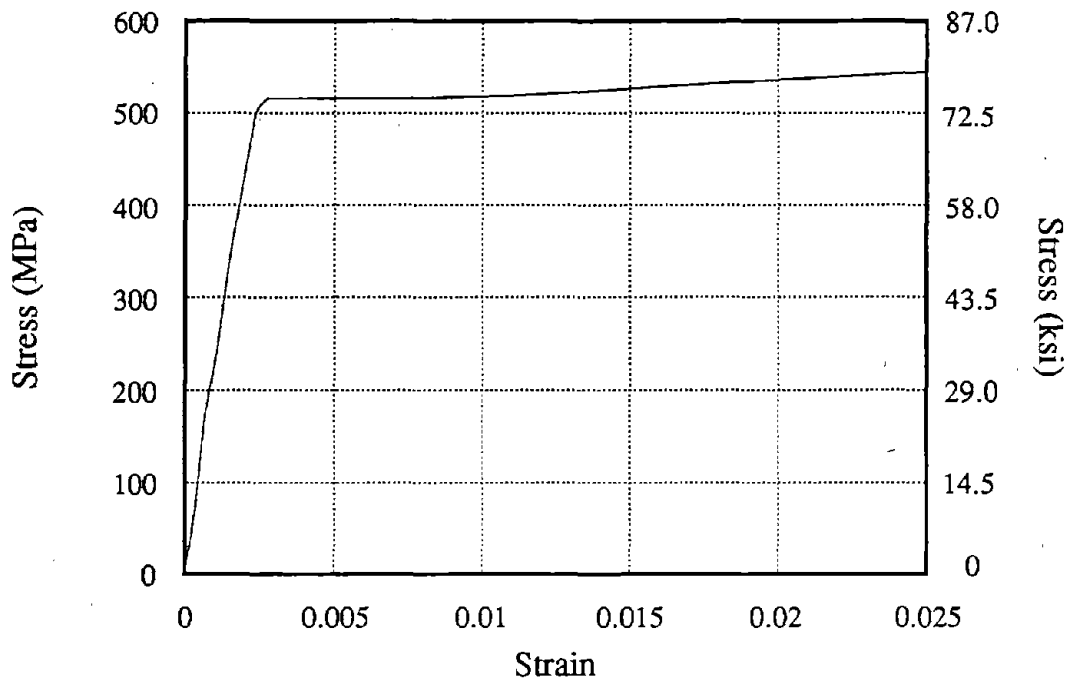


Figure C4. Stress-Strain Curve for Smooth Wire Used for Ties.

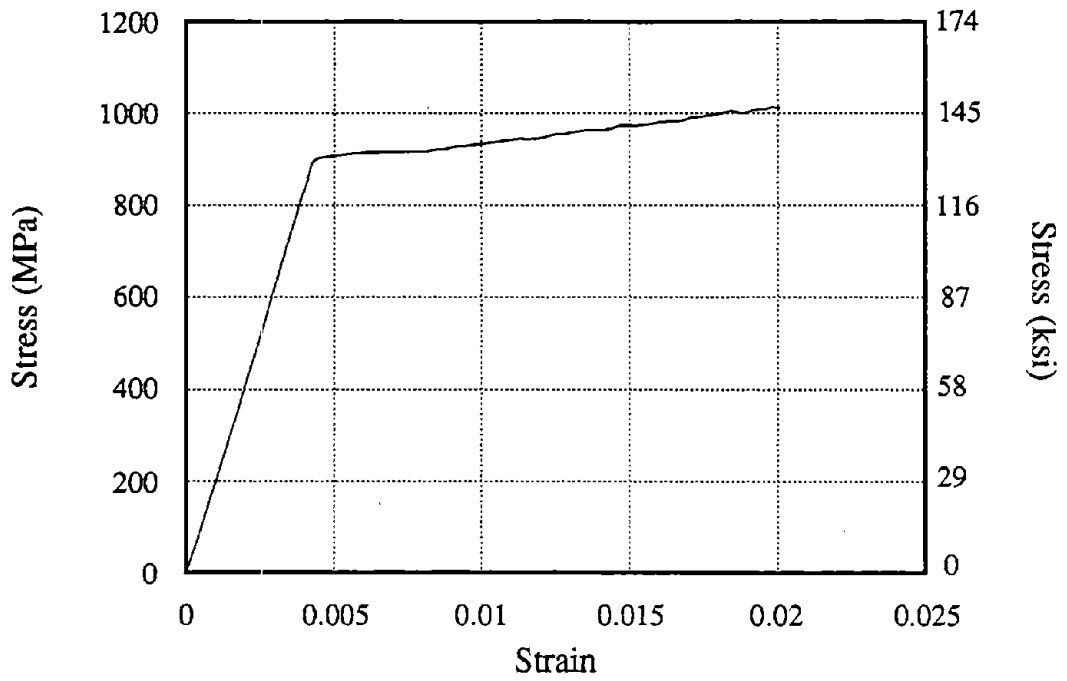


Figure C5. Stress-Strain Curve for Dywidag Bar - J-P-Z4.

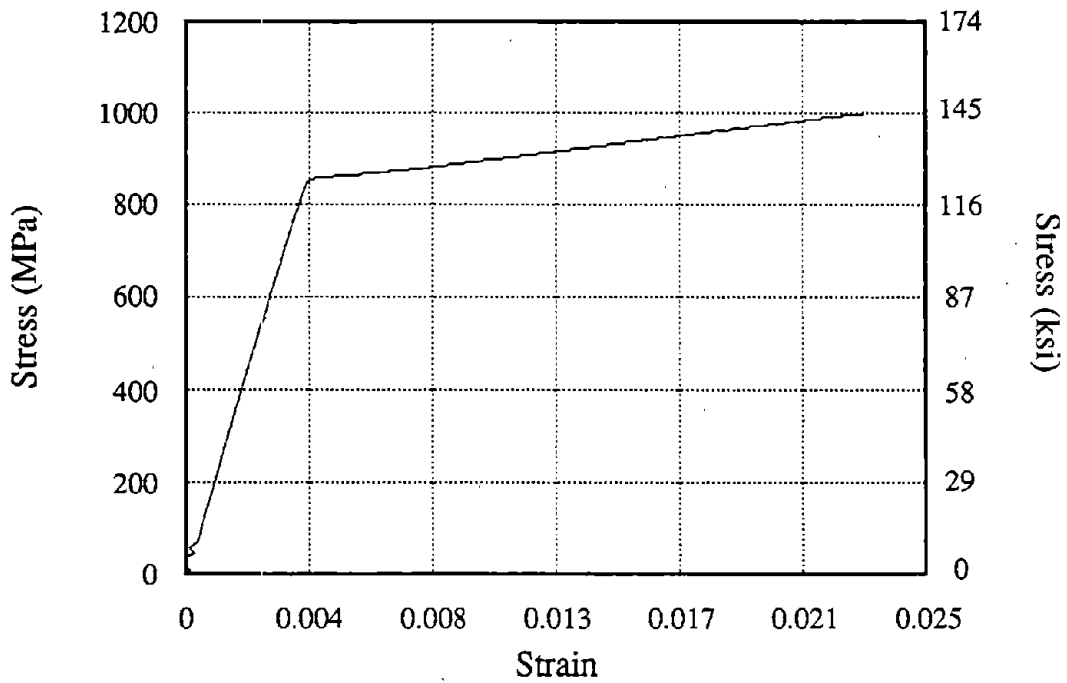


Figure C6. Stress-Strain Curve for Dywidag Bar - L-P-Z4 B.

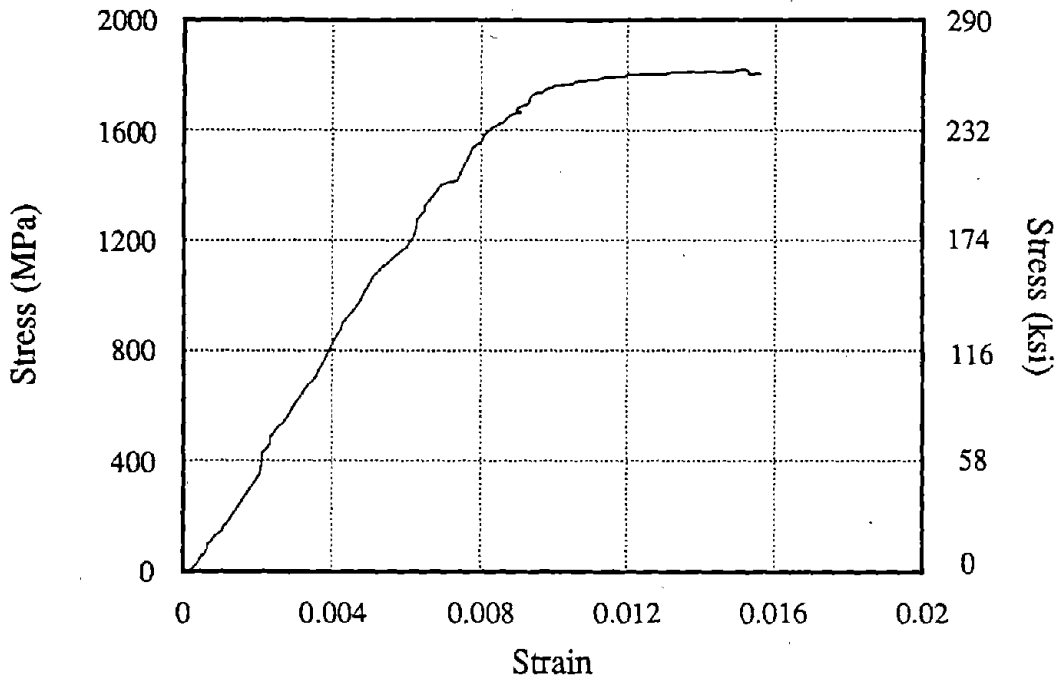


Figure C7. Stress-Strain Curve for 9 mm, Grade 270 Strand - L-P-Z4 C.

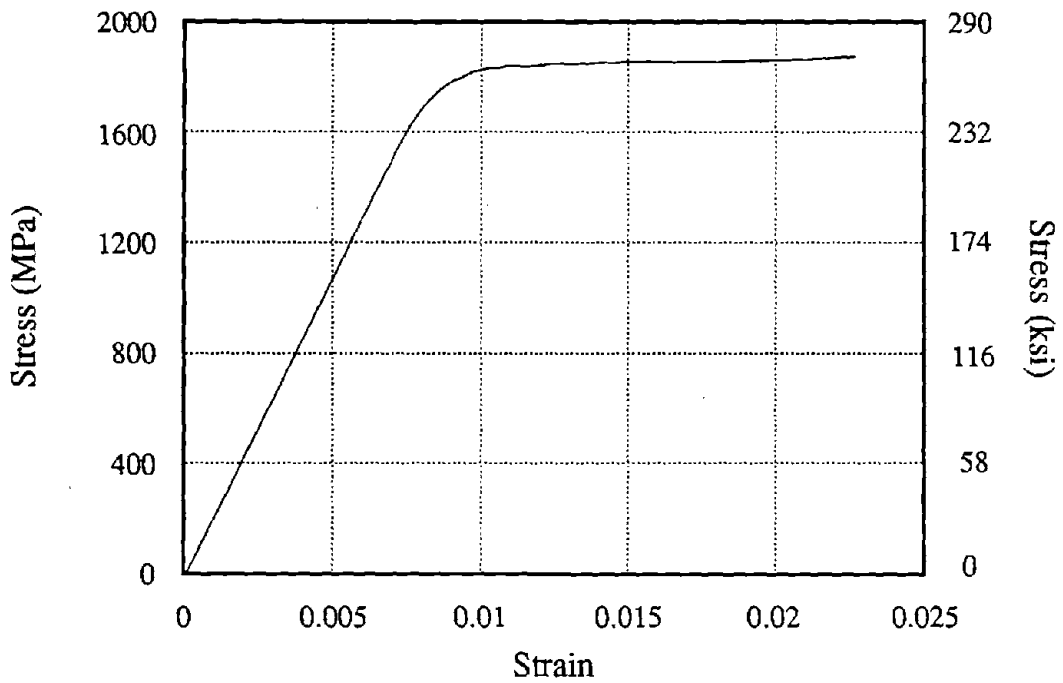


Figure C8. Stress-Strain Curve for 11 mm, Grade 270 Strand - L-P-Z4 A.

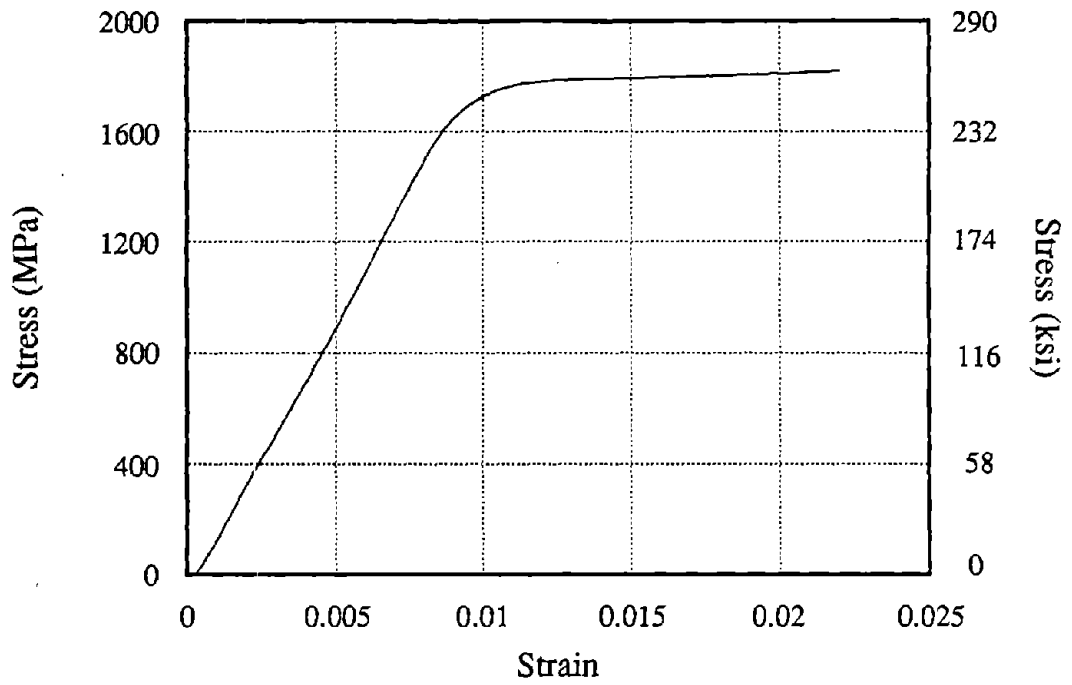


Figure C9. Stress-Strain Curve for 13 mm, Grade 270 Strand - I and K P-Z4.

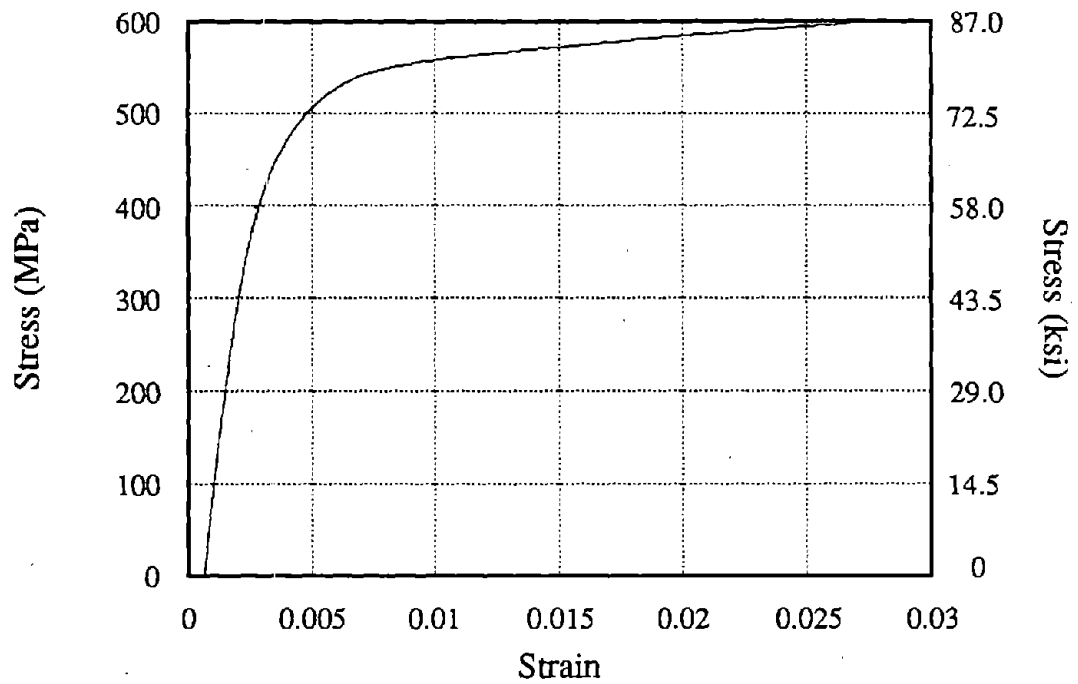
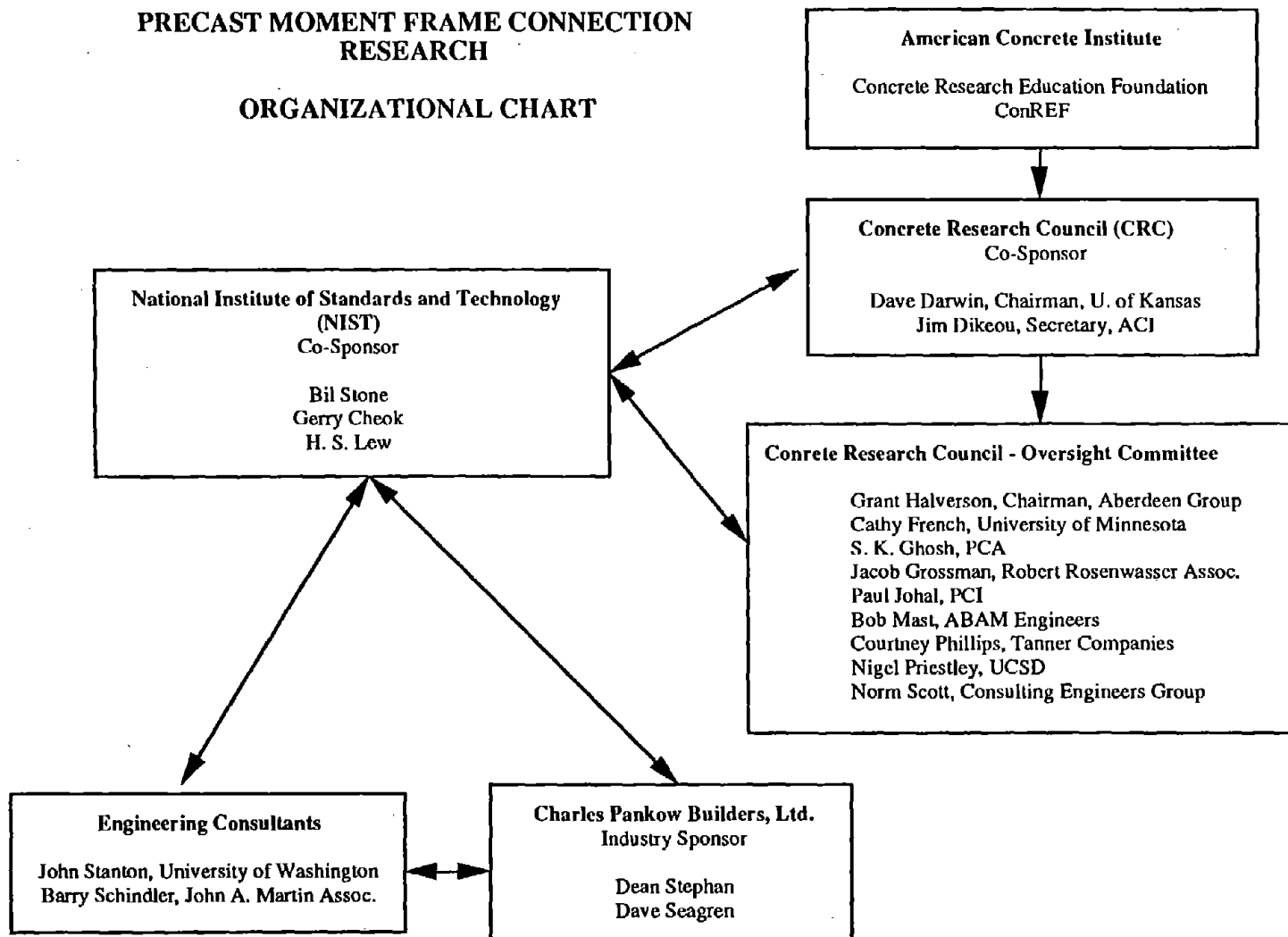


Figure C10. Stress-Strain Curve for 1026 Steel Tube - L-P-Z4 C.

**PRECAST MOMENT FRAME CONNECTION
RESEARCH**

ORGANIZATIONAL CHART



APPENDIX E: DOCUMENTATION FOR PROGRAM B6.FOR

Program B6.FOR is written in Lahey Fortran for a PC. The program requires the file called COMMON.FOR when compiling. The file COMMON.FOR contains all the declaration type statements and common blocks. For precast beam-to-column connections with partially unbonded tendons, this program computes the moments and rotations for:

1. A given geometry, steel areas (mild and PT), and material properties.
2. A given geometry and material properties. The steel areas are changed to meet a user specified target moment and the percentage of total moment contributed by the mild steel.

The program imposes an incremental length change, $gap(j)^1$, on the steel layer (Layer 1) that experiences the highest tensile strains - in a sense, this is an imposed beam rotation. The convention used in this program is compression is at the top of beam and tension at the bottom of beam. This increase in length is converted to a strain level in the steel by dividing the increase in length by the unbonded length. The steel strain is assumed to be equal over the entire unbonded length. The stress in the steel is then obtained from a typical stress-strain curve for that material. The stress-strain curves for each different type of steel are in separate subroutines and are comprised of a series of points that define the curve. For values that fall between these pre-defined points, the stresses are obtained by linear interpolation.

The changes in length and therefore the strains in the other layers of steel are determined through the use of similar triangles using the top most layer, layer(n), of steel as the initial assumed "pivot" point. The distance between the steel in layer 1 to this pivot point is defined as the distance y as shown in Fig. E1. The forces in each layer of steel, tension and compression, are then calculated.

¹Alphanumeric characters in *italics* are the variable names as used in program b6.for

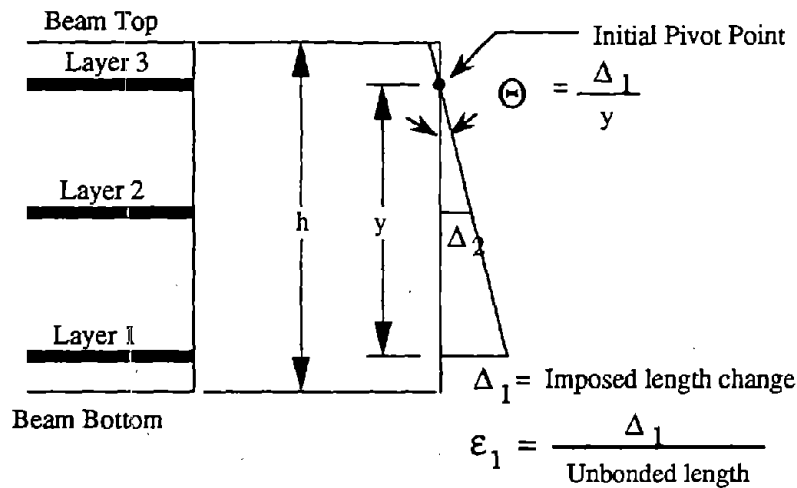


Figure E1. Determination of Length Change in Steel Layer.

The program then computes the concrete compression force, C_c [cc]. This is done by starting with an initial value for the neutral axis depth, $NA(j)$, 0.1 in. For steel strains in Layer 1 less than yield, C_c is computed using the following equation:

$$C_c = 0.5 \times f'_c \times b \times NA \quad (E-1)$$

where

f'_c = concrete compressive strength

b = beam width

NA = Neutral axis depth

For steel strains in Layer 1 greater than or equal to yield, C_c is computed using the following equation:

$$C_c = 0.85 \times f'_c \times b \times \beta_1 \times NA \quad (E-2)$$

where

β_1 = Factor as defined in ACI 10.2.7.3 [ACI, 1989]

The program will then check for equilibrium of the forces. As the neutral axis depth is small to begin with, the total compression force [*ctot*] will always be less than the total tension force [*ptot*] and the program will increment the neutral axis depth until a force balance is found. Equilibrium is satisfied if the difference between the tension and compression forces is less than or equal to a set tolerance [*tol_force*]. This tolerance is presently set to 5% of the total tension force.

The location of the "pivot" point is checked next. In this program the pivot point is defined as the centroid of the compression forces. If the difference between the actual y value, *y_act*, and the initial assumed y value is greater than a set tolerance [*tol_y*], then the program will recalculate the strains in each layer of steel based on this new y value. The tolerance on y is equal to 5% of the initial y value. The procedure to compute C_c is repeated. If the actual y and the initial assumed y value are within the tolerance, the program computes the moment [*mom(j)*], rotation [*theta(j)*], the fraction of the total moment that is contributed by the mild steel [*momratio(j)*], shear at column face [*shear(j)*], and the resistance provided by the friction between the beam and the column [*v_prov(j)*]. A check is made to see if the provided shear resistance is greater than the applied shear and the number of times this check is failed is tabulated in the variable *shear_count*. The rotation, *theta*, is defined as the *gap(j)* divided by *y_act*. The story drift is then set equal to this rotation. This definition of story drift is not entirely correct as it does not account for other components which contribute to the story drift such as joint shear deformation, elastic column deformation, inelastic beam deformations, etc.

If a target moment [*targetmom*] is set, the program will check if the maximum moment capacity of the section [*maxmom*] is within 0 [*lowermom*] to 5% [*uppermom*] of the target moment. If the maximum moment is less than the target moment, the amount of mild steel in layer 1 [*a(1)*] and layer n (n = total number of steel layers) [*a(n)*] is increased and vice versa. If the maximum moment is within the tolerance, the program will then check if the ratio of the moment contributed by the mild steel to the total moment [*targetmratio*] is within 0 [*lowerratio*] to 2% [*upperratio*] of the target ratio. If the ratio is less than the target ratio, the amount of PT steel is decreased. If the ratio is greater than the target ratio, the amount of PT steel is increased. The procedure described in the previous paragraphs is repeated.

The program terminates when bar fracture is encountered in steel layer 1 or a beam rotation/story drift of 5% is reached or when the number of solutions is greater than 2000. The output file contains the time and date that the program was executed. Therefore, a problem may arise from the differences in format between systems for the time and date. The variable that stores the time [*time1*] is in A11 format and the variable that stores the date [*date1*] is in A8 format. The subroutines that call for the time and data in subroutine OUTPUT and the write statements for the time and date may be commented out or changed if a problem is encountered. If the formats of the time and date are changed, changes to the declaration statements in the file COMMON.FOR will also have to be made.

A flowchart of the program is given in Figs. E2 - E5 and a program listing is given at the end of this appendix.

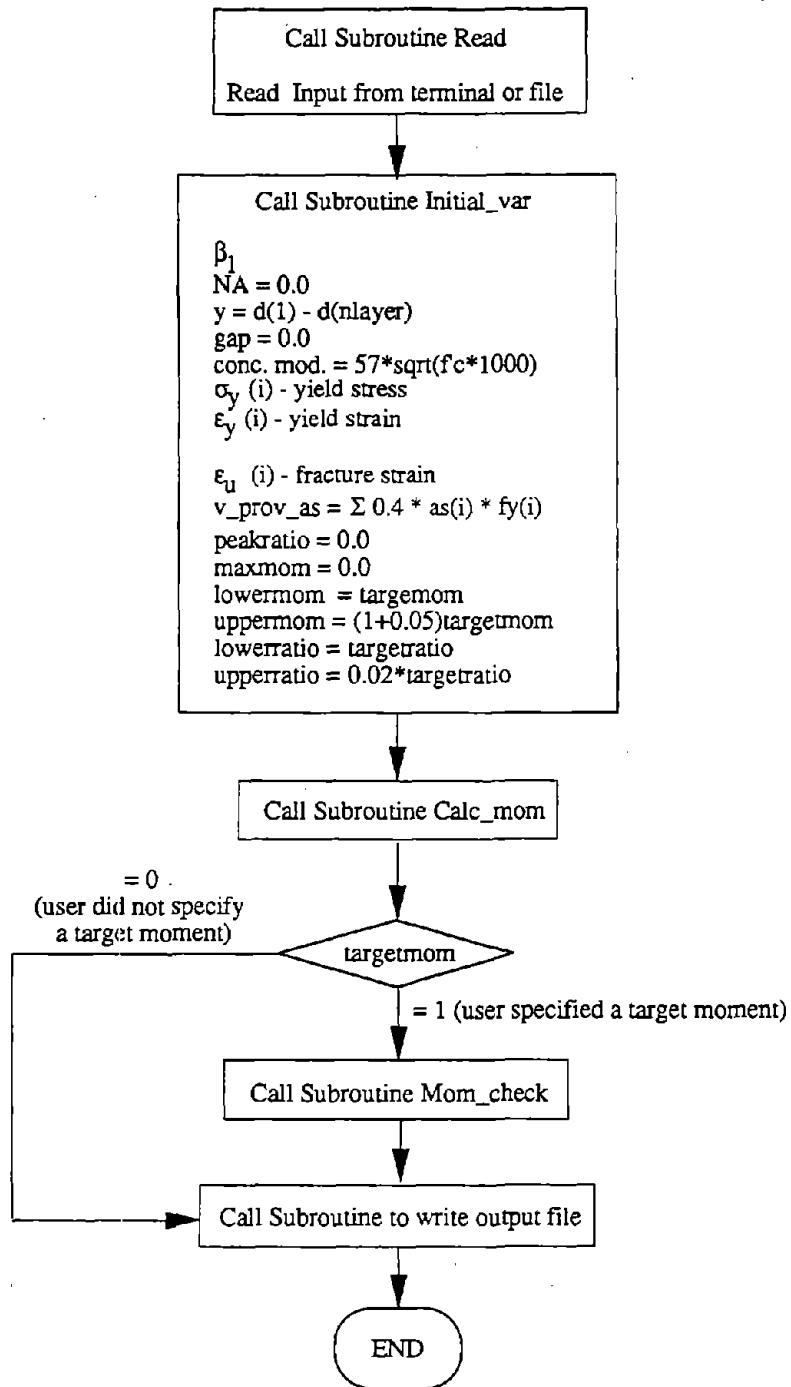


Figure E2. Flowchart for program B6.FOR.

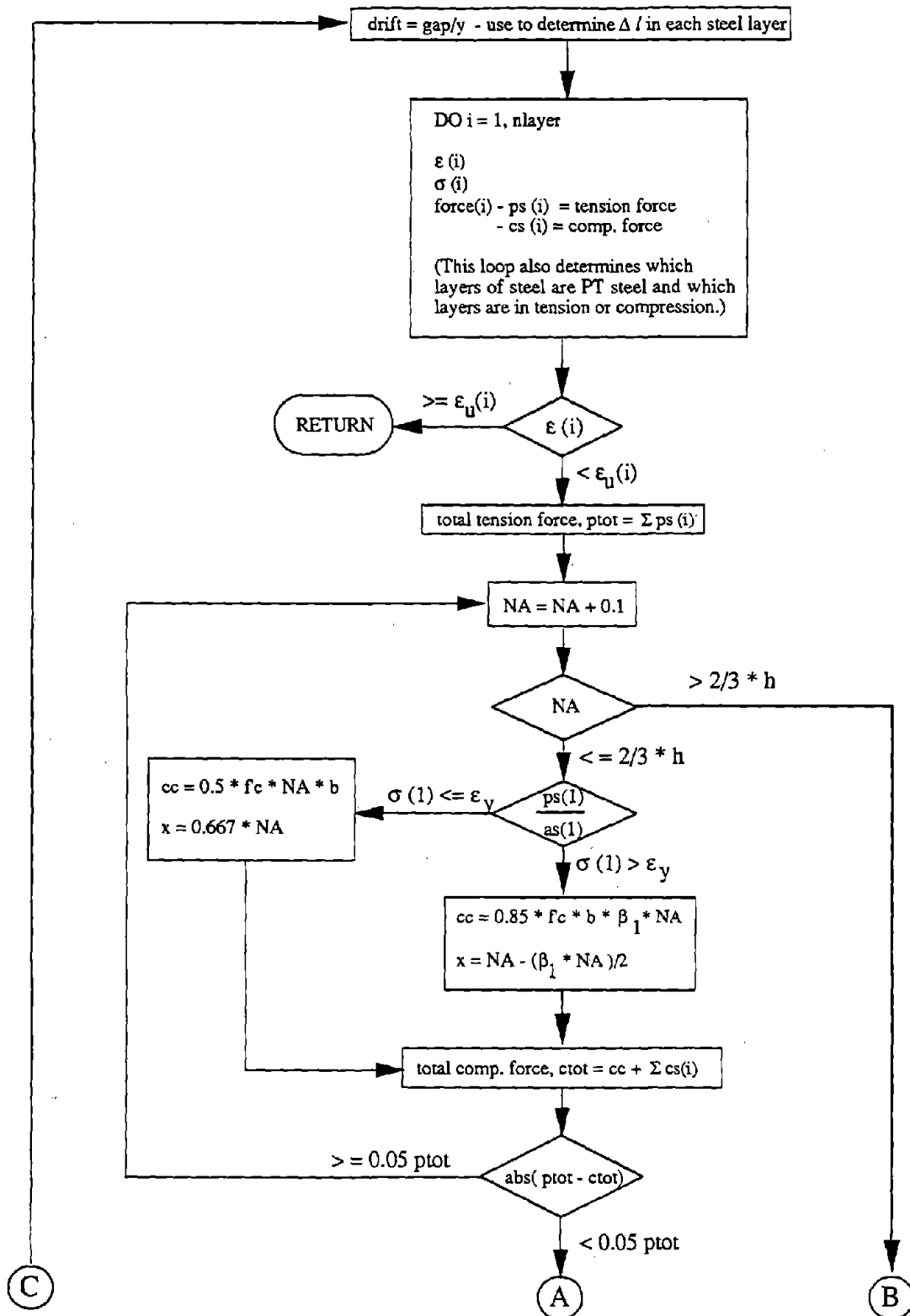


Figure E3. Flowchart for Subroutine Calc_mom.

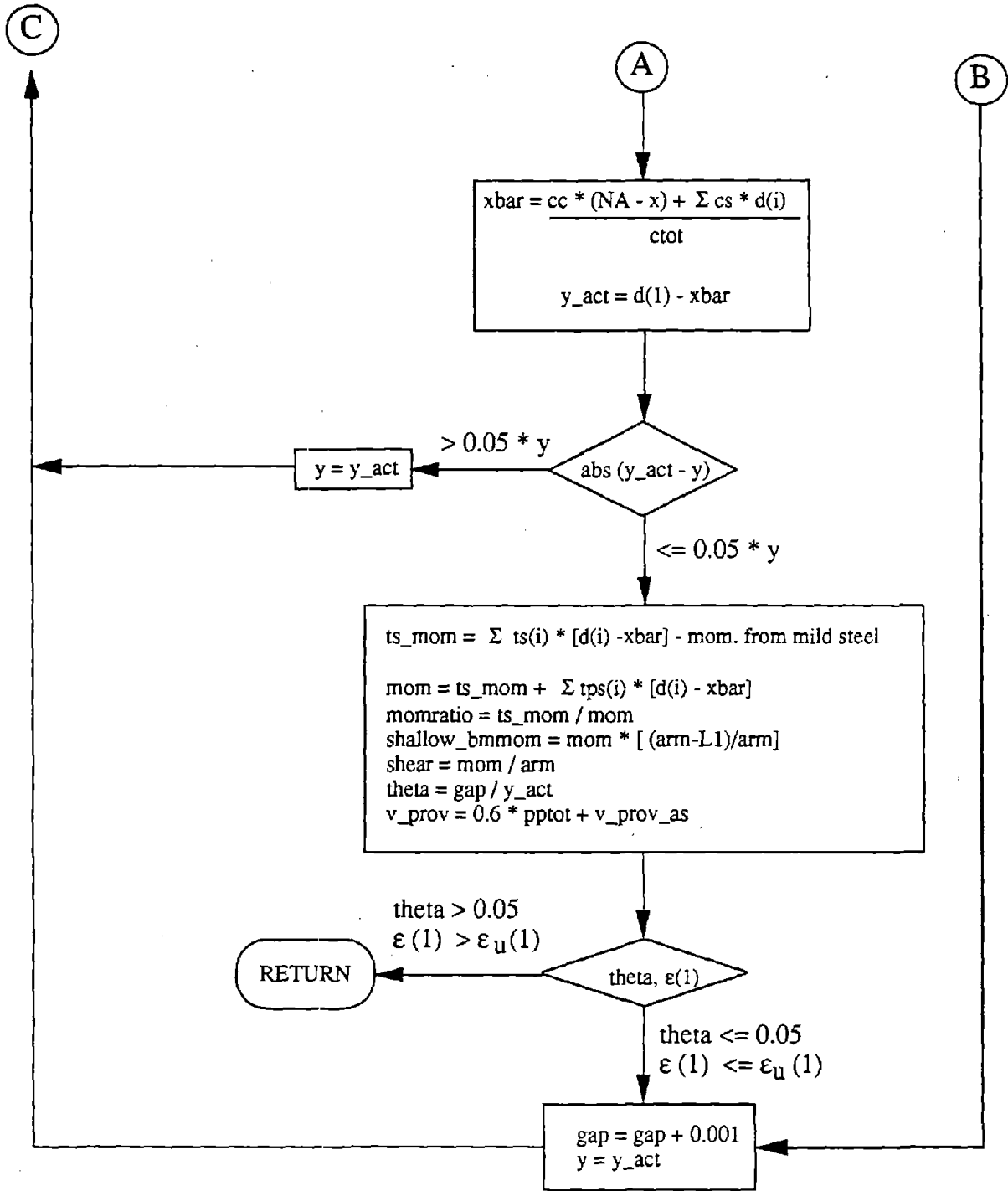


Figure E4. Flowchart for Subroutine Calc_mom (cont.).

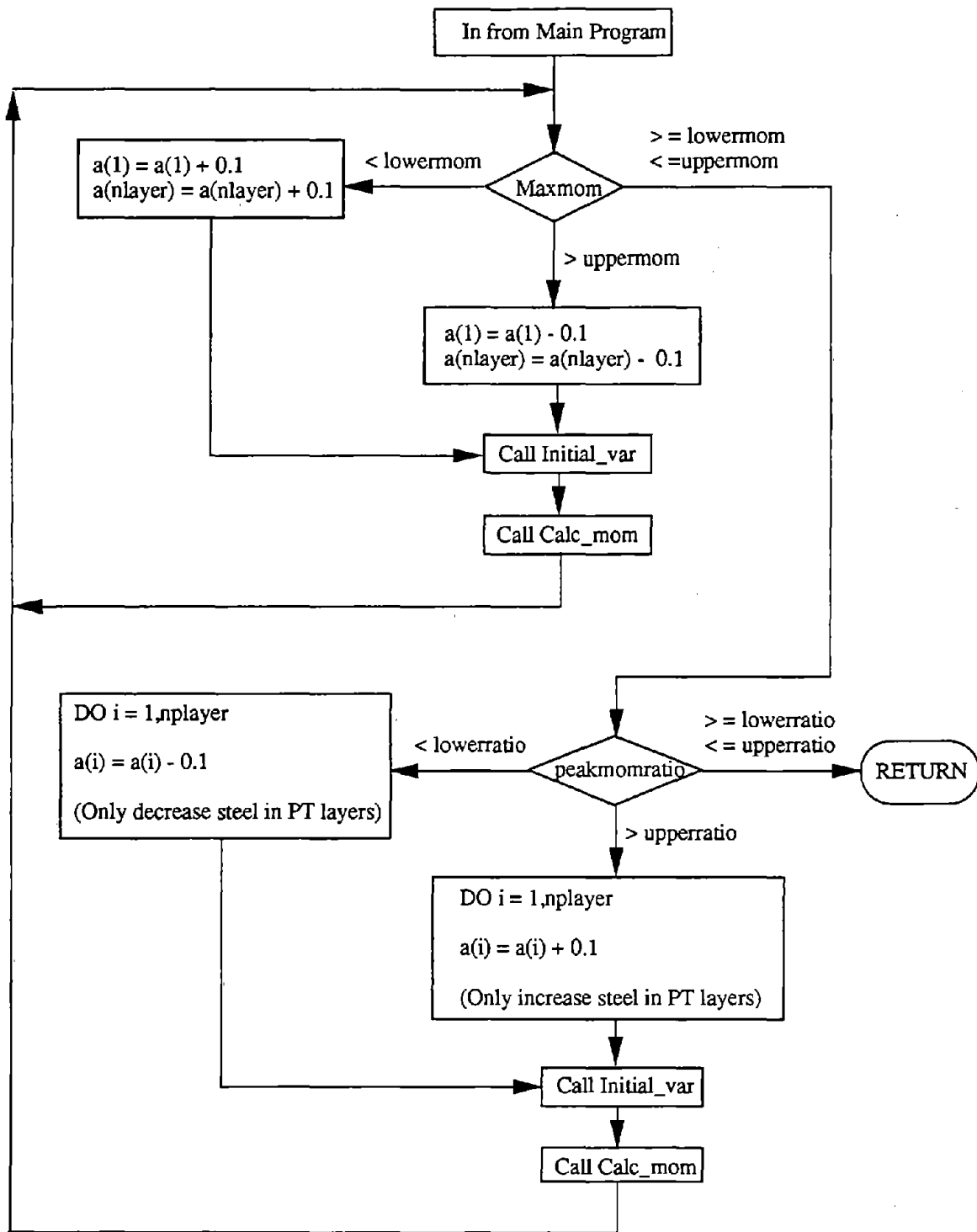


Figure E5. Flowchart for Subroutine Mom_check.

In the output file, the columns headings and their explanations are as follows:

<i>Theta</i>	Beam rotation in radians
<i>Delta</i>	The imposed change in length of the steel in layer 1, in.
<i>Non-PT</i>	The total tension force from the mild steel, k.
<i>PT</i>	The total tension force from the PT steel, k.
<i>Xbar</i>	The distance from the top of the beam to the centroid of the total compression force, in.
<i>Mcol</i>	Moment in the beam at the column face, k-ft.
<i>Mbm</i>	Moment in the beam at the point in which the mild steel ends in the beam, k-ft.
<i>Shear</i>	Shear force at the column face due to applied moment, k.
<i>Ms/Mtot</i>	Ratio of moment provided by mild steel to total moment.
<i>V_{prov}</i>	Shear resistance provided by friction between the beam and the column caused by the PT force and the shear resistance of the mild steel, k. This is equal to $0.6 (PT \text{ force}) + 0.4 A_s f_y$
<i>V_{Check}</i>	An asterisk (*) in the output column means that the provided shear is less than the applied shear. If no asterisk appears the provided shear is greater than the applied shear.

Note: 1 in. = 25.4 mm
 1 k = 4.448 kN
 1 k-ft = 1.356 kN-m

The type of steels that are available for use with this program are:

<u>Type</u>	<u>Steel</u>
1	A36
2	Grade 40, reinforcing bar
3	Grade 60, reinforcing bar
4	Stainless steel 304
5	1026 Steel tube
6	7/16", 7-wire strand, grade 270
7	3/8", 7-wire strand, grade 270
8	1/2", 7-wire strand, grade 270

The format of the input file is free and the order of the input data is as follows:

line 1: Title line (80 characters) - *Title1*
 line 2: Title line (80 characters) - *Title2*

- line 3: Title line (80 characters) - *Title3*
- line 4: Name of output file including file extension (20 characters) - *Outfile*
- line 5: f_c (ksi) - *fc*
- line 6: f_{pe} (ksi) initial PT stress after losses - *fpe*
- line 7: Total number of layers of steel - *nlayer*
- line 8: Type of steel in layer i , where $i = 1, nlayer$ - *type(i)*
- line 9: Area of steel in layer i (in**2) - *a(i)*
- line 10: Distance from top of beam to steel (in.) - *d(i)*
- line 11: Debonded length of steel (in.) as measured from the center of the column.
Use a value of 1 for totally bonded steel - *lunb(i)*

Repeat lines 8 - 11 n times for n layers of steel

- line 12: Length of mild steel from column face to point where it ends in the beam
- the dogbone length. This used to be the dogbone length. (in.) - *L1*
- line 13: 1/2 the clear span between the columns (in.) - *arm*
- line 14: Width of beam (in.) - *b*
- line 15: Height of beam (in.) - *h*

The input order for the steel layers is the first layer of steel, layer 1, should be the one closest to the beam bottom (highest tensile strains) and the last layer of steel, layer n , should be the one closest to the beam top (highest compressive strains). The following list is a sample of an input data file - characters in [] are descriptions of the input values and are not included in an actual input file.

Sample Input File

Col 1
↓

line 1:	Test run case T2	[title/description line 1]
line 2:	20% of moment from Gr.60 Bars, 80% from 1/2 PT strand	[title/description line 2]
line 3:		[title/description line 3]
line 4:	t2.out	[output file name with extension]
line 5:	5	[f' _c]
line 6:	189	[f _{pe}]
line 7:	3	[Total number of steel layers]
line 8:	3	[Steel type of layer 1, grade 60 rebar]
line 9:	1.2	[Area of steel in layer 1]
line 10:	45	[Dist. from top of beam to centroid of steel layer 1]
line 11:	5	[Unbonded length of steel in layer 1]
line 12:	6	[Steel type in layer 2, 7/16" PT strand]
line 13:	2.57	[Area of steel in layer 2]
line 14:	24	[Dist. from top of beam to centroid of steel layer 2]
line 15:	36	[Unbonded length of steel in layer 2]
line 16:	3	[Steel type in layer 3, grade 60 rebar]
line 17:	1.2	[Area of steel in layer 3]
line 18:	3	[Dist. from top of beam to centroid of steel layer 3]
line 19:	5	[Unbonded length of steel in layer 3]
line 20:	36	[Length of mild steel in the beam]
line 21:	90	[1/2 clear span between the columns]
line 22:	24	[beam width]
line 23:	48	[beam height]

The following is a sample output file:

Sample Output File

National Institute of Standards & Technology
Bldg 226/ B168, Structures Division
Gaithersburg, MD 20899

Program B6: Analysis of Arbitrary Partially
Prestressed Precast Beam Column Joints

Date: 07/23/93 Time: 14:40:29.42

Input File: t2.inp

TITLE/NOTES:

Test run case T2

20% of moment from Gr.60 Bars, 80% from 1/2 PT strand

INPUT DATA

fc = 5.00 ksi
fpe = 189.00 ksi
b = 24.00 in.
h = 48.00 in.

STEEL LAYERS

Type	Layer	D (in.)	As (in**2)	Py (k)	L unb (in.)
3	1	45.00	1.400	84.00	5.00
6	2	24.00	4.470	1099.62	36.00
3	3	3.00	1.400	84.00	5.00

Initial concrete strain = 0.000182

Initial PT strain = 0.006300

Initial PT stress = 0.70 fpu

----- RUN SUMMARY -----

Target Moment = 2000.00 k-ft

Max. Moment = 2082.97 k-ft

Max. ratio M (non pt) / M (total) = 0.2190

Max. Drift (beam) = 0.0155

Max. Shear = 277.73k

Max. PT Force = 1126.51 k Max PT strain = 0.0139 PT Steel Yielded? Y

Max. Non. PT Force = 324.51 k Max Non PT strain = 0.1200 Non. PT Steel Yield? Y

V_prov < V_req: 0. times

MESSAGES: Bar fracture in layer 1

----- RESULTS -----

Theta	Delta	Non PT	PT	Xbar	Mcol	Mbm	Shear	Ms/Mtot	V_prov	V_Check
0.00000	0.00000	0.0	822.9	4.3623	1346.7	808.0	179.56	0.000	560.95	
0.00002	0.00100	9.3	824.5	4.4289	1375.0	825.0	183.34	0.022	561.89	
0.00005	0.00200	18.6	826.0	4.4622	1405.6	843.3	187.41	0.043	562.82	
0.00007	0.00300	27.9	827.6	4.5288	1433.7	860.2	191.16	0.063	563.76	
0.00010	0.00400	37.3	829.1	4.5954	1461.7	877.0	194.89	0.083	564.68	
0.00012	0.00500	46.7	830.7	4.6287	1491.9	895.2	198.93	0.101	565.61	
0.00015	0.00600	56.1	832.2	4.6953	1519.7	911.8	202.63	0.119	566.54	
0.00017	0.00700	65.6	833.8	4.7619	1547.3	928.4	206.31	0.136	567.46	
0.00020	0.00800	75.1	835.3	4.8285	1574.8	944.9	209.97	0.153	568.37	
0.00022	0.00900	83.7	836.8	4.8618	1601.6	961.0	213.55	0.167	569.29	
0.00025	0.01000	86.8	838.3	4.8951	1610.1	966.1	214.68	0.171	570.21	
0.00027	0.01100	88.2	839.9	4.8951	1615.4	969.3	215.39	0.172	571.12	
0.00030	0.01200	89.2	841.4	4.3600	1661.2	996.7	221.50	0.171	572.05	
0.00032	0.01300	88.1	843.2	4.3600	1664.7	998.8	221.97	0.171	573.15	
0.00034	0.01400	88.5	844.8	4.3600	1667.6	1000.6	222.35	0.171	574.08	
0.00037	0.01500	88.9	846.4	4.3600	1670.5	1002.3	222.74	0.171	575.02	
↓	↓	↓	↓	↓	↓	↓	↓	↓	↓	
0.01528	0.59100	231.0	1125.0	6.3200	2082.7	1249.6	277.70	0.204	742.23	
0.01530	0.59200	230.9	1125.2	6.3200	2082.8	1249.7	277.70	0.204	742.34	
0.01533	0.59300	230.9	1125.4	6.3200	2082.8	1249.7	277.70	0.204	742.45	
0.01536	0.59400	230.8	1125.6	6.3200	2082.8	1249.7	277.71	0.204	742.56	
0.01538	0.59500	230.8	1125.8	6.3200	2082.8	1249.7	277.71	0.204	742.68	
0.01541	0.59600	230.7	1126.0	6.3200	2082.8	1249.7	277.71	0.204	742.79	
0.01543	0.59700	230.7	1126.2	6.3200	2082.9	1249.7	277.71	0.203	742.90	
0.01546	0.59800	230.6	1126.4	6.3200	2082.9	1249.7	277.72	0.203	743.02	
0.01549	0.59900	230.6	1126.5	6.3200	2082.8	1249.7	277.70	0.203	743.08	
0.01551	0.60000	230.5	1126.5	6.3200	2082.6	1249.5	277.68	0.203	743.10	

Listing of Program B6.FOR

```
c*****
c Program: B6.for
c
c Purpose: Calculates the moments in a beam for a series of drift levels.
c
c Subroutines:
c
c 1. A36          ! Mild steel stress-strain curve
c 2. g40         ! Grade 40 deformed rebar stress strain curve
c 3. g60         ! Grade 60 deformed rebar stress strain curve
c 4. ss304       ! 304 Stainless steel stress strain curve
c 5. steel1026   ! J55 high strength drill pipe stress strain curve
c 6. pt_strand716 ! 7/16" (and 1/2") 7-wire 270 ksi tendon stress/strain
c 7. pt_strand38 ! 3/8" 7-wire 270 ksi tendon stress strain curve
c 8. pt_bar      ! Dywidag prestress bar stress strain curve
c 9. read_inp    ! Gets initial problem data (file or user)
c 10. init_var   ! initializes problem variables
c 11. calc_mom   ! determines moment-drift curve for given section
c 12. mom_check  ! adjustment logic for targeting specified moment
c                ! and percentage of moment provided by non-pt steel
c 13. output     ! write data to output file
c
c Installation:
c
c 1) Verify that you have the two files B6.FOR and COMMON.FOR
c 2) Using Lahey F77 compiler type "f771 B6" (return)
c 3) Following compilation (ignore warnings) type "optlink B6"
c    and answer all the questions with a blank carriage return.
c    This creates the executable file "B6.EXE"
c 4) To run the program type "B6" (return). The program will
c    ask whether you want to read an existing input file (fastest)
c    or manually enter a problem from the key board (with prompts).
c 5) The program is iterative and will automatically target a
c    design moment if requested. The initial input data can therefore
c    be an educated guess to serve as seed data. The final
c    values of As and Aps for each layer are printed in the output
c    file. Only the outermost layer of As (top and bottom) is
c    modified in this process; ALL Aps layers are modified, however
c    and set to a common trial level for the next iteration.
c
c
c Version: July 7, 1993: Includes improved printout, error checking
c                        plus design limit checking ... and, it seems
c                        to yield reasonable results for both bonded and
c                        partially debonded BC joints. For the fully
c                        bonded condition, set the debond lengths to
c                        1 inch. Program handles multiple (n) layers
c                        of mixed (prestress and non-PT) steel. A total of 10
c                        layers is allowed. All rotation (drift) is presumed
```

c to take place at the beam-column face. For certain column
 c and (underreinforced) beam conditions the
 c predicted drift can be as much as two times
 c less than would be measured under actual
 c experiment. The minimum drift capacity
 c predicted by this program is therefore
 c CONSERVATIVE.

c Written by: G.Cheok & B. Stone, NIST
 c Tel: 301-975-6075
 c FAX: 301-869-6275
 c email: "wins%"<stone@sdvax.cbt.nist.gov>"
 c email: "wins%"<cheok@sdvax.cbt.nist.gov>"

c *****

include 'common.for'

c -----
 print *,'
 print *,'
 print *,'*****'
 print *,' NIST...NIST...NIST...NIST...NIST...NIST...NIST'
 print *,'
 print *,' PC Program: B6'
 print *,'
 print *,' Input: Section geometry, material property,'
 print *,' prestressed and non-prestressed steel.'
 print *,' Output: Moment vs Drift plot data to ultimate'
 print *,' for arbitrary partially prestressed beams'
 print *,'
 print *,' ***** WARNING *****'
 print *,'
 print *,' THIS IS RESEARCH CODE: USE AT YOUR OWN RISK'
 print *,'
 print *,'*****'
 print *,'

c -----

c Begin main program:

```

call read_inp          ! read input values
iterationcount=0      ! initialize the iteration counter
call initial_var      ! initialize variables
call calc_mom         ! calculate moments

if(mtargflag.eq.1) then ! user specified target moment
  call mom_check      ! auto design for target moment and target moment ratio
endif

call output           ! open output file and write headers,
                    ! input variables

```

```

close (2)                ! close output file

print *,'Number of solutions found: ',nsoIn

stop
end

c
c*****
c
c  subroutine: mom_check
c
c  Purpose:  Check that the maximum moment of the section falls within
c            specified bounds.  If not, then either increase or
c            decrease the mild steel (both compression and tension).
c
c            If such a target moment is requested the user is also asked
c            to provide a moment ratio for the portion of the ultimate
c            moment that is provided by non-prestressed steel.  The
c            program automatically iterates to solve both the desired
c            moment and to satisfy the specified moment ratio.
c
c  Subroutines called:
c
c  1. Initial_var
c  2. Calc_mom
c
c-----
c
c  subroutine mom_check
c
c  include 'common.for'
c  print *,'
c  print *,'-----'
c  print *,'
c  print *,'**Entering Iteration Phase**'
c  print *,'
c  print *,'Inc. Aps = increasing prestress area'
c  print *,'Dec. Aps = decreasing prestress area'
c  print *,'Inc. As  = increasing non-prestress area'
c  print *,'Dec. As  = decreasing non-prestress area'
c  print *,'
c  print *,'-----'
c  print *,'
c
c  Case 1: Moment is within bounds of target moment
c
c  411  continue
c
c      if (maxmom .ge. lowermom .and. maxmom .le. uppermom) then
c
c          check moment ratio (M[non-prestressed steel] / M[total])
c

```

```

c      Case 1a: Moment ratio is also satisfied; print results
c
1      if(peakratio .ge. lowerratio .and.
      peakratio .le. upperratio) then      ! mom ratio within bounds
      print *,'
      print *,'** Successful Solution !! ... Exiting **'
      goto 2001
c
c      Case 1b: Moment ratio too high: increase quantity of PT steel
c
      elseif( peakratio .gt. upperratio) then      ! mom ratio too low,
      ! increase Apt

      do jj = 1,nplayermax-1

      a( player(jj) ) = a( player(jj) ) + 0.1
      iterationcount=iterationcount+1
      print *,'Iteration # ',iterationcount
      print *,'Inc. Aps'

      enddo
      goto 1001
c
c      Case 1c: Moment ratio too low: decrease quantity of PT steel
c
      elseif( peakratio .lt. lowerratio) then      ! mom ratio too high;
      ! decrease Apt

      do jj = 1,nplayermax-1

      a( player(jj) ) = a( player(jj) ) - 0.1

      enddo

      iterationcount=iterationcount+1
      print *,'Iteration # ',iterationcount
      print *,'Dec. Aps'
      goto 1001

      endif
c
c-----
c
c      Case 2: Insufficient non-prestressed steel to meet target moment
c      (increase area and re-evaluate)
c
c      elseif (maxmom .lt. lowermom) then      ! moment lower than
      ! lower bound
      a(1) = a(1) + 0.1      ! increase tension steel
      a(nlayer) = a(nlayer) + 0.1      ! increase compression steel
      iterationcount=iterationcount+1
      print *,'Iteration # ',iterationcount

```



```

    print *, 'Inc. As'

    goto 1001                ! repeat computation
c
c-----
c
c   Case 3: Too much non-prestressed steel: target moment exceeded
c           (decrease non-PT steel area and re-evaluate)
c
    elseif (maxmom .gt. uppermom) then      ! moment over upper
                                           ! bound
        a(1) = a(1) - 0.1                    ! decrease tension steel
        a(nlayer) = a(nlayer) - 0.1        ! decrease compression steel
        iterationcount = iterationcount + 1
        print *, 'Iteration # ', iterationcount

    print *, 'Dec. As'

    goto 1001                ! repeat computation

endif

c
c-----
c
c   Re-Evaluation

c
1001 call initial_var          ! initialize variables
    call calc_mom             ! calculate new moments
    goto 411                  ! check moments, ratios
c
c-----
c
c   Successful Completion:
c
2001 continue

    return
end

c
c*****
c
c Subroutine: Calc_mom
c
c Purpose: Calculate moments corresponding to a series of drift levels.
c
c The routine works as follows:
c
c 1. Set an initial "gap" between the beam and column.
c 2. Set initial pivot point at compression steel level.
c 3. Calc. strains in the mild and PT steels.

```

- c 4. Calc. tension and compression forces.
- c 5. Check for force equilibrium.
- c 6. Set pivot point to centroid of compression forces.
- c 7. Repeat steps 3 - 6 until there is a convergence in the
c initial and actual strains
- c 8. Calc. moment and rotation.
- c 9. Increase gap width
- c 10. Set initial pivot point at the previous pivot point (step 6).
- c 11. Repeat steps 3 to 9.

```
c
c*****
```

```
c
  subroutine calc_mom

  include 'common.for'

1000 if(index.ge.2000) then
      print *,'Array size > 2000 ... End this Cycle'
      message = 'Array size > 2000. End program.'
      goto 4000
    endif

      drift = gap(index)/y ! drift = rotation angle in radians for << angles
```

```
c reinitialize variables
```

```

  na(index) = 0.0
  cstot = 0.0
  ctot = 0.0
  ptot = 0.0
  pstot(index) = 0.0
  ppttot(index) = 0.0
  nplayer = 1
  ntlayer = 1
  nclayer = 1

c   print *,'index = ',index,' gap = ',gap

c === Begin Steps 3 & 4 =====
```

```
c
c Calc. forces in mild and PT steels
c
c -----
```

```

  do i = 1, nlayer ! calc. strains and forces for each layer of steel
c
c   steel strain divided by unbonded length:
c
c   estr(i) = (( y-( d(1)-d(i))) * drift ) / lunb(i)

  if (estr(i) .ge. eu(i) ) then ! bar fracture
    print *,'Bar Fracture ... End this Cycle'
```

```

write (frac_layer,'(i1)') i
message = 'Bar fracture in layer '//frac_layer
goto 4000
endif

```

```

if (type(i) .eq. 1) then      ! get stress for a given strain for A36 steel
  call a36( estr(i),sigma)   ! strain is negative if steel is in
                             ! compression

```

- c Check if steel in compression or tension by location of
- c steel w/ respect to pivot point
- c If steel layer is above pivot point, steel is in compression.

```

if ( estr(i) .lt. 0.0 ) then
  clayer(nclayer) = i      ! layer in compression
  nclayer = nclayer + 1
  cs(i) = sigma * a(i)     ! compression force in layer
  cstot = cstot + cs(i)   ! total commpression force
else
  if (estr(i) .gt. es_max) then
    es_max = estr(i)      ! max. steel strain
    if (es_max .ge. ey(i) ) nonpt_yield = 'Y' ! check if steel yielded
  endif
  tlayer(ntlayer) = i     ! layer in tension
  ntlayer = ntlayer + 1
  ps(i) = sigma * a(i)    ! tension force in layer
  if (ps(i).ge.nonpt_max) nonpt_max = ps(i)
  pstot(index) = pstot(index) + sigma * a(i) ! total tension force
endif
endif

```

```

if (type(i) .eq. 2) then    ! get stress for a given strain for G40 rebar
  call g40( estr(i),sigma)

```

- c Check if steel in compression or tension by
- c location of steel w/ respect to pivot point
- c If steel layer is above pivot point, steel is in compression.

```

if ( estr(i) .lt. 0.0 ) then
  clayer(nclayer) = i      ! layer in compression
  nclayer = nclayer + 1
  cs (i) = sigma * a(i)    ! compression force in layer
  cstot = cstot + cs(i)   ! total commpression force
else
  if (estr(i) .gt. es_max) then
    es_max = estr(i)      ! max. steel strain
    if (es_max .ge. ey(i) ) nonpt_yield = 'Y' ! check if steel yielded
  endif
  tlayer(ntlayer) = i     ! layer in tension
  ntlayer = ntlayer + 1
  ps(i) = sigma * a(i)    ! tension force in layer
  if (ps(i).ge.nonpt_max) nonpt_max = ps(i)

```

```

    pstot(index) = pstot(index) + ps(i)      ! total tension force
  endif
endif

```

```

if (type(i) .eq. 3) then      ! get stress for a given strain for G60 rebar
  call g60( estr(i),sigma)

```

- c Check if steel in compression or tension by
- c location of steel w/ respect to pivot point
- c If steel layer is above pivot point, steel is in compression.

```

if ( estr(i) .lt. 0.0 ) then
  clayer(nclayer) = i      ! layer in commpression
  nclayer = nclayer + 1
  cs(i) = sigma * a(i)      ! compression force in layer
  cstot = cstot + cs(i)    ! total compression force
else
  if (estr(i) .gt. es_max) then
    es_max = estr(i)      ! max. steel strain
    if (es_max .ge. ey(i) ) nonpt_yield = 'Y' ! check if steel yielded
  endif
  tlayer(nlayer) = i      ! layer in tension
  nlayer = nlayer + 1
  ps(i) = sigma * a(i)      ! tension force in layer
  if (ps(i).ge.nonpt_max) nonpt_max = ps(i)
  pstot(index) = pstot(index) + ps(i)      ! total tension force
endif
endif

```

```

if (type(i) .eq. 4) then      ! get stress for a given strain for
                              ! stainless steel 304
  call ss304( estr(i),sigma)

```

- c Check if steel in compression or tension by
- c location of steel w/ respect to pivot point
- c If steel layer is above pivot point, steel is in compression.

```

if ( estr(i) .lt. 0.0 ) then
  clayer(nclayer) = i      ! layer in commpression
  nclayer = nclayer + 1
  cs(i) = sigma * a(i)      ! compression force in layer
  cstot = cstot + cs(i)    ! total commpression force
else
  if (estr(i) .gt. es_max) then
    es_max = estr(i)      ! max. steel strain
    if (es_max .ge. ey(i) ) nonpt_yield = 'Y' ! check if steel yielded
  endif
  tlayer(nlayer) = i      ! layer in tension
  nlayer = nlayer + 1
  ps(i) = sigma * a(i)      ! tension force in layer
  if (ps(i).ge.nonpt_max) nonpt_max = ps(i)
  pstot(index) = pstot(index) + ps(i)      ! total tension force

```

```

endif
endif

if (type(i) .eq. 5) then    ! get stress for a given strain for 1026 steel
  call steel1026( estr(i),sigma)

```

- c Check if steel in compression or tension by
- c location of steel w/ respect to pivot point
- c If steel layer is above pivot point, steel is in compression.

```

if ( estr(i) .lt. 0.0 ) then
  clayer(nclayer) = i      ! layer in compression
  nclayer = nclayer + 1
  cs(i) = sigma * a(i)     ! compression force in layer
  cstot = cstot + cs(i)    ! total compression force
else
  if (estr(i) .gt. es_max) then
    es_max = estr(i)      ! max. steel strain
    if (es_max .ge. ey(i) ) nonpt_yield = 'Y' ! check if steel yielded
  endif
  tlayer(ntlayer) = i     ! layer in tension
  ntlayer = ntlayer + 1
  ps(i) = sigma * a(i)    ! tension force in layer
  if (ps(i) .ge. nonpt_max) nonpt_max = ps(i)
  pstot(index) = pstot(index) + ps(i)    ! total tension force
endif
endif

```

```

if (type(i) .eq. 6) then ! get stress for a given strain
  ! for 7/16" PT strand

```

```

  player (nplayer) = i    ! player is array which stores the layer # that is PT steel
  nplayer = nplayer + 1  ! nplayer is the number of layers of steel that are PT steel
  if(nplayermax.le.nplayer) nplayermax=nplayer
  estr(i) = estr(i) + epsini ! add the initial strain to
  ! increment in strain
  call pt_strand716(estr(i),sigma) ! net force in PT is assumed
  ! to be always in tension
  if (estr(i) .gt. ept_max) then
    ept_max = estr(i) ! max. PT steel strain
    if (ept_max .ge. ey(i)) PT_yield = 'Y' ! check if PT yielded
  endif
  ppt(i) = sigma * a(i) ! PT force in layer
  if (ppt(i) .ge. pt_max) pt_max = ppt(i)
  ppttot(index) = ppttot(index) + ppt(i) ! total PT force

```

```

endif

```

```

if (type(i) .eq. 7) then ! get stress for a given
  ! strain for 3/8" PT strand
  player (nplayer) = i
  nplayer = nplayer + 1

```

```

if(nplayermax.le.nplayer) nplayermax=nplayer
estr(i) = estr(i) + epsini      ! add the initial strain to
                                ! increment in strain
call pt_strand38(estr(i),sigma) ! net force in PT is assumed
                                ! to be always in tension
if (estr(i) .gt. ept_max) then
  ept_max = estr(i)      ! max. PT steel strain
  if (ept_max .ge. ey(i)) PT_yield = 'Y' ! check if PT yielded
endif
ppt(i) = sigma * a(i)      ! PT force in layer

if (ppt(i) .ge. pt_max) pt_max = ppt(i)
ppttot(index) = ppttot(index) + ppt(i)      ! total PT force
endif

if (type(i) .eq. 8) then      ! get stress for a given strain for PT bar
  player (nplayer) = i
  nplayer = nplayer + 1
  if(nplayermax.le.nplayer) nplayermax=nplayer
  estr(i) = estr(i) + epsini      ! add the initial strain to
                                  ! increment in strain
  call pt_bar( estr(i),sigma)      ! net force in PT is assumed
                                  ! to be always in tension
  if (estr(i) .gt. ept_max) then
    ept_max = estr(i)      ! max. PT steel strain
    if (ept_max .ge. ey(i)) PT_yield = 'Y' ! check if PT yielded
  endif

  ppt(i) = sigma * a(i)      ! PT force in layer
  if (ppt(i) .ge. pt_max) pt_max = ppt(i)
  ppttot(index) = ppttot(index) + ppt(i)      ! total PT force
endif

enddo

ptot = ppttot(index) + pstot(index)      ! Total Tension force, ptot

```

c -- Calc. Concrete Comp. Force -----

c

c Computation of Cc is done following the method

c outlined in Park and Paulay's

c "Reinforced Concrete Structures", Wiley and Sons,

c 1975, p. 204. and example 6.1. pp. 212 - 216.

c "The stress-strain curve for concrete is approximately linear

c up to 0.75 fc; hence if the concrete stress does not exceed this value

c when the steel reaches yield

c strength, the depth to the neutral axis may be calculated using the elastic

c (straight line) theory formula, derived in Chapter 10."

c For steel strains <= yield: $C_c = 1/2 * f_c * b * NA$

c For steel strains > yield: $C_c = 0.85 * f_c * b * beta1 * NA$

c -----

c For a given neutral axis depth, compute Cc.

2000 na(index) = na(index) + 0.1 ! incr. neutral axis depth by 0.1"

if (na(index) .gt. 2.0*h/3.0) then ! assume no soln. found if NA > 2/3 h
! goto next rotation w/o incrementing index
y_act = y ! actual y not set at this point
goto 6000

endif

if (ntlayer .eq. 1) then ! no mild steel, only PT steel
cc = 0.85 * fc * b * beta1 * na(index) ! use equivalent rect. stress block
x = na(index) - beta1 * na(index) / 2.0 ! dist. from NA to centroid of cc
goto 2100

endif

if (ps(1)/a(1) .le. fy(1)) then ! compute comp. force, cc

cc = 0.5 * fc * na(index) * b ! use triangular stress distribution
c ! for steel stress < yield
x = 0.667 * na(index) ! dist. from neutral axis to
! centroid of cc

else

cc = 0.85 * fc * b * beta1 * na(index) ! use equivalent rect. stress block
c ! for steel strains > yield
x = na(index) - beta1 * na(index) / 2.0 ! dist. from NA to centroid of cc

endif

2100 ctot = cstot + cc ! total compression force, ctot = steel + conc force

c === Step 5 =====

c Set the tolerance for check the forces to be 5% of total tension force

tol_force = 0.05 * ptot

if (abs (ptot-ctot) .lt. tol_force) then ! check that diff. in forces
! within tolerance

sum = 0.0 ! find centroid of comp. forces, xbar
do i = 1, nlayer ! sum the mult. of comp. force in steel with
! dist. to top of beam
sum = cs(clayer(i)) * d(clayer(i)) + sum

enddo

c

c xbar is measured from beam top (outermost compression fiber)

$$\text{xbar}(\text{index}) = (\text{cc} * (\text{na}(\text{index}) - \text{x}) + \text{sum}) / \text{ctot}$$

c ==== Step 6 =====

c Compute the distance between the bottom layer of tension steel and the
c centroid of the compression forces, y. This is the height used to compute
c the rotation = gap/y

$$\text{y_act} = \text{d}(1) - \text{xbar}(\text{index})$$

c ==== Step 7 =====

c Check that this height is equal to the height assumed at the beginning
c of the iteration. Check that the diff. in the assumed height and the
c actual height is within 5% of the actual height. If this is true then
c compute moment. If not, recalc. forces using the "new" height to compute
c strains.

$$\text{tol_y} = 0.05 * \text{y}$$

if (abs(y_act - y) .le. tol_y) then

c ===== Step 8 =====

c Calc. moment at column face and in the shallow part of beam, rotation,
c shear force at col. face,

ts_mom = 0.0 ! sum tension forces about compression force

```
do i = 1, ntlayer
  ts_mom = ps( tlayer(i) ) * (d(tlayer(i)) - xbar(index))
1      + ts_mom ! moment due to ten. steel, ts_mom
enddo
```

```
tps_mom = 0.0 ! sum PT forces about compression force
do i = 1, nplayer
  tps_mom = ppt(player(i)) * (d(player(i)) - xbar(index))
1      + tps_mom ! mom. due to PT steel, tps_mom
enddo
```

mom(index) = (tps_mom + ts_mom) / 12.0 ! Moment at col. face in kip-ft

momratio(index) = ts_mom / (mom(index) * 12.0) ! % of total moment due
! to non-PT steel

c Calc. moment in the beam where the mild steel stops, shear at col. face,
c and drift (= theta), provided shear resistance
c


```

shallow_bmmom(index)= mom(index)*((arm - L1)/arm)      ! moment in beam
c
shear(index) = mom(index) / (arm/12.0)      ! shear at column face

theta(index) = gap(index) / y_act          ! beam rotation at col. face
c
c shear capacity available from shear friction and from non-PT steel.
c Friction coefficient is conservatively estimated at 0.6
c
v_prov(index) = 0.6*ppttot(index) + v_prov_as
c
c check that the provided shear resistance is greater than the required shear.
c
if (v_prov(index) .le. shear(index)) then
v_check(index) = '**'
c
c count the number of times the required shear exceeds the provided shear:
c
shear_count = shear_count + 1
else
v_check(index) = ''
endif

c get the maximum moment and shear capacity of the beam section

if (mom(index) .gt. maxmom) maxmom = mom(index)
if (shear(index) .gt. v_max) v_max = shear(index)

if (momratio(index) .gt. peakmratio) then
peakmratio=momratio(index)
endif

nsoln = nsoln + 1      ! number of solutions found

c Stop calculations for drift levels greater than 5% or mild
c steel fractures. The outermost layer is checked as this would be the most
c likely layer of steel to fracture.

if (theta(index).gt.0.05.or.estr(1).gt.eu(1)) goto 4000      ! end program.

goto 5000      ! continue program with another rotation value

else

c === Step 7 =====
c Initial assumed drift height, y, and actual drift height are not equal.
c Recalculate strains based on the "new" pivot height, y
c Repeat steps 3 - 6

y = y_act
goto 1000

```

```

        endif
    else
c No force balance was found, increment neutral axis depth and try again
        goto 2000
    endif
5000 continue

    index = index + 1      ! increment counter

c === Step 9 =====
c Increase gap width and get corr. moment.
6000 if (index .eq. 1) then
    gap(index) = gap(index) + 0.001    ! increment gap by 0.001
else
    gap(index) = gap(index-1) + 0.001
endif

c === Step 10 =====
c
c Set the new y to the last y values

    y = y_act

c ===== Step 11 =====

    goto 1000

4000 continue

    return
end

c*****
c
c Subroutine: read_inp
c
c Purpose: read in input variables
c
c*****

subroutine read_inp

```

```

include 'common.for'

print *, '
print *, 'Input data from terminal [T] or file (F)? '
read (5,100) ans
100 format (a1)
if (ans.eq.'T'.or. ans.eq.'t' .or. ans.eq.' ') goto 400

print *, 'Enter input file name including extension - '
read (5,200) infile
200 format(a20)

c -----

c read data in from file

open (1,file=infile,access='sequential',status='old')

read (1,300) title1 ! title line 1
read (1,300) title2 ! title line 2
read (1,300) title3 ! title line 3
read (1,200) outfile ! name of output file
read (1,*) fc ! concrete compressive stress, ksi
read (1,*) fpe ! init. stress in PT steel after all losses, ksi

c Types of steel for which stress-strain are available in this program
c 1 = A 36
c 2 = Grade 40 reinforcing bar
c 3 = Grade 60 reinforcing bar
c 4 = Stainless steel 304
c 5 = 1026 Steel (J55 tubing)
c 6 = 7-wire strand, Grade 270 [7/16 inch dia.]
c 7 = 7-wire strand, Grade 270 [3/8 inch dia.]
c 8 = High strength bar - Dywidag bar, fpu = 150 ksi

read (1,*) nlayer ! number of layers of steel - all types

c The convention used is that the top of the beam is in
c compression and the bottom is in tension.
c
c Read in the type of steel, area of steel, distance from top of beam to
c centroid of steel layer, unbonded length of steel layer. The first layer
c MUST be the one closest to the bottom of the beam - highest tensile
c strains.

c ***** NOTES: *****

c 1. The unbonded length of the PT steel should be measured from the
c center of the column to the point at which the debonding stops.
c 2. The unbonded length of the mild steel should include intentional
c debonding and predicted debonding length which occurs during the test

```

```

c   when the actual stress > bond stress.
c
do i = 1, nlayer
  read (1,*) type(i)   ! type of steel in the layer
  read (1,*) a(i)     ! area of non-prestressed steel, in**2
  read (1,*) d(i)     ! dist. from top of beam to tension steel, in
  read (1,*) lumb(i)  ! unbonded length of the steel, in.
enddo

read (1,*) L1         ! length mild steel from column face to the point
                    ! at which the mild steel ends in the beam, in.
read (1,*) arm       ! length from mid-span of bay (beam pin) to col.
                    ! face, in.

read (1,*) b         ! width of beam, in
read (1,*) h         ! height of beam, in

close (1)

300 format (a80)

goto 1000

c -----
c read in data from terminal

400 continue

print *,'Enter title line 1 (80 characters)'
print *,'
read (5,300) title1           ! title line 1

print *,'Enter title line 2 (80 characters)'
print *,'
read (5,300) title2           ! title line 2

print *,'Enter title line 3 (80 characters)'
print *,'
read (5,300) title3           ! title line 3

print *,'Enter name of output file including extension '
read (5,200) outfile          ! name of output file

print *,'Enter concrete compressive strength, fc, in ksi '
read (5,*) fc                 ! concrete compressive stress, ksi

print *,'Enter the initial stress in the PT steel, fpe, in ksi '
read (5,*) fpe                ! init. stress in PT steel after all losses, ksi

print *,'Enter total number of layers of steel '
read (5,*) nlayer             ! number of layers of steel - all types

```

```

print *, 'The convention used is that the top of the beam is in
print *, 'compression and the bottom is in tension.'

```

```

print *, 'The first layer MUST be the one closest to the bottom'
print *, 'of the beam (highest tensile strains).'

```

```

print *, '
print *, ' ***** NOTES: *****

```

```

print *, '1. The unbonded length of the PT steel should be',
1 ' measured from'

```

```

print *, ' the center of the column to the point at which',
1 ' the debonding stops.'

```

```

print *, '2. The unbonded length of the mild steel should',
1 ' include intentional debonding'

```

```

print *, ' and predicted debonding length which occurs',
1 ' during the test'

```

```

print *, ' when the actual stress > bond stress.'

```

```

print *, 'Types of steel for which stress-strain are available',
1 ' in this program:'

```

```

print *, '

```

```

print *, ' 1 = A 36 steel'

```

```

print *, ' 2 = Grade 40 reinforcing bar'

```

```

print *, ' 3 = Grade 60 reinforcing bar'

```

```

print *, ' 4 = Stainless steel 304'

```

```

print *, ' 5 = 1026 Steel (Similar to J-55)'

```

```

print *, ' 6 = 7-wire strand, 7/16", Grade 270'

```

```

print *, ' 7 = 7-wire strand, 3/8", Grade 270'

```

```

print *, ' 8 = High strength bar - Dywidag bar',
1 ' fpu = 150 ksi'

```

```

print *, '

```

```

do i = 1, nlayer

```

```

print *, 'Enter type of steel in layer ', i, ' '

```

```

read (5, *) type(i) ! type of steel in the layer

```

```

print *, 'Enter area of steel in layer ', i, ' (sq. in) '

```

```

read (5, *) a(i) ! area of non-prestressed steel, in**2

```

```

print *, 'Enter dist. from top of beam to steel in layer ', i,
1 ' (in) '

```

```

read (5, *) d(i) ! dist. from top of beam to tension steel, in

```

```

print *, 'Enter the debonded length of steel in layer ', i,

```

```

1 ' (in) '

```

```

read (5, *) lunb(i) ! unbonded length of the steel, in.

```

```

enddo

```

```

print *, 'Enter length of mild steel DUCT in beam (in.) '

```

```

print *, '[previously, this was "dogbone" length]'

```

```

read (5, *) L1 ! length mild steel from column face to the point at which
! the mild steel ends in the beam, in.

```

```

print *, 'Enter length of beam to column face (in.) '

```

```

read (5, *) arm ! length from mid-span of bay (beam pin) to col. face, in.

```

```

print *, 'Enter width of beam, inches'
read (5,*) b                ! width of beam, in

print *, 'Enter overall height of beam, inches'
read (5,*) h                ! height of beam, in

c -----

1000 continue

print *, 'Is there a target moment to be met? [Y]/N '
read (5,100) ans

if( ans.eq.'Y' .or. ans.eq.'y' .or. ans.eq.' ' ) then

    print *, 'Enter Target Moment (kip-ft) '
    read (5,*) targetmom
    print *, 'Enter Percentage of Total Moment to be provided'
    print *, 'by Non-PT [Energy Dissipative] Steel'
    print *, 'as a DECIMAL value '
    print *, ' '
    read (5,*) targetmratio

    mtargflag = 1            ! target moment is specified
else
    targetmom = 0
    mtargflag = 0            ! no target moment; solve given section
endif

2000 continue

print *, 'Computation Cycle Begins'

return
end

c*****
c
c Subroutine: Initial_var
c
c Purpose: Initialize variables
c
c*****

subroutine initial_var

include 'common.for'

index = 1                    ! counter
shear_count = 0              ! counter for # of times the provided
                             ! shear is less than the req. shear

```

```

nplayermax = 0          ! counter for number of prestress steel layers
nsoln = 0              ! number of solutions found
maxmom = 0.0          ! computed max moment of section.
peakmratio = 0.0      ! computed maximum moment fraction from mild steel
ept_max = 0.0         ! max. strain in PT steel
es_max = 0.0          ! max. strain in steel
PT_yield = 'N'        ! flag for yielding of PT steel
nonpt_yield = 'N'     ! flag for yielding of Non-PT steel

```

```
v_max = 0.0
```

```

gap(1) = 0.0          ! init. gap betw'n bm and col. at location of
                    ! tension steel
y = d(1) - d(nlayer) ! initial height for calc. of theta. This initial height
                    ! is set to the diff. in the two extreme d's.

```

c Indices to track the layers of steel that are in tension or
c compression and the layers of steel that at PT steel. The numbers of the
c layer is stored in arrays nlayer, nlayer and nplayer. This is necessary so
c that the moment of the section and the centroid of the compression forces
c may be found later.

```

nlayer = 1
nlayer = 1
nplayer = 1

```

```

ec_mod = 57*sqrt(fc*1000) ! modulus for concrete, ksi
eps_mod = 30000.0         ! modulus for PT steel as taken for the
                          ! stress-strain curves

```

c set the yield stresses and strains and strain at fracture for each type of steel

```

do i = 1,nlayer
  if (type(i) .eq. 1) then
    fy(i) = 36.0          ! yield stress of A36
    ey(i) = 0.00124
    eu(i) = 0.34         ! strain at fracture
  elseif (type(i) .eq. 2) then
    fy(i) = 42.0          ! yield stress of g40 rebar
    ey(i) = 0.00145
    eu(i) = 0.19         ! strain at fracture
  elseif (type(i) .eq. 3) then
    fy(i) = 60.0          ! yield stress of g60 rebar
    ey(i) = 0.00207
    eu(i) = 0.12         ! strain at fracture
  elseif (type(i) .eq. 4) then
    fy(i) = 45.0          ! yield stress of stainless steel 304
    ey(i) = 0.0021
    eu(i) = 0.53         ! strain at fracture
  elseif (type(i) .eq. 5) then
    fy(i) = 78.0          ! yield stress of 1026 rod
    ey(i) = 0.0058

```

```

eu(i) = 0.026          ! strain at fracture
elseif (type(i) .eq. 6) then
  fy(i) = 246.0        ! yield stress of 7/16" PT strand g270
  ey(i) = 0.01
  eu(i) = 0.058        ! strain at fracture

elseif (type(i) .eq. 7) then
  fy(i) = 255.0        ! yield stress of 3/8" PT strand grad 270
  ey(i) = 0.01
  eu(i) = 0.015        ! strain at fracture
elseif (type(i) .eq. 8) then
  fy(i) = 145.0        ! yield stress of PT bar
  ey(i) = 0.0069
  eu(i) = 0.038        ! strain at fracture
endif
enddo

if (fc .gt. 4.0) then
  beta1 = 0.85 - 0.05*(fc - 4.0)
  if (beta1 .lt. 0.65) beta1 = 0.65      ! beta1 >= 0.65  ACI 10.2.7.3
else
  beta1 = 0.85
endif

area = b*h            ! area of concrete, transformed steel area ignored.

v_prov_as = 0.0
do i = 1,nlayer      ! Determine the shear resistance
                    ! contributed by non_PT steel
  if (type(i) .lt. 6) then
    v_prov_as = 0.4*a(i)*fy(i) + v_prov_as
  endif
enddo

apstot = 0.0         ! total area of PT steel

do i = 1,nlayer      ! Look only for steel layers that are PT.
  if (type(i) .eq. 6 .or. type(i) .eq. 7) fpu = 270 ! Set ultimate stress for
  ! strand, grade 270
  if (type(i) .eq. 8) fpu = 150      ! Set ultimate stress PT bar

  if (type(i) .ge. 6) then          ! This is assuming that the PT steel is
    apstot = a(i) + apstot         ! all one type - strands or bars - and no
  endif                             ! combination.
enddo

pptini = apstot*fpe      ! initial post-tensioning force
sigini = pptini/area     ! initial stress in concrete
ecini = sigini/ec_mod    ! initial strain in concrete

```



```

epsini = fpe/eps_mod      ! initial strain in PT steel
if (fpu .eq. 0) then
  ptini = 0.0             ! init. PT force as a ratio of ult. PT stress
else
  ptini = fpe/fpu
endif

v_prov(index) = v_prov_as + 0.6*ptini    ! total resistance to shear by
                                           ! PT and non-PT steels
v_check(index) = 'Y'

cstot = 0.0               ! sum of compression steel forces

do i = 1,2000
  pstot(i) = 0.0          ! sum of tension forces
  pptot(i) = 0.0          ! sum of PT forces
  mom(i) = 0.0            ! initial value for moment vector
  theta(i) = 0.0         ! initial value for theta vector
  na(i) = 0.0             ! initial value for neutral axis depth
enddo

econ = ecini              ! initial concrete strain
ppt(index) = pptini       ! initial force in PT steel

tolmoment = 0.05         !5% band +/- on moment target
tolratio = 0.02          !1% variance on desired moment ratio
if( mtargflag.eq.1) then !user has selected a target design moment
  lowermom = targetmom
  uppermom = (1+tolmoment)*targetmom
  lowerratio=targetmratio
  upperratio=tolratio+targetmratio
endif

return
end

```

```

c*****
c
c Subroutine: Output
c
c Purpose: Write output file.
c
c*****

```

subroutine output

include 'common.for'

```

call time(time1)      ! get time from system clock
call date(date1)      ! get date from system clock

```

c open file to write output

```

open (2,file=outfile,access='sequential',status='unknown')

write (2,1700)
write (2,1701)

write (2,1702)
write (2,1703)
write (2,1704)
write (2,1705)
write (2,1706)

write (2,1800) date1, time1, infile
write (2,1900) title1, title2, title3
write (2,2000) fc,fpe,b,h
write (2,2010)
write (2,2020) (type(ii), ii, d(ii), a(ii),
1 a(ii)*fy(ii), lunb(ii),ii=1,nlayer)
write (2,2070) ecini,epsini,ptini

1700 format (1x,'*****')
1701 format (1x,'National Institute of Standards & Technology')
1702 format (1x,'Bldg 226/ B168, Structures Division')
1703 format (1x,'Gaithersburg, MD 20899',/)
1704 format (1x,'Program B6: Analysis of Arbitrary Partially')
1705 format (1x,'Prestressed Precast Beam Column Joints')
1706 format (1x,'*****',/)
1800 format (1x,t35,'Date: ',a8,
1 5x,'Time: ',a11,
1 /1x,'Input File: ',A20,
1 //1x,'TITLE/NOTES:')
1900 format (1x,a80)

2000 format (/t30,'INPUT DATA',
1 /1x,'fc = ',f5.2,' ksi',
2 /1x,'fpe = ',f6.2,' ksi',
3 /1x,'b = ',f6.2,' in.',
3 /1x,'h = ',f6.2,' in.')

2010 format(/t20,'STEEL LAYERS',
1 //2x,'Type',2x,'Layer',3x,'D (in.)',3x,
2 'As (in**2)',3x,'Py (k)',3x,'L unb (in.)'/)
2020 format(3x,i2,4x,i2,5x,f6.2,5x,f7.3,4x,f7.2,4x,f5.2)

2070 format(//1x,'Initial concrete strain = ',f9.6,
1 /1x,'Initial PT strain = ',f9.6,
2 /1x,'Initial PT stress = ',f4.2,' fpu')

write (2,3100) targetmom, maxmom, peakratio,
1 theta(index-1), v_max, pt_max, ept_max, pt_yield,
2 nonpt_max, es_max, nonpt_yield, shear_count

3100 format(/1x'-----',

```

```

1 ' RUN SUMMARY -----',
1 //1x,'Target Moment = ',f7.2,' k-ft',
2 /1x,'Max. Moment = ',f7.2,' k-ft',
2 /1x,'Max. ratio M (non pt) / M (total) = ',f6.4,
3 /1x,'Max. Drift (beam) = ',f6.4,
4 /1x,'Max. Shear = ',f6.2,'k',
5 /1x,'Max. PT Force = ',f8.2,' k',t35,'Max PT strain = ',
6 f6.4,t65,'PT Steel Yielded? ',a1,
7 /1x,'Max. Non. PT Force = ',f8.2,' k',t35,'Max',
8 ' Non PT strain = ',f6.4,t65,'Non. PT Steel Yield? ',a1,
9 /1x,'V_prov < V_req: ',f4.0,' times')

```

```

write (2,2060) message
2060 format (/1x,'MESSAGES: ',a80)

```

```

write (2,2050)
2050 format (/1x,'-----',
1 ' RESULTS -----')

```

```

write (2,2080)
2080 format (/2x,'Theta',5x,'Delta',5x,'Non PT',5x,
1 'PT',5x,'Xbar',5x,'Mcol',6x,'Mbm',6x,'Shear',3x,
2 'Ms/Mtot',3x,'V_prov',4x,'V_Check'//)

```

c write results to file

```

do i = 1,index-1
write (2,3000) theta(i), gap(i),pstot(i), ppptot(i),
1 xbar(i),mom(i), shallow_bmmom(i), shear(i),
2 momratio(i),v_prov(i),v_check(i)

enddo
3000 format (1x,f7.5,3x,f7.5,3x,f6.1,3x,f6.1,3x,f6.4,3x,
1 f6.1,3x,f6.1,3x,f6.2,3x,f6.3,4x,f6.2,6x,a1)
return
end

```

c*****

c Compute stress for A36 steel given the strain. fy = 36 ksi
c Use ultimate steel strain of 0.34. Source: Salmon and Johnson, "Steel
Structures", 2nd ed., Harper and Row, 1980, pp.37.

c Variable passed in: strain

c Variable returned: sigma

c -----

```

subroutine a36(strain,sigma)

```

```

dimension e(35), s(35)

```

```

data e /0,0.0017391,0.0052172,0.0078258,0.0086953,0.012173,
1 0.013913,0.016521,0.023477,0.032173,0.041738,0.05652,0.069563,
2 0.079997,0.092170,0.10347,0.12086,0.13826,0.15043,0.16173,
3 0.17391,0.18521,0.19304,0.20173,0.21217,0.22260,0.23564,
4 0.24695,0.26086,0.27477,0.28955,0.30260,0.31912,0.33651,
5 0.34955/

```

```

data s /0,35.59,35.59,35.59,35.59,34.57,34.91,35.59,36.61,
1 38.30,40.68,43.05,44.74,46.44,48.13,50.51,52.20,54.57,
2 55.25,56.27,56.61,56.95,56.95,57.29,56.95,55.93,55.59,
3 54.23,53.22,51.52,49.83,47.79,45.42,42.71,40.68/

```

```

c -----
strain = abs(strain)
if ( strain .le. 0.34 ) then

do i = 2,35          ! interpolate values from stress-strain curve

if (strain .ge. e(i-1) .and. strain .lt. e(i)) then
sigma = ( strain-e(i-1) )/( e(i)-e(i-1) ) *
1 ( s(i)-s(i-1) ) + s(i-1)
endif

enddo

elseif ( strain .gt. 0.34 ) then
sigma = 0.0          ! consider bar to have fractured

endif

return
end

```

```

c *****
c
c subroutine to obtain the stress for grade 40 rebar.
c
c The stress-strain curve used is as defined in "Design of Concrete
c Structures", 8th ed. Winter and Nilson, McGraw-Hill, 1985, p 31. Upon
c strain-hardening values between given points (6 total) are linearly
c interpolated. Pick strain = 0.19 as fracture strain.
c
c variable returned: stress
c
c variable passed in: strain

```

```

c -----
subroutine g40(strain,sigma)

```

dimension e(35), s(35)

```
data e/0.0000,0.0012496,0.0013483,0.0015456,0.0019402,  
1 0.0044066,0.020761,0.023727,0.027681,0.030976,  
2 0.034931,0.040533,0.044817,0.048442,0.055032,  
3 0.062282,0.067884,0.080736,0.087327,0.093588,  
4 0.098861,0.10644,0.11501,0.11995,0.12522,  
5 0.13017,0.13709,0.14335,0.14829,0.15719,0.16345,  
6 0.17531,0.18223,0.19113,0.19706/
```

```
data s/0.0000,39.390,40.748,41.835,42.922,42.922,  
1 43.294,44.938,46.856,48.500,50.692,52.884,  
2 54.802,56.446,59.460,62.200,63.845,69.325,  
3 70.695,72.613,73.435,75.353,76.997,77.545,  
4 78.093,78.641,78.641,78.093,77.545,76.723,  
5 75.627,72.613,70.421,67.955,66.037/
```

```
c -----  
  
strain = abs(strain)  
if ( strain .le. 0.19 ) then  
  
do i = 2,35          ! interpolate values from stress-strain curve  
  
if (strain .ge. e(i-1) .and. strain .lt. e(i)) then  
    sigma = ( strain-e(i-1) )/( e(i)-e(i-1) ) *  
1 ( s(i)-s(i-1) ) + s(i-1)  
endif  
  
enddo  
  
elseif ( strain .gt. 0.19 ) then  
    sigma = 0.0          ! consider bar to have fractured  
  
endif  
  
return  
end
```

```
c*****  
c  
c subroutine to obtain the stress for grade 60 rebar.  
c The stress-strain curve used is as defined in "Design of Concrete  
c Structures", 8th ed. Winter and Nilson, McGraw-Hill, 1985, p 31. Upon  
c strain-hardening values between given points are linearly interpolated.  
c Choose strain = 0.12 as the strain at fracture  
  
c variable returned: stress  
  
c variable passed in: strain  
  
c -----
```

```
subroutine g60(strain,sigma)
```

```
dimension e(53), s(53)
```

```
data e /0.0000,0.0017429,0.0018087,0.0019073,  
1 0.0021375,0.0023677,0.0030583,0.0035844,  
2 0.0041106,0.0052287,0.0058864,0.0065112,  
3 0.0071360,0.0080568,0.0091748,0.010424,  
4 0.011411,0.012858,0.014042,0.015390,0.016574,  
5 0.017758,0.018580,0.019303,0.019829,0.022227,  
6 0.024881,0.027535,0.028862,0.031847,0.036160,  
7 0.040804,0.044122,0.047439,0.050756,0.054406,  
8 0.057723,0.060709,0.064358,0.068670,0.072983,  
9 0.077296,0.081608,0.082604,0.087912,0.094215,  
1 0.10052,0.10549,0.11014,0.11545,0.12042,  
2 0.12507,0.12905/
```

```
data s/0.0000,55.961,57.320,58.678,59.493,  
1 60.036,60.308,60.036,60.308,60.308,60.308,60.851,  
2 61.938,63.296,64.111,65.469,66.827,68.186,69.816,  
3 71.174,73.076,74.162,75.249,76.064,76.335,78.372,  
4 80.564,83.030,84.400,86.044,89.333,91.525,93.443,  
5 95.361,97.005,98.649,99.746,100.57,101.94,103.03,  
6 103.58,104.68,104.68,104.68,104.68,103.86,103.03,  
7 102.21,101.39,100.57,99.197,98.101,96.731/
```

```
c -----
```

```
strain = abs(strain)
```

```
if (strain .le. 0.12 ) then      ! interpolate from stress-strain curve
```

```
do i = 2,53
```

```
  if (strain .ge. e(i-1) .and. strain .lt. e(i)) then  
    sigma = ( strain-e(i-1) )/( e(i)-e(i-1) ) *  
1  ( s(i)-s(i-1) ) + s(i-1)  
  endif
```

```
enddo
```

```
elseif ( strain .gt. 0.12 ) then
```

```
  sigma = 0.0                      ! consider bar to have fractured
```

```
endif
```

```
return
```

```
end
```

```
c*****
```

```
c
```

```
c subroutine to obtain the stress in a 7/16" 7 wire prestress
```

```
c strand given the strain. Twelve points along the stress-strain
```

c curve are defined. Values between these points are linearly
 c interpolated. Data is obtained from a tension test of a 7/16" strand.
 c Choose strain = 0.058 as strain at fracture

c variable returned: stress

c variable passed in: strain

c -----

```
subroutine PT_strand716(strain,stress)
```

```
dimension epsilon(12), sigma(12)
```

```
data epsilon /0.0,0.005497,0.006609,0.007783,0.009389,  
1 0.011427,0.013898,0.019025,0.029958,0.039964,  
2 0.04997,0.058/
```

```
data sigma /0,163.17,192.15,212.94,230.58,243.81,  
1 252.0,255.78,262.71,267.12,269.64,272.16/
```

c -----

```
astr = abs(strain)
```

```
if (astr .gt. 0.058) then          ! Strand fracture  
  stress = 0.0  
  return  
endif
```

```
do 100 i = 2,12
```

```
  if (astr .ge. epsilon(i-1) .and. astr .lt. epsilon(i)) then  
    stress = ( astr-epsilon(i-1) )/( epsilon(i)-epsilon(i-1) ) *  
1 ( sigma(i)-sigma(i-1) ) + sigma(i-1)  
  endif
```

```
100 continue
```

```
return  
end
```

c *****

c
 c subroutine to obtain the stress in a 3/8" 7 wire prestress
 c strand given the strain. Thirty-four points along the stress-strain
 c curve are defined. Values between these points are linearly
 c interpolated. Data is obtained from a tension test of a 3/8" strand.
 c File is 38strande_lesspts.dat which is a subset of 38strande.lis.
 c Choose strain = 0.035 as strain at fracture. This is the minimum
 c elongation as required by A 416-87a. Our test data stopped at 0.015
 c strain.

c variable returned: stress

c variable passed in: strain

c -----

subroutine PT_strand38(strain,stress)

dimension e(34), s(34)

data e /0.0000, 0.000637, 0.00102, 0.00148,
1 0.0017700, 0.0020600, 0.0021300, 0.0023400,
2 0.0028000, 0.0031600, 0.0035900, 0.0037900,
3 0.0041100, 0.0048200, 0.0050600, 0.0053600,
4 0.0060000, 0.0063000, 0.0064900, 0.0068100,
5 0.0072400, 0.0077700, 0.0081400, 0.0088000,
6 0.0094300, 0.0097000, 0.0100000, 0.011400,
7 0.012000, 0.013000, 0.014100, 0.015000,
8 0.015200, 0.035000/

data s /0.0000, 11.882, 20.941, 32.471,
1 41.765, 51.412, 62.353, 70.235,
2 80.824, 91.765, 102.59, 110.82,
3 122.35, 144.71, 152.94, 160.00,
4 170.59, 182.35, 191.76, 200.00,
5 211.76, 222.35, 230.59, 240.00,
6 248.24, 252.94, 255.29, 260.00,
7 261.18, 261.18, 262.35, 263.53,
8 263.53, 263.53/

c -----

astr = abs(strain)

if (astr .gt. 0.0350) then ! Strand fracture
 stress = 0.0
 return
endif

do 100 i = 2,34

 if (astr .ge. e(i-1) .and. astr .lt. e(i)) then
 stress = (astr-e(i-1))/(e(i)-e(i-1))*
1 (s(i)-s(i-1)) + s(i-1)
 endif

100 continue

return
end

c*****

c
 c subroutine to obtain the stress for 1/2" to 1-1/4" PT bar given
 c the strain. Thirty-nine points along the stress-strain
 c curve are defined. Values between these points are linearly
 c interpolated. The curve was that taken out of "Design of Prestressed
 c Concrete Structures", 3rd ed., Lin & Burns, 1981, p. 54.
 c Choose strain = 0.039 as strain at fracture

c variable returned: stress

c variable passed in: strain

c -----

subroutine PT_bar(strain,stress)

dimension epsilon(39), sigma(39)

data epsilon /0.0E+00,0.40309E-02,0.44030E-02,0.47131E-02,
 1 0.49611E-02,0.52092E-02,0.55193E-02,0.57673E-02,0.61394E-02,
 2 0.65115E-02,0.68836E-02,0.73797E-02,0.76898E-02,0.83719E-02,
 3 0.89301E-02,0.94882E-02,0.99223E-02,0.10915E-01,0.12279E-01,
 4 0.13643E-01,0.15256E-01,0.16682E-01,0.18108E-01,0.19907E-01,
 5 0.21271E-01,0.22697E-01,0.24062E-01,0.25550E-01,0.27162E-01,
 6 0.28465E-01,0.29643E-01,0.31255E-01,0.32496E-01,0.33736E-01,
 7 0.35100E-01,0.36402E-01,0.37643E-01,0.38821E-01,0.39937E-01/

data sigma /0.0E+00,0.12000E+03,0.12562E+03,0.13000E+03,
 1 0.13312E+03,0.13562E+03,0.13812E+03,0.14000E+03,0.14250E+03,
 2 0.14500E+03,0.14750E+03,0.14875E+03,0.15062E+03,0.15125E+03,
 3 0.15187E+03,0.15250E+03,0.15375E+03,0.15375E+03,0.15437E+03,
 4 0.15500E+03,0.15625E+03,0.15625E+03,0.15687E+03,0.15750E+03,
 5 0.15750E+03,0.15875E+03,0.15937E+03,0.16000E+03,0.16062E+03,
 6 0.16062E+03,0.16062E+03,0.16187E+03,0.16187E+03,0.16250E+03,
 7 0.16312E+03,0.16312E+03,0.16312E+03,0.16437E+03,0.16437E+03/

c -----

astr = abs(strain)

if (astr.gt.0.039) then ! PT bar fracture
 stress = 0.0
 return
endif

do 100 i = 2,39

if (astr .ge. epsilon(i-1) .and. astr .lt. epsilon(i)) then
 stress = (astr-epsilon(i-1))/(epsilon(i)-epsilon(i-1)) *
 1 (sigma(i)-sigma(i-1)) + sigma(i-1)
endif

100 continue

return
end

c*****
c subroutine to obtain the stress for stainless steel 304 bar given
c the strain. Thirty-one points along the stress-strain
c curve are defined. Values between these points are linearly
c interpolated. The curve was that taken out of "Metals Handbook", 10th
c ed., Vol. 1, American Society of Metals, 1990, p. 853.
c Choose strain = 0.53 as strain at fracture

c variable returned: stress

c variable passed in: strain

c -----

subroutine ss304 (strain,sigma)

dimension e(31), s(31)

data e /0,0.024521,0.030651,0.036781,0.049042,0.061302,0.076628,
1 0.085823,0.098084,0.11647,0.13180,0.14713,0.16552,0.18084,
2 0.19617,0.21149,0.22069,0.23601,0.25747,0.27586,0.29119,
3 0.31264,0.33410,0.35555,0.37394,0.40153,0.42912,0.45670,
4 0.48122,0.50268,0.53333/

data s /0,42.40,46.37,48.58,51.67,53.88,57.41,59.18,61.39,
1 64.48,67.13,69.34,72.43,75.08,76.85,78.17,79.50,81.26,83.47,
2 84.35,85.68,86.56,87.89,88.77,89.21,90.54,90.98,91.42,
3 91.41,91.42/

c -----

strain = abs(strain)
if (strain .le. 0.53) then ! interpolate from stress-strain curve

do i = 2,31

if (strain .ge. e(i-1) .and. strain .lt. e(i)) then
sigma = (strain-e(i-1))/(e(i)-e(i-1)) *
1 (s(i)-s(i-1)) + s(i-1)
endif

enddo

elseif (strain .gt. 0.53) then ! consider bar to have fractured
sigma = 0.0

endif

```
return
end
```

```
c*****
c
c subroutine to obtain the stress for 1026 steel given
c the strain. Twenty-nine points along the stress-strain
c curve are defined. Values between these points are linearly
c interpolated. The curve was obtained from actual tension test of 1026 rod
c used in specimen L-P-Z4 C. Original data file is tube_shortlist.tmp which
c is a subset of tube.lis
c Choose strain = 0.026 as strain at fracture

c variable returned: stress

c variable passed in: strain
```

```
c -----
```

```
subroutine steel1026 (strain,sigma)
```

```
dimension e(29), s(29)
```

```
data e /0.0000, 0.00093, 0.001235, 0.001540,
1 0.0019000, 0.0021150, 0.0023700, 0.0026700,
2 0.0030450, 0.0035550, 0.0043050, 0.0054000,
3 0.0060000, 0.0065000, 0.0070000, 0.0075000,
4 0.0080000, 0.0085000, 0.0095000, 0.0100000,
5 0.011500, 0.013050, 0.015000, 0.017000,
6 0.019100, 0.021100, 0.023500, 0.025450,
7 0.026800/
```

```
data s /0.0000, 10.761, 21.521, 30.297,
1 40.326, 45.132, 50.355, 55.370,
2 60.176, 65.190, 70.205, 75.010,
3 76.682, 77.727, 78.562, 79.189,
4 79.607, 80.025, 80.861, 81.070,
5 81.697, 82.323, 82.950, 83.786,
6 84.413, 85.040, 85.875, 86.502,
7 86.711/
```

```
c -----
```

```
strain = abs(strain)
if (strain .le. 0.026 ) then      ! interpolate from stress-strain curve
```

```
do i = 2,29
```

```
if (strain .ge. e(i-1) .and. strain .lt. e(i)) then
sigma = ( strain-e(i-1) )/( e(i)-e(i-1) ) *
1 ( s(i)-s(i-1) ) + s(i-1)
endif
```

```
enddo
elseif ( strain .gt. 0.026 ) then
    sigma = 0.0          ! consider bar to have fractured
endif
return
end
```

Listing of Common.FOR

```
c *****
c
c file containing the declaration type statements and common statements
c used in program beammom.for
c
c *****
c
c declaration statements
c
c   character infile*20, outfile*20, title1*80, title2*80, title3*80
c   character time1*11, date1*8, ans, v_check(2000), frac_layer
c   character message*80, pt_yield, nonpt_yield
c
c   real mom (2000), na(2000), mom_y, lunb(10), L1, maxmom,
c   1 lowermom, momratio(2000), lowerratio, nonpt_max
c
c   dimension a(10), d(10), estr(10), ppt(10), ps(10), theta(2000)
c   dimension cs(10), gap(2000), shallow_bmmom(2000), shear(2000)
c   dimension eu(10), fy(10),pstot(2000),ppttot(2000), v_prov(2000)
c   dimension xbar(2000), ey(10)
c
c   integer type(10), clayer(10), tlayer(10), player(10)
c -----
c
c common block for input variables
c
c   common /input/ fc, fpe, fu, b, h, d, a, nlayer,
c   1 type, lunb, arm, L1, targetmom, mtargflag,
c   2 targetmratio, player, iterationcount, infile,
c   3 time1, date1, outfile, title1, title2, title3,
c
c common block for intial values
c
c   common /initval/ sigini, ecini, epsini, nsoln,
c   1 fy, eu, ppt, ps, index, beta1, gap, pstot, cstot,
c   2 ppttot, ptini, y, na, nlayer, nclayer, nplayer,
c   3 maxmom, lowermom, uppermom, peakmratio,
c   4 lowerratio, upperratio, nplayermax, v_max, v_prov,
c   5 v_prov_as, apstot, shear_count, ept_max, es_max,
c   6 pt_max, nonpt_max, ey, pt_yield,
c   7 nonpt_yield, v_check, frac_layer
c
c common block for output variables
c
c   common /output/ mom, theta, mom_y, theta_y,
c   1 shear, shallow_bmmom, momratio, xbar, message
```

